Report of Investigations No. 128

FACIES AND STRATIGRAPHY OF THE SAN ANDRES FORMATION, NORTHERN AND NORTHWESTERN SHELVES OF THE MIDLAND BASIN, TEXAS AND NEW MEXICO

Paul J. Ramondetta

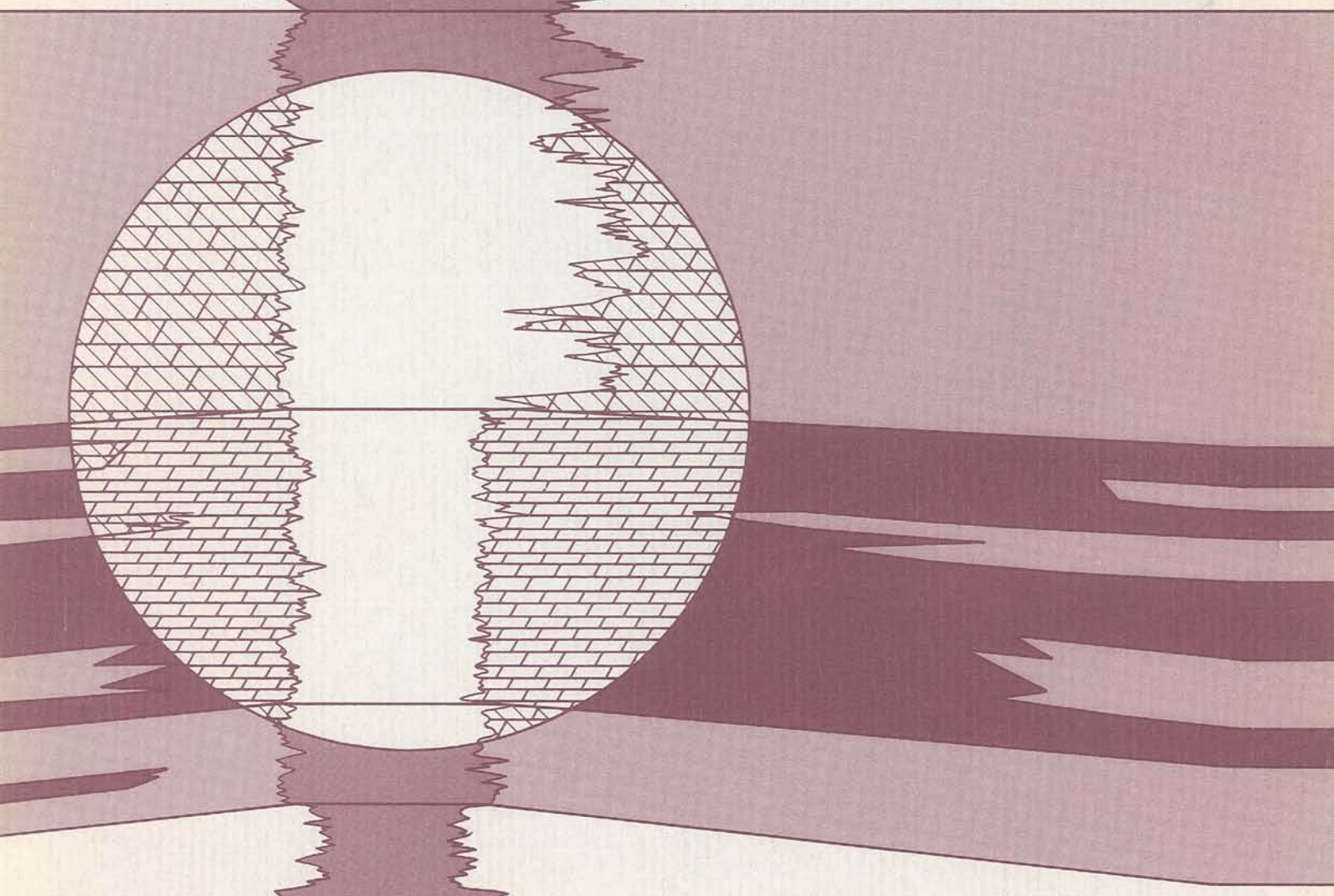

1982

Bureau of Economic Geology
W. L. Fisher, Director
The University of Texas at Austin
Austin, Texas 78712

Report of Investigations No. 128

FACIES AND STRATIGRAPHY OF THE SAN ANDRES FORMATION, NORTHERN AND NORTHWESTERN SHELVES OF THE MIDLAND BASIN, TEXAS AND NEW MEXICO

Paul J. Ramondetta*

Assisted by

David D. Guetzow
Rick Dauzat
Robert Merritt
John Garza
Lee Holman
Dominick Roques

Project funded by
the U.S. Department of Energy,
Contract No. DE-AC97-80ET-46615

Bureau of Economic Geology
W. L. Fisher, Director
The University of Texas at Austin
Austin, Texas 78712

*Currently with Cities Service Company, Wichita, Kansas.

CONTENTS

FIGURES

TABLES

ABSTRACT

The San Andres Formation on the Northern and Northwestern Shelves of the Midland Basin is a progradational stratigraphic unit consisting predominantly of carbonate facies. Lithofacies include dolomite, laminated anhydrite and dolomite, massive bedded anhydrite, limestone, salt, and red beds. These lithofacies represent depositional environments that include deep-water outer shelf, shallow-water inner shelf, shallow-water to emergent shoals, and a sabkha complex that comprises intertidal to supratidal algal mud flats, hypersaline lagoons or brine pans, and terrigenous mud flats.

Deposition was cyclic; a cycle began with a transgression followed by a gradual shoaling-upward sequence. Cycles commonly terminated with subaerial exposure before renewed transgression initiated a new cycle. Much of the dolomitization probably occurred during periods of subaerial exposure in schizohaline environments. Likewise, porosity was probably also developed during subaerial exposure. Surface topography probably exerted considerable control on dolomitization and porosity development. Additional diagenetic alteration of carbonates may have occurred as a result of an influx of hypersaline brine.

San Andres reservoirs of the Northern and Northwestern Shelves yielded 12.7 percent of the total oil production for the State of Texas in 1980. Trapping mechanisms for the oil are both structural and stratigraphic. Maps and cross sections in this report document the nature of these mechanisms.

Large volumes of oil are trapped in a discontinuous, structurally high, and stratigraphically thin belt that rims the deep northern Midland Basin and that overlies older shelf margins. Porosity zones thin updip from this belt; source rocks are subjacent to this belt of porosity. Additional oil is trapped in a series of steplike, updip porosity pinch-outs exhibiting little or no structural control. Regional porosity pinch-outs control the northern limits of oil production in the Northern and Northwestern Shelves of Texas and eastern New Mexico.

INTRODUCTION

This investigation was designed to describe and interpret the facies and stratigraphy of the San Andres Formation on the Northern and Northwestern Shelves of the Midland Basin and to document, with subsurface maps, cross sections, and production data (fig. 1), the nature of oil entrapment. Assessment of San Andres oil and gas potential in the Palo Duro Basin is important because San Andres salt deposits are being evaluated for possible storage of nuclear waste. The study area is shown in figure 1. The Texas and New Mexico state line is arbitrarily used in this report as the boundary between the Northern and Northwestern Shelves.

The Northern Shelf is separated from the northern Midland Basin by the Abo Reef trend. This reef trend is a long, narrow belt of dolomitized reef and carbonate bank deposits of Lower Permian age, stretching from Eddy County, New Mexico, to Hockley County, Texas (Sax and Stenzel, 1968; Wright, 1962). Shelf-margin deposits ranging in age from Strawn to Clear Fork are found along this belt (fig. 2; table 1). To the south, the San Andres shelf extends onto the Central Basin Platform, and to the west in New Mexico, it is called the Northwestern Shelf (figs. 1 and 2). San Andres carbonate facies deposited on this broad marine shelf extend

Table 1. Stratigraphic chart, northern Midland Basin.

System	Series or Group	Group or Formation	
Tertiary		Ogallala	
Cretaceous			
Triassic		Dockum	
Permian		**Shelf Facies**	**Basinal Facies**
	Ochoa	Dewey Lake Rustler Salado	Dewey Lake Rustler Salado
	Guadalupe	Artesia Upper San Andres Lower San Andres ("Yellowhouse dolomite")	Delaware Sand San Andres
	Leonard	Upper Clear Fork-Yeso-Glorieta Lower Clear Fork Wichita-Albany-Abo	Upper Spraberry Lower Spraberry-Dean
	Wolfcamp		
Pennsylvanian	Cisco Canyon Strawn Bend		
Mississippian	Chester Meramec Osage Kinderhook		
Devonian	Woodford Post-Fusselman Pre-Woodford		
Silurian	Fusselman		
Ordovician	Montoya Simpson Ellenburger		
Cambrian	Upper Cambrian		

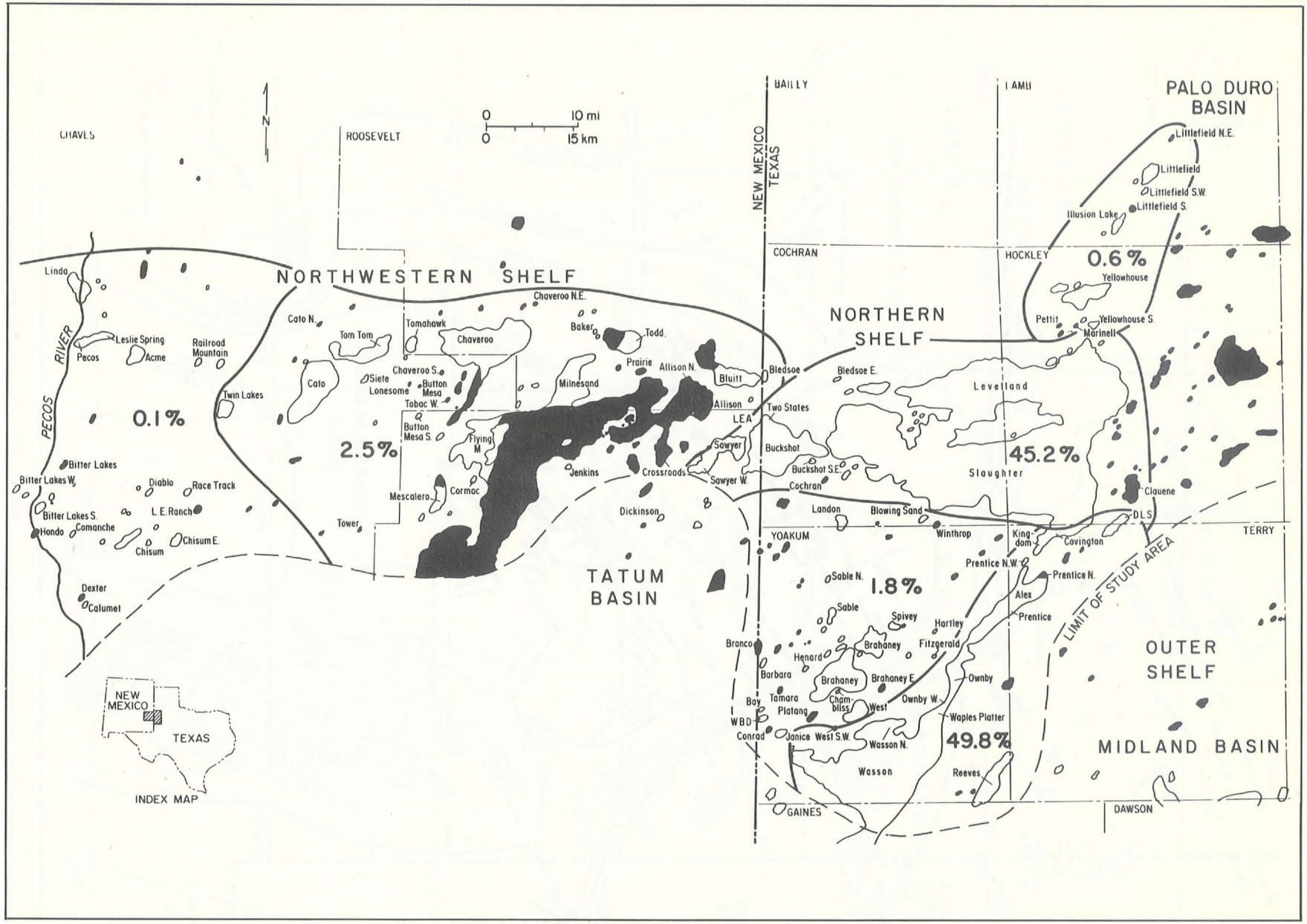

Figure 1. Map of the Northern and Northwestern Shelves showing oil fields and percent total accumulative San Andres oil production within each region. Darkened fields produce from pre-San Andres strata.

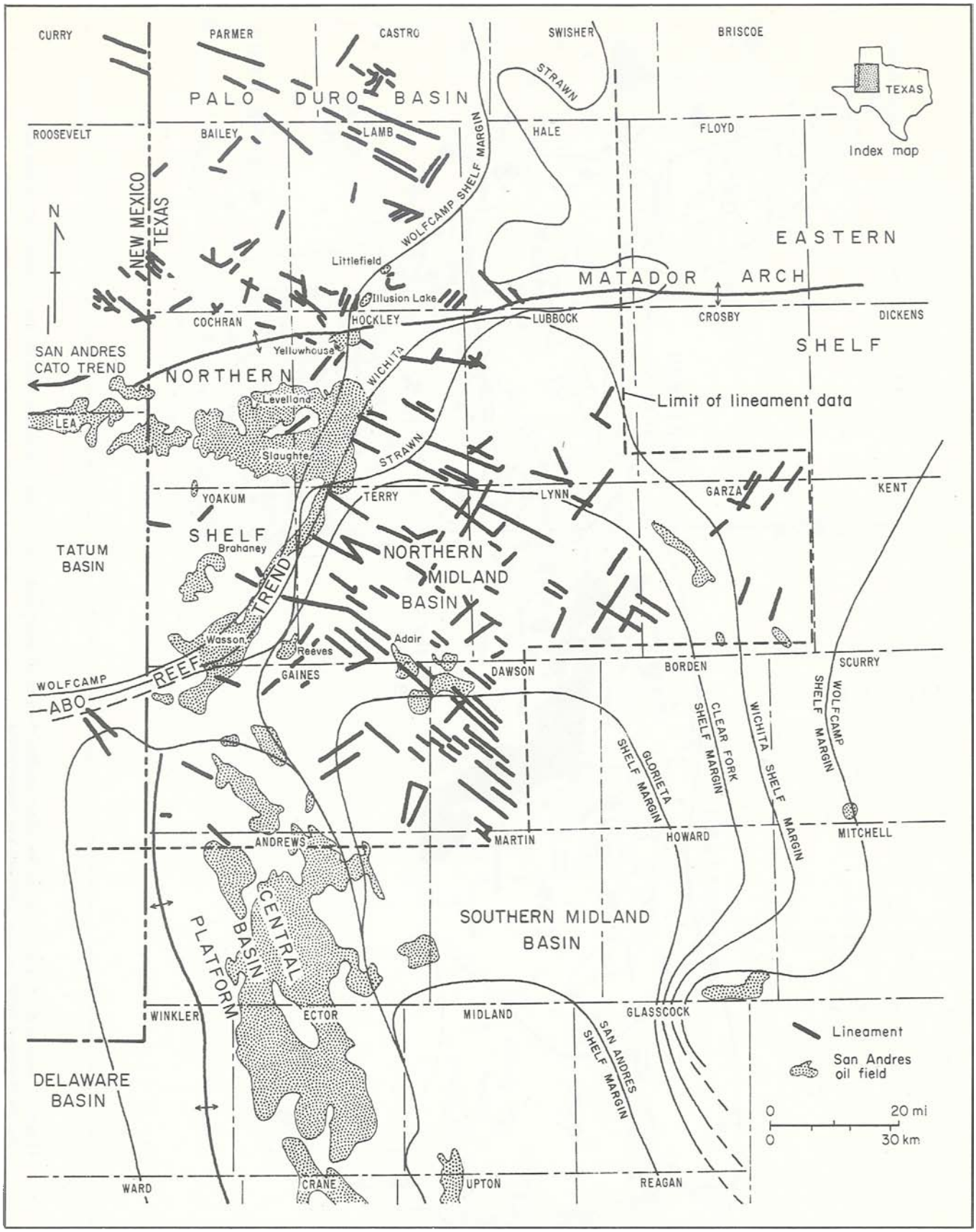

Figure 2. Map of study area in Texas showing San Andres oil production, shelf margins, and surface lineaments. Surface lineaments are from Finley and Gustavson (1981), and shelf-margin positions are from J. H. Nicholson (personal communication, 1980).

northward into the Palo Duro Basin, where they grade into sabkha evaporites and terrigenous continental deposits.

More than 80 percent of the oil produced on the Northern Shelf has been from lower San Andres reservoirs; in 1980 this production constituted 12.7 percent of total Texas oil production (Railroad Commission of Texas, 1981).

San Andres carbonate facies, which currently are hydrocarbon reservoirs in the southern Palo Duro Basin just north of the Matador Arch, intertongue to the north with relatively massive San Andres salt facies. The presence of hydrocarbons within potential San Andres dolomite reservoirs could limit the use of intercalated salt as a nuclear waste repository host rock.

Oil that is produced from San Andres dolomites is not indigenous to the San Andres Formation but has migrated onto the Northern Shelf from deep Wolfcampian basinal shales. This migration occurred mostly along vertical fractures in the Abo Reef trend (Ramondetta, 1982).

METHODS

Maps and cross sections presented in this report were made on the basis of approximately 3,000 well logs from the northern Midland Basin and Palo Duro Basin, Texas and New Mexico (fig. 3). The names and locations of well control are on open file at the Bureau of Economic Geology. A minimum spacing of 1 mi was maintained between control wells where well density is high.

All maps were originally prepared at a scale of 1 inch equaling 8,000 ft; these maps and other maps of intermediate scale are also on open file at the Bureau. Important marker horizons in the San Andres are shown on cross sections. The top and the base of the San Andres differ from those selected by Presley for the Palo Duro Basin (Gustavson and others, 1980); therefore, thickness and structure values vary somewhat in overlapping areas. Most maps in this report display all well control. However, many wells do not penetrate the lower San Andres horizons, and our mapping of these horizons is based on fewer control points than might be inferred from the maps. The well control used to prepare each map is on open file at the Bureau.

STRATIGRAPHY

The San Andres Formation (Upper Permian) consists predominantly of carbonate facies that extend from Central Texas to Arizona and Utah. In the Permian Basin, San Andres carbonates grade northward into anhydrite, salt, and red beds in the northern Texas Panhandle, Oklahoma, and Kansas. Red bed, dolomite, and gypsum facies crop out along a north-south belt in the eastern part of the Texas Panhandle (Blaine Formation) and have been described by M. W. Presley (personal communication, 1981). Similarly, a predominantly carbonate section (Kelly, 1971) equivalent to the San Andres is exposed along the eastern flank of the Sacramento Mountains, New Mexico. Kelly divided the San Andres into three members: (1) the thickly bedded Rio Bonito, (2) the thinly bedded Bonnie Canyon, and (3) the gypsiferous Fourmile Draw.

The San Andres Formation was originally described by Lee and Girty (1909). In subsequent years, controversy developed about whether the San Andres is Leonardian or Guadalupian in age. Some of the early workers include Darton (1922), Dickey (1940), Lewis (1941), King (1942), Galley (1958), and Hayes (1959, 1964). Dickey (1940) and Hayes (1959, 1964) inferred two apparent ages: Leonardian in the Delaware Basin and on the Northwestern Shelf, and Guadalupian in the Midland Basin. This apparent contradiction was explained by Todd (1976), who interpreted the San Andres as an eastward-prograding sequence in the Delaware and Midland Basins.

Lithofacies range from deep-water limestones to shallow-water oolite bar deposits to shallow shelf or lagoonal carbonates containing siliciclastics and anhydrite and, finally, to sabkha, brine-pan, and mud-flat deposits (Todd, 1976; Perez de Mejia, 1977). The distribution of depositional environments on the Northern Shelf during a regressive phase in early San Andres time is shown schematically in figure 4. Progradation of this facies tract proceeded, with cyclic interruptions, from north to southeast across the Northern Shelf and into the Midland Basin (figs. 5 and 6). Deposition during early San Andres time was

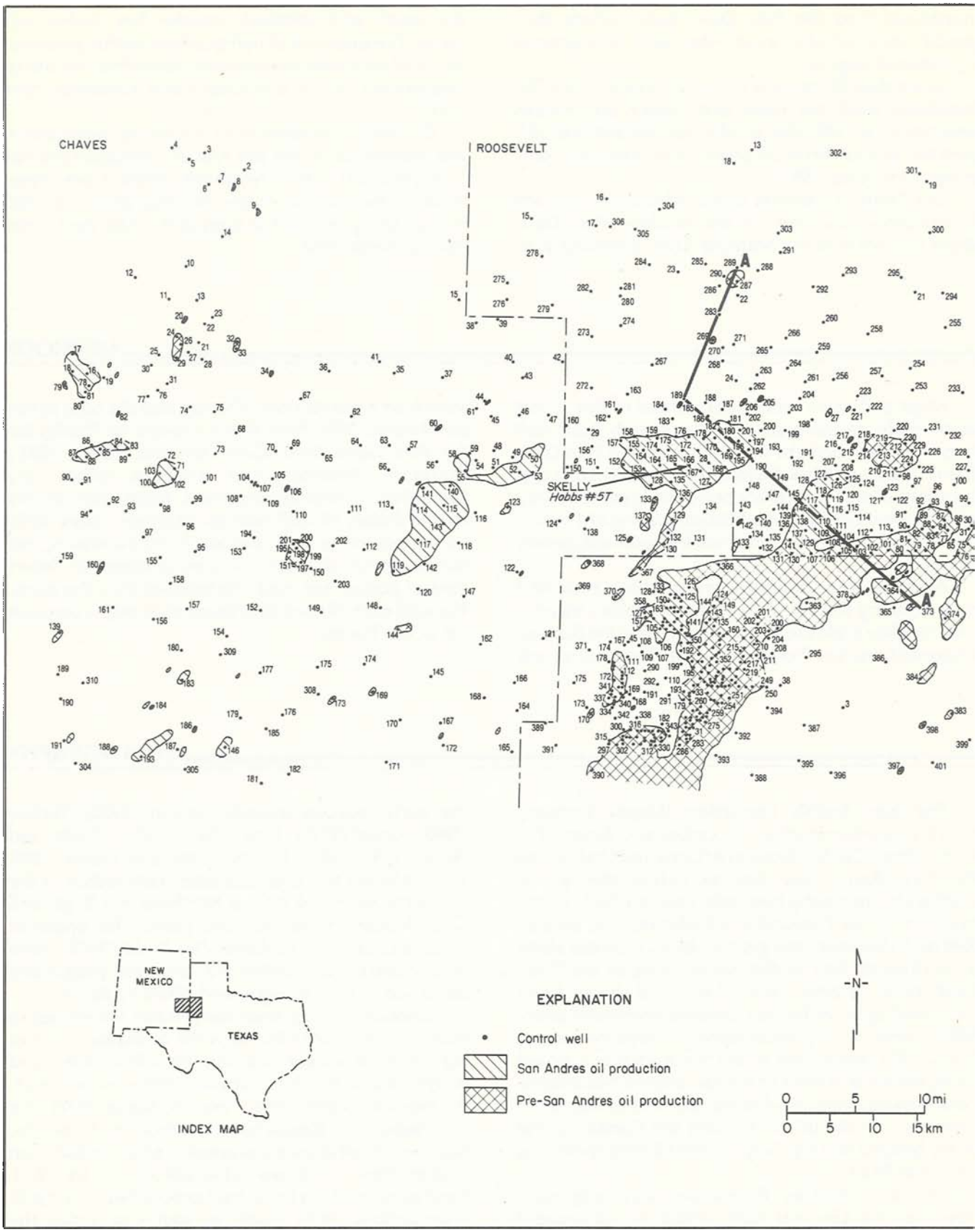

Figure 3. Map of the Northern and Northwestern Shelves showing well control and lines of cross section.

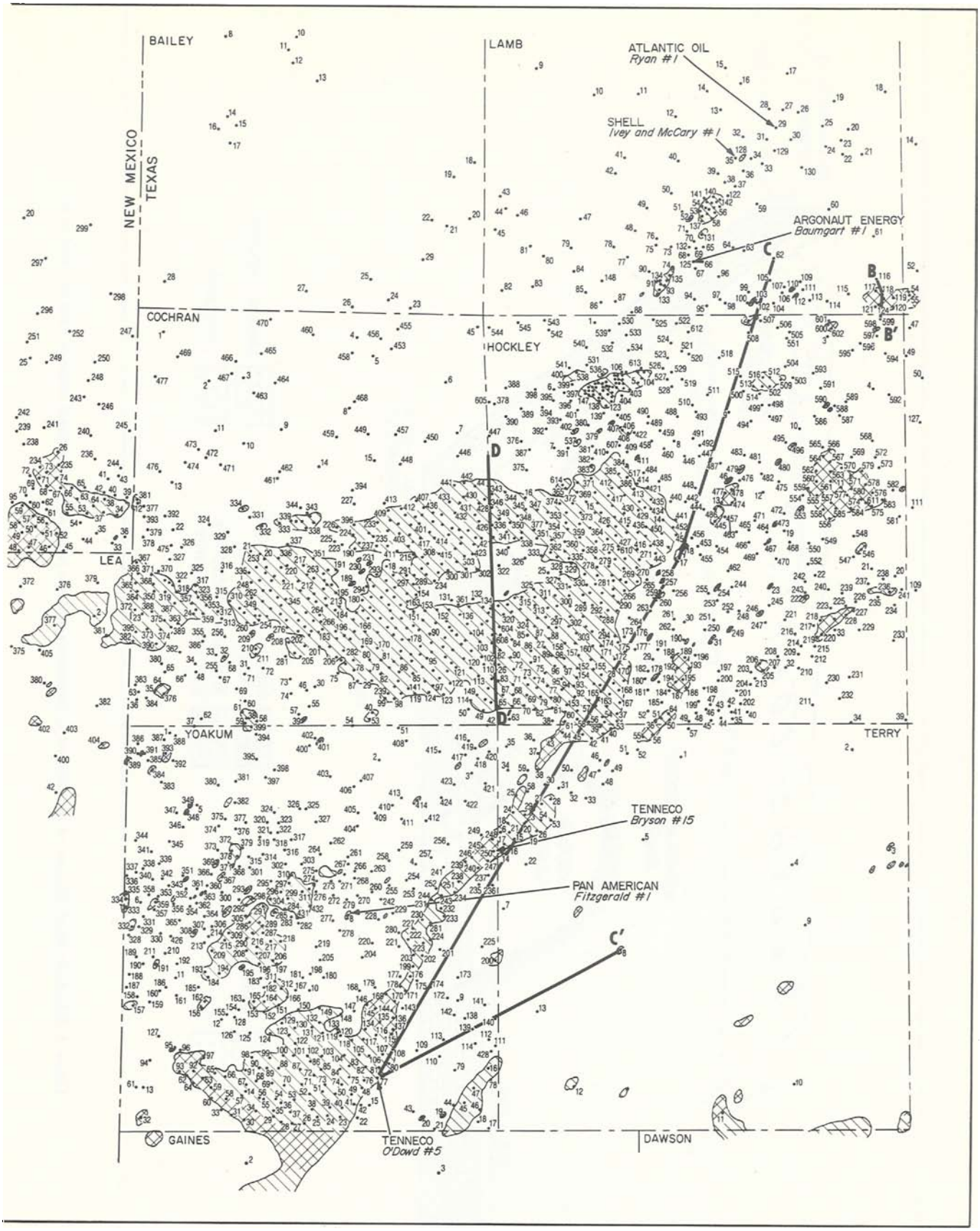

Figure 3 ***(continued)*.**

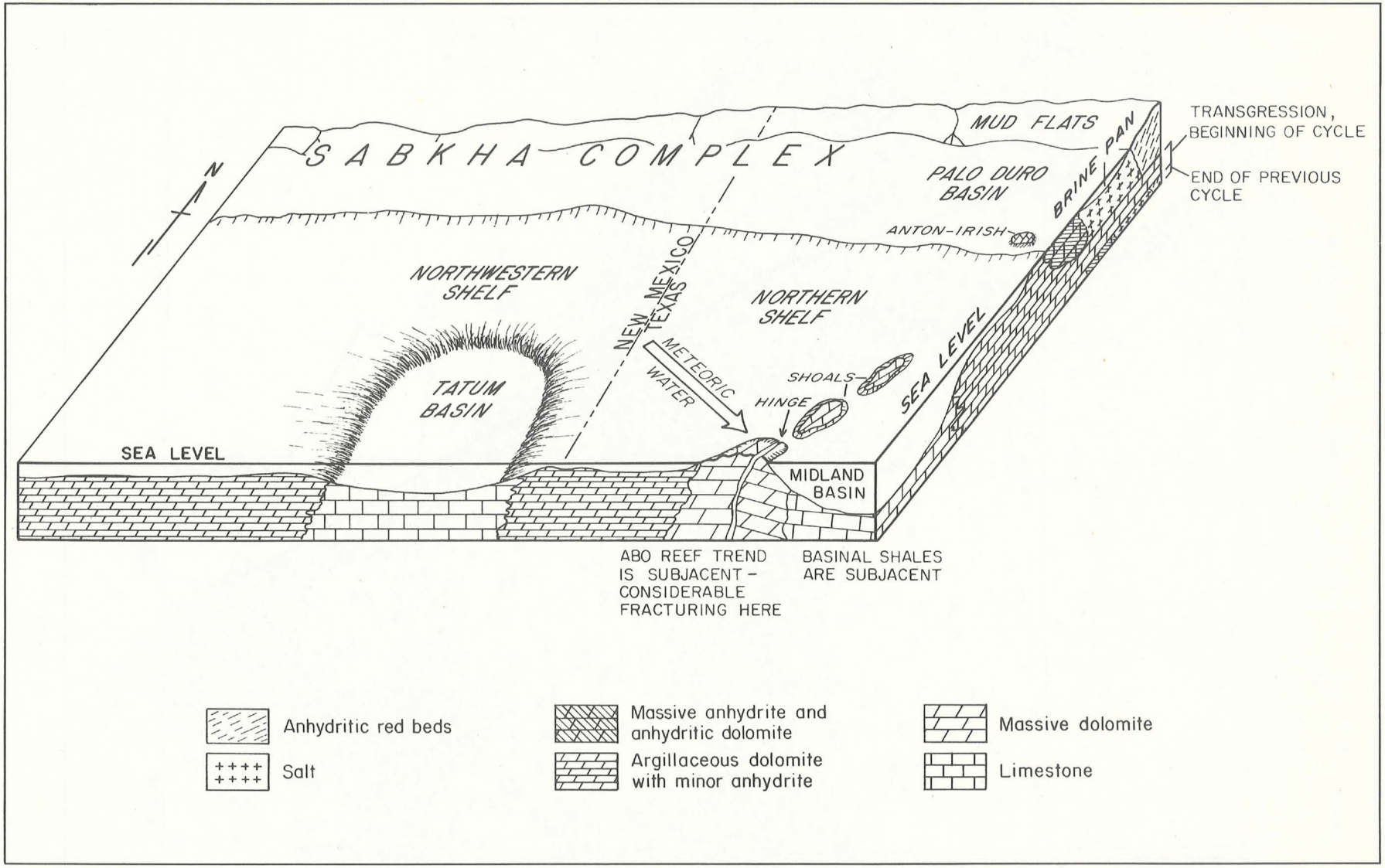

Figure 4. Schematic block diagram of depositional environments during a regressive depositional phase in early San Andres time.

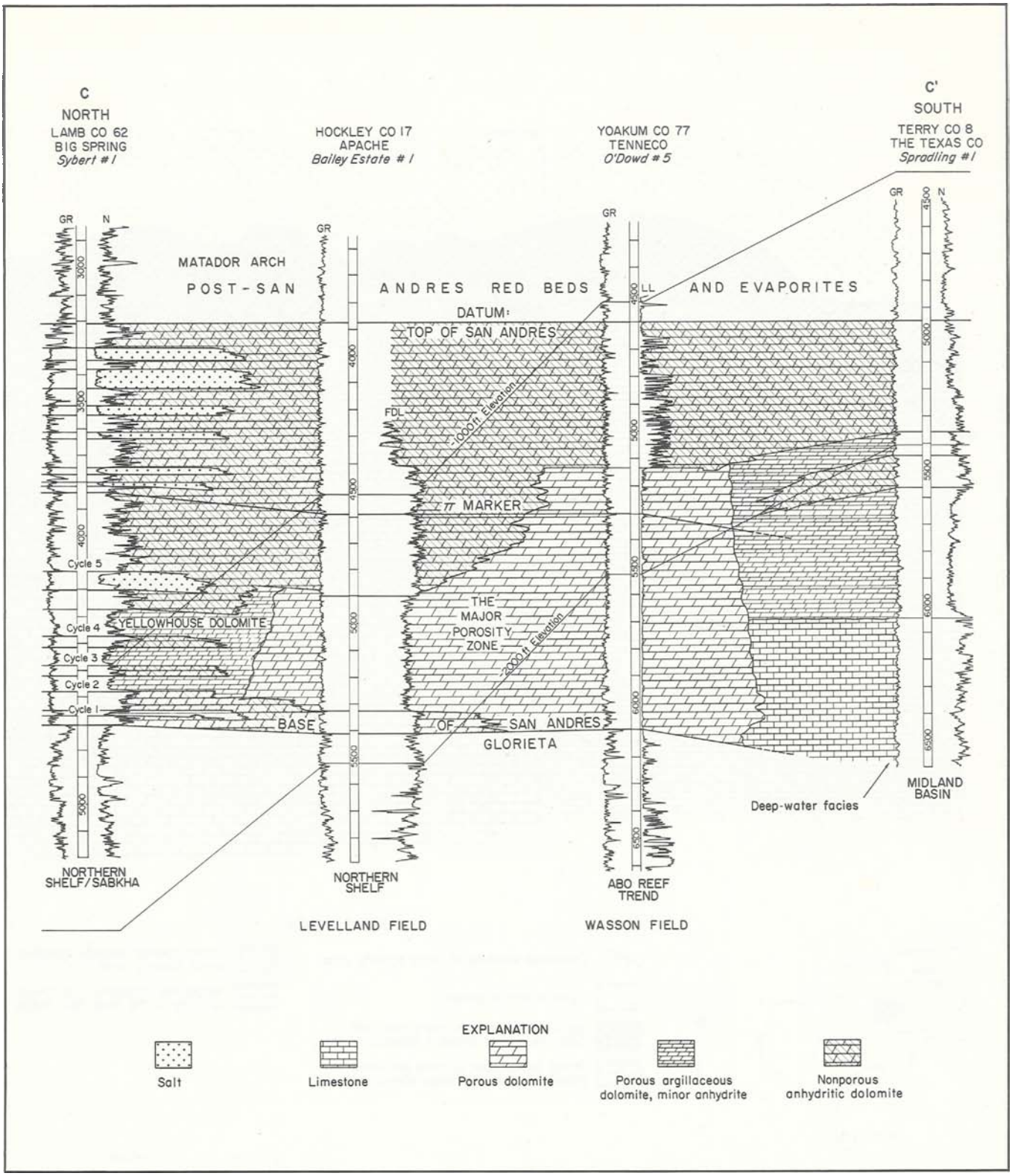

Figure 5. North-south cross section of San Andres Formation across the Northern Shelf. Line of section C-C′ illustrated in figure 3.

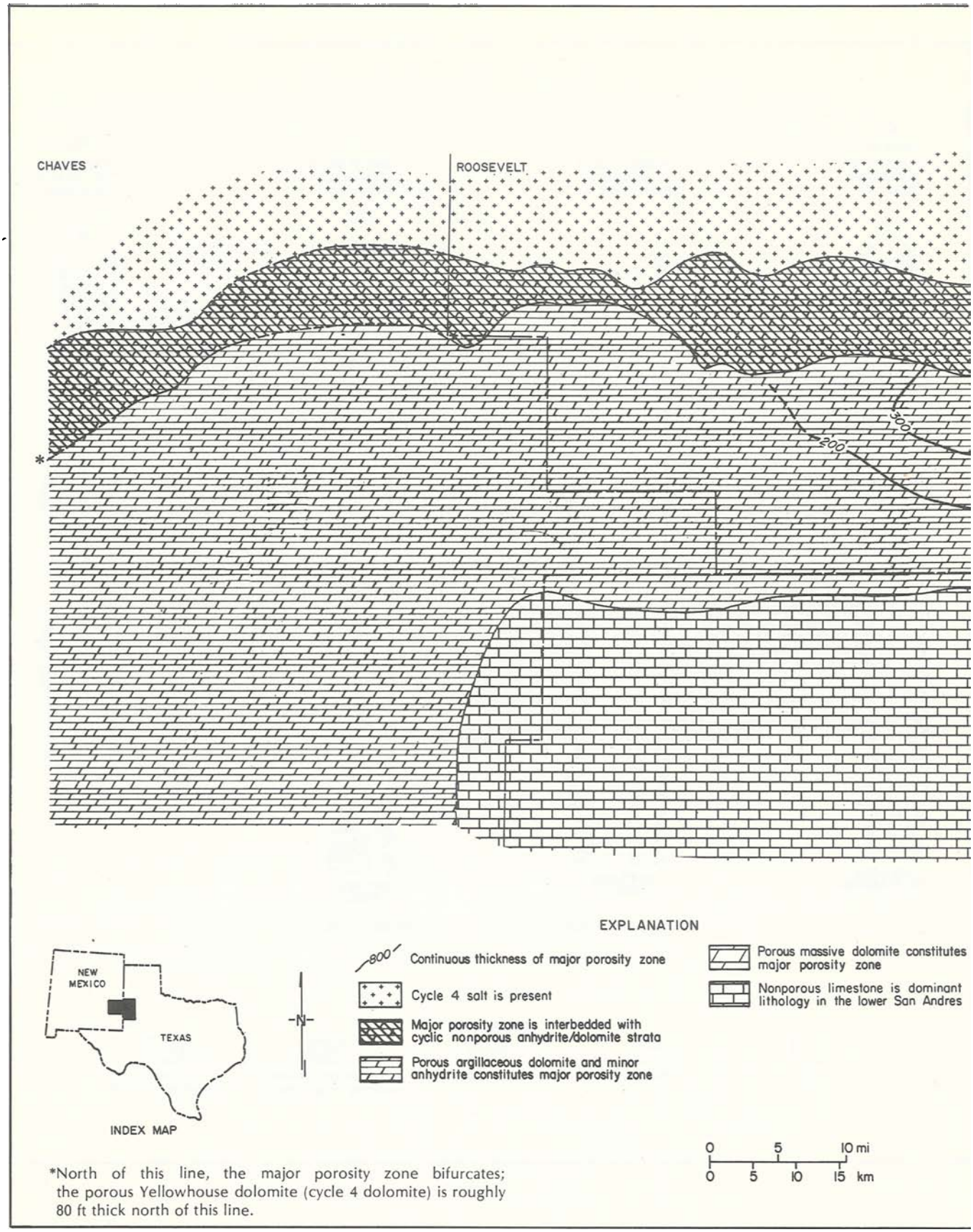

Figure 6. Distribution of lithofacies during much of early San Andres time. The thickness of the major porosity zone is also shown.

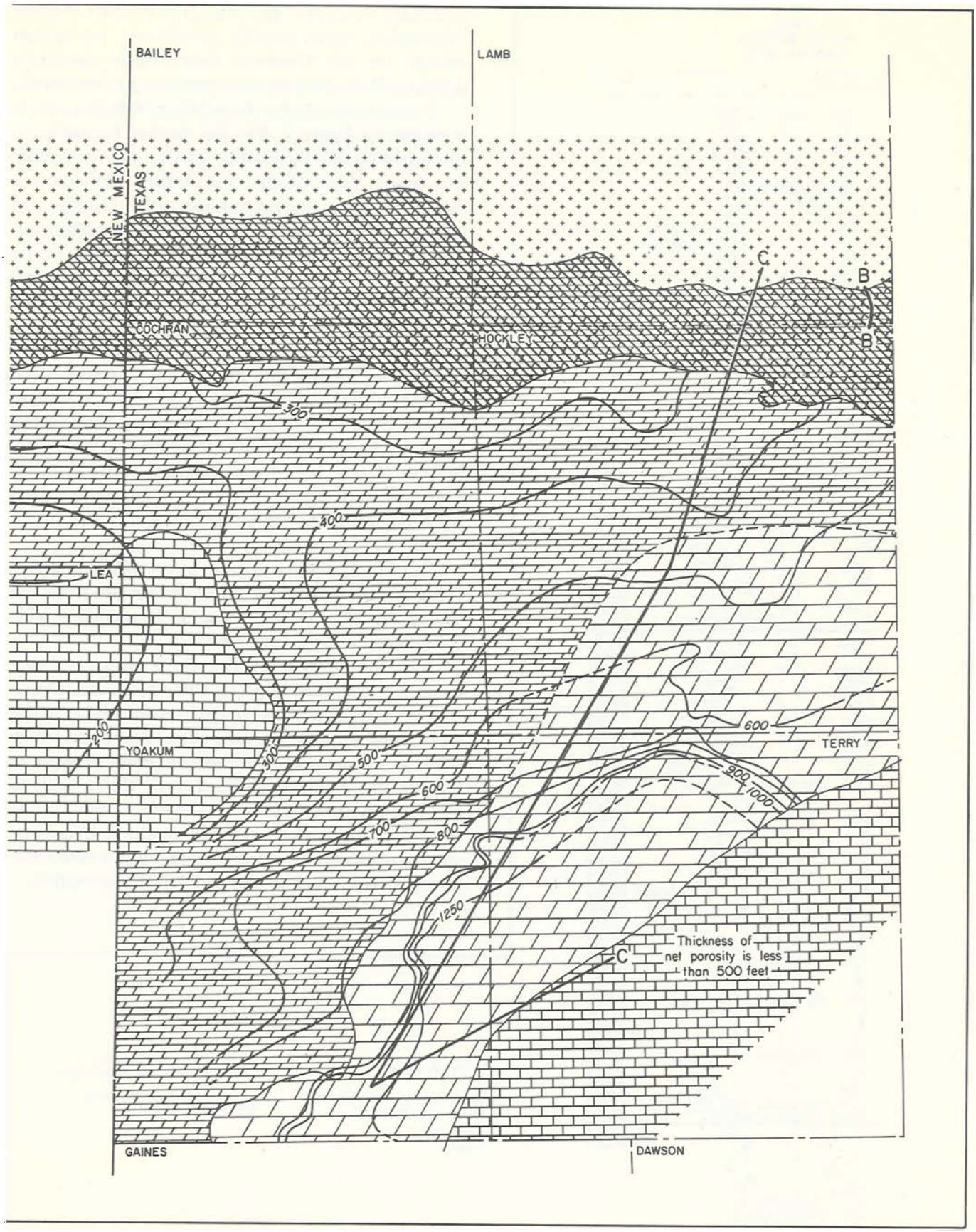

Figure 6 ***(continued)***.

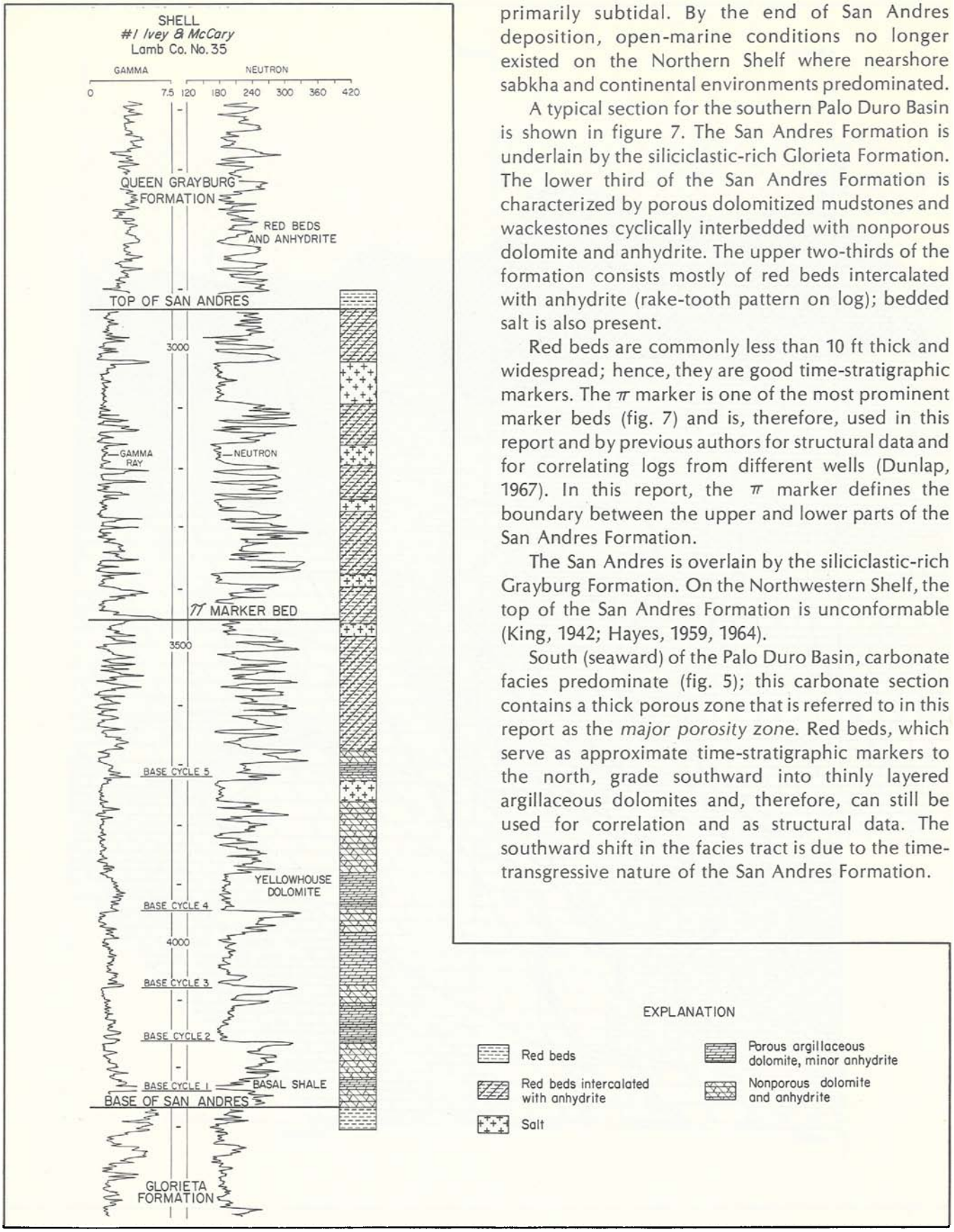

primarily subtidal. By the end of San Andres deposition, open-marine conditions no longer existed on the Northern Shelf where nearshore sabkha and continental environments predominated.

A typical section for the southern Palo Duro Basin is shown in figure 7. The San Andres Formation is underlain by the siliciclastic-rich Glorieta Formation. The lower third of the San Andres Formation is characterized by porous dolomitized mudstones and wackestones cyclically interbedded with nonporous dolomite and anhydrite. The upper two-thirds of the formation consists mostly of red beds intercalated with anhydrite (rake-tooth pattern on log); bedded salt is also present.

Red beds are commonly less than 10 ft thick and widespread; hence, they are good time-stratigraphic markers. The π marker is one of the most prominent marker beds (fig. 7) and is, therefore, used in this report and by previous authors for structural data and for correlating logs from different wells (Dunlap, 1967). In this report, the π marker defines the boundary between the upper and lower parts of the San Andres Formation.

The San Andres is overlain by the siliciclastic-rich Grayburg Formation. On the Northwestern Shelf, the top of the San Andres Formation is unconformable (King, 1942; Hayes, 1959, 1964).

South (seaward) of the Palo Duro Basin, carbonate facies predominate (fig. 5); this carbonate section contains a thick porous zone that is referred to in this report as the *major porosity zone*. Red beds, which serve as approximate time-stratigraphic markers to the north, grade southward into thinly layered argillaceous dolomites and, therefore, can still be used for correlation and as structural data. The southward shift in the facies tract is due to the time-transgressive nature of the San Andres Formation.

Figure 7. Gamma-ray, neutron log, and lithic interpretation of San Andres strata, Shell Ivey and McCary No. 1, Lamb County, Texas.

DOLOMITE

Dolomitized mudstone (fig. 8) is the most common rock type in the lower part of the San Andres Formation. The size of dolomite rhombs (fig. 9) ranges from 2 to 96 microns (Barone, 1976); limpid dolomite is generally absent. Dolomitized wackestones, packstones, and grainstones (fig. 10) are also present, although they are not as common. Porosity is best developed in mudstones and wackestones (Chuber and Pusey, 1967) and is mostly finely intercrystalline (fig. 9) or finely intergranular (Schneider, 1943; Barone, 1976). Coarser moldic porosity, which tends to be less permeable than the fine intercrystalline porosity, and fracture porosity, which causes locally high permeabilities, are also present.

These dolomites are generally bioturbated (fig. 10), fossiliferous (fig. 11), highly stylolitized, and contain varying amounts of anhydrite and siliciclastics. The siliciclastic-rich dolomites are typically thin bedded and, hence, are useful for correlation. Fossils include brachiopods, pelecypods, echinoderms, ostracods, bryozoans, sponge spicules, algal debris, worm jaws, foraminifers, membranous plant debris, and plant cuticles (Chuber and Pusey, 1967; Ramondetta, 1982); corals and fusulinids are absent (Chuber and Pusey, 1967). Nonskeletal grains, such as pellets, ooliths, and intraclasts, are more abundant than skeletal grains (Chuber and Pusey, 1967). Amounts of organic material vary; black, organic-rich lentils may have as much as 4 percent organic carbon (Ramondetta, 1982).

Dolomite may also occur as thin beds intercalated with anhydrite (fig. 12a, b, c, and d). This association is typical of intertidal to supratidal stromatolitic sequences; fenestral cavities are common. Such

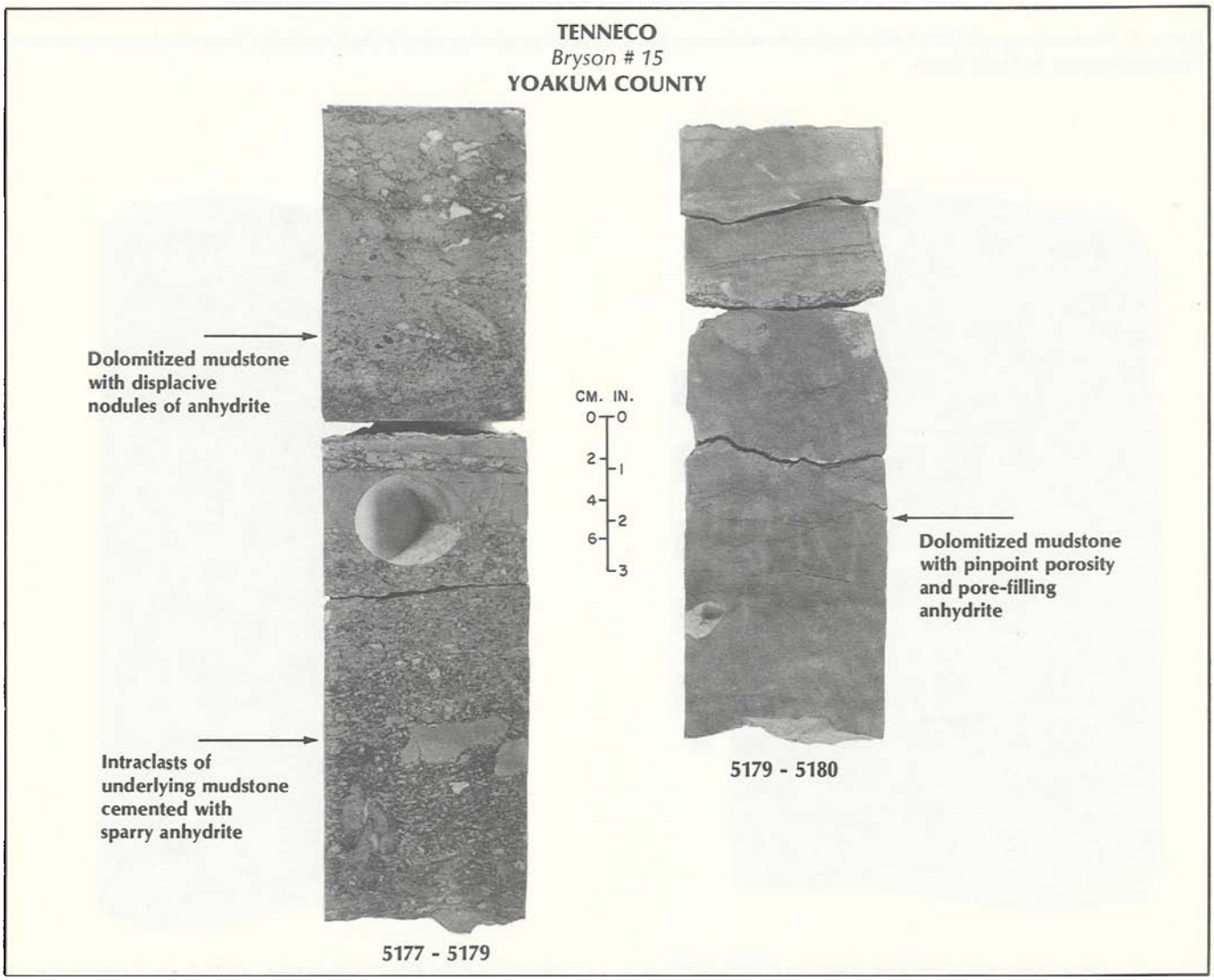

Figure 8. Dolomitized mudstone and intraclasts, Tenneco Bryson No. 15, Yoakum County, Texas.

Figure 9. Photomicrograph (SEM) of dolomite rhombs from a San Andres oil-producing zone in the Cato field, Chaves County, New Mexico. Photomicrograph by Holly Lanan.

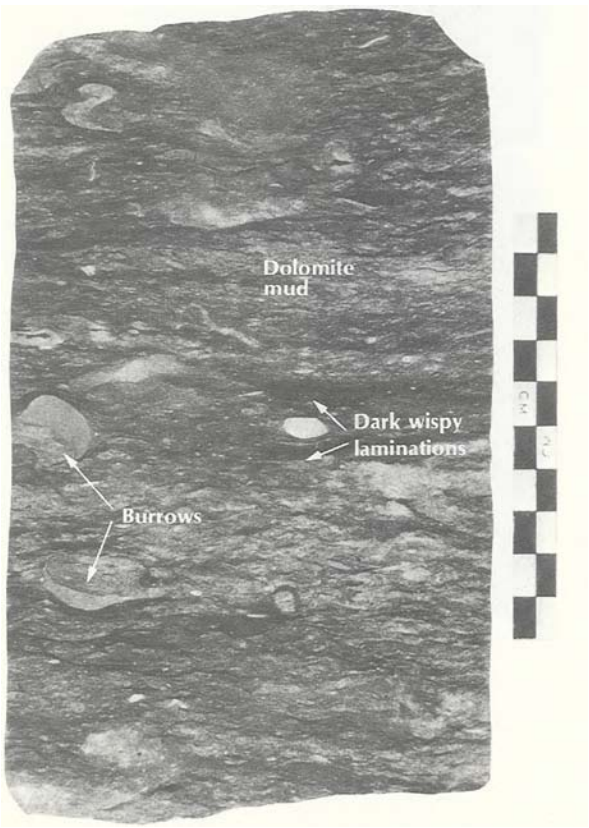

Figure 10. Wispy-laminated crinoidal packstone, Atlantic Oil Ryan No. 1, Lamb County, Texas. Photograph by M. W. Presley.

Figure 11. Fossiliferous dolomite, DOE-Gruy Grabbe No. 1, Swisher County, Texas.

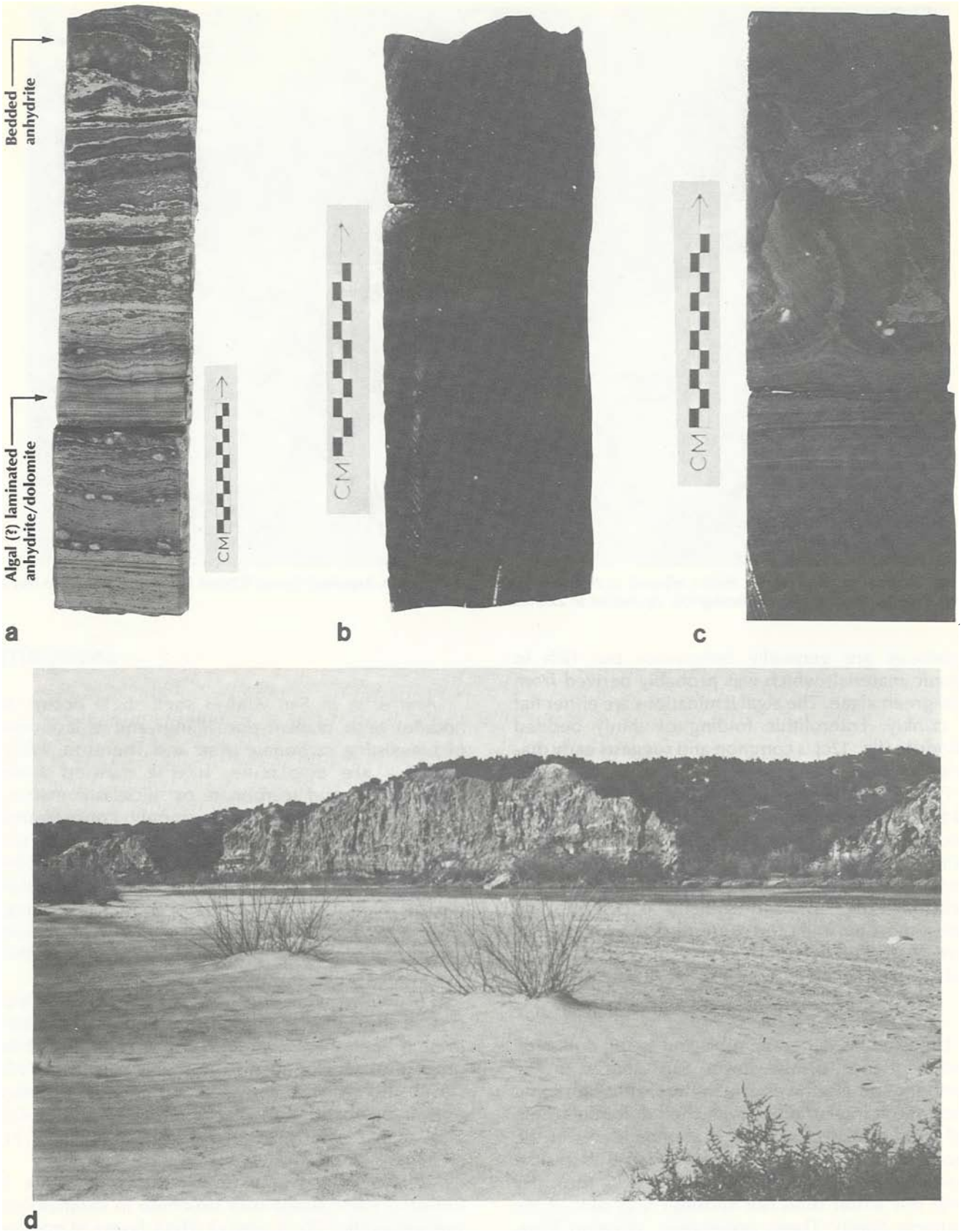

Figure 12. (a) Laminated, nonporous anhydrite and dolomite, lower San Andres Formation, Atlantic Oil Ryan No. 1, Lamb County, Texas. (b) Laminated anhydrite and dolomite, DOE-Gruy Grabbe No. 1, Swisher County, Texas. (c) Laminated anhydrite and dolomite with enterolithic folding, DOE-Gruy Grabbe No. 1, Swisher County, Texas. (d) Massive gypsum in outcrop, Cottle County, Texas. Photographs a through c by M. W. Presley.

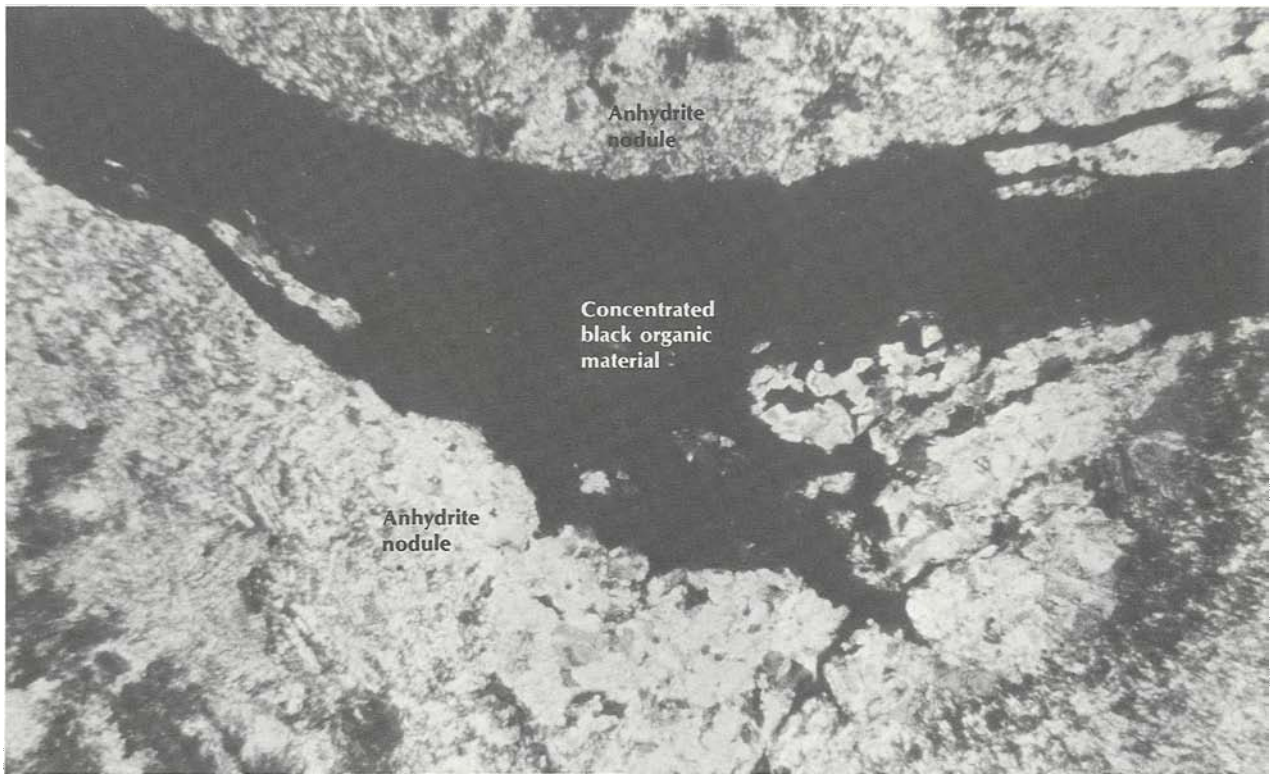

Figure 13. Concentrated organic matter adjacent to displacive nodules of anhydrite, Argonaut Energy (Crown Petroleum) Baumgart No. 1, Lamb County, Texas. Width of photograph equivalent to 2.66 mm of thin section.

sequences are generally nonporous but rich in organic material, which was probably derived from blue-green algae. The algal laminations are either flat or crinkly. Enterolithic folding of thinly bedded anhydrite (fig. 12c) is common and suggests early diagenetic volume changes.

Further subdivision of carbonate lithofacies was made by Bein and Land (1982) as follows: dolomudstone (fig. 8), pellet-oolite packstone-grainstone, filamentous (*Girvanella*-like) grainstone, sponge-spicule packstone, wispy-laminated crinoid packstone (fig. 10), and skeletal packstone and grainstone. Bein and Land contended that these facies were controlled by salinity of the surrounding water body.

LIMESTONE

Limestone is generally subjacent to the dolomitic shelf sequence of the lower San Andres in the Northern and Northwestern Shelves, although some limestone is interstratified with shelf dolomites (Bein and Land, 1982). Limestone is abundant east of the Abo Reef trend (fig. 6), which during San Andres time was a deeper part of the carbonate shelf (or the outer shelf; this writer does not consider it as part of the Northern Shelf). These nonporous, siliceous limestones are micritic and, except for siliceous sponge spicules and small foraminifers, are generally void of fossils (Todd, 1976).

ANHYDRITE

Anhydrite in San Andres shelf strata occurs as nodules, beds, cement, pore fillings, and replacement of preexisting carbonate (Kerr and Thomson, 1963). Nodules are displacive, having pushed aside surrounding mud (carbonate or siliciclastic matrix), and organic material is commonly concentrated around them (fig. 13). Pyrite typically rims the nodules. Internally the nodules consist of a complex multicrystalline fabric of felted, lathlike crystals (fig. 13). Nodules vary in size and density of packing. They may occur alone or be so densely packed (nodular mosaic) that they mimic bedded anhydrite (Kerr and Thomson, 1963).

Pore-filling anhydrite consists of coarse, clear crystals and is more common in carbonates deposited in high-energy environments (fig. 8); this anhydrite probably is analogous to the sparry calcite of Folk (1959). Pore-filling anhydrite commonly destroys porosity. Anhydrite also is present as a replacement mineral, particularly in burrows and shells (figs. 10, 11, and 14).

Thinly bedded (1 to 2 cm thick) anhydrite is normally intercalated with dolomite in stromatolitic sequences (fig. 12a, b, and c). Thick layers of massive laminated anhydrite are also present; in the eastern part of the Texas Panhandle they (Blaine Formation) crop out as low but rugged ridges of heavily

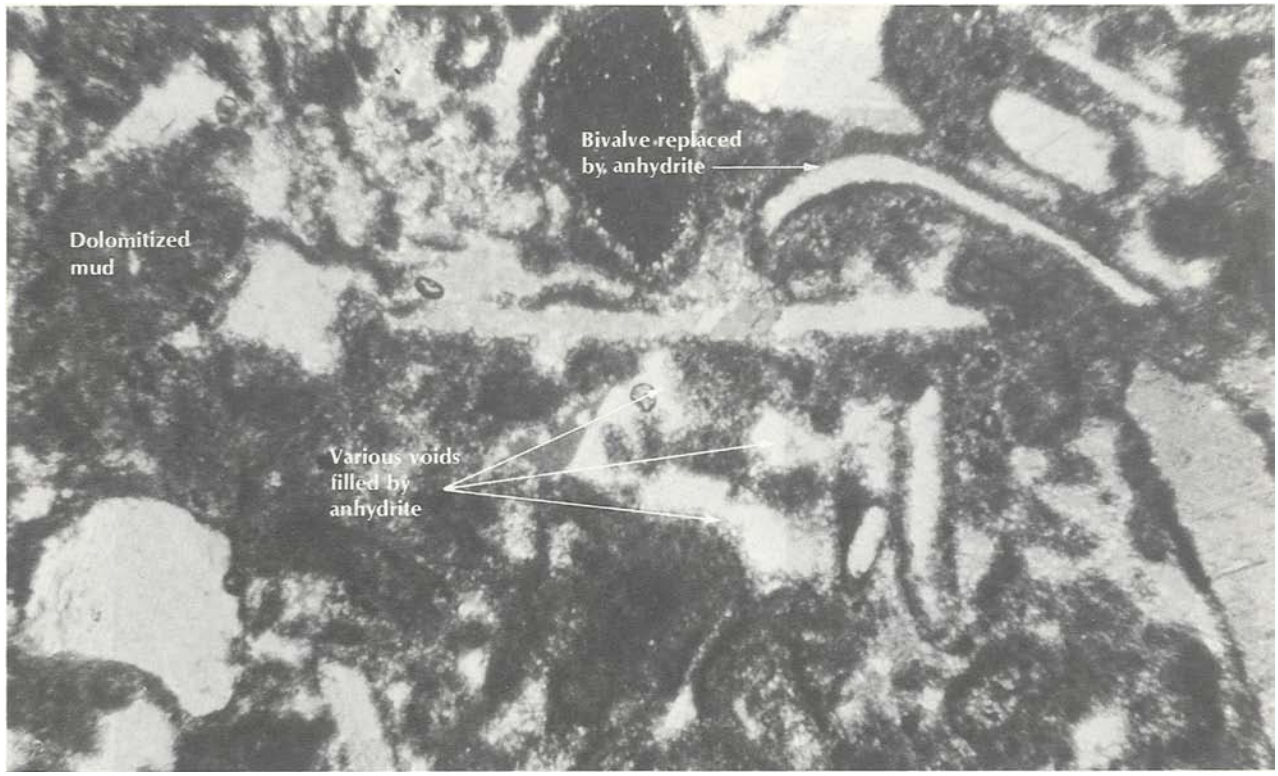

Figure 14. Replacement of skeletal debris and voids by secondary anhydrite, Argonaut Energy (Crown Petroleum) Baumgart No. 1, Lamb County, Texas. Width of photograph equivalent to 2.66 mm of thin section.

recrystallized gypsum (fig. 12d), which is quarried for plaster. Sequences containing bedded anhydrite are generally nonporous and indicative of supratidal brine-pan sabkha conditions. These form effective sealing beds over porous dolomites.

RED BEDS

Red beds (mostly siltstone) are abundant in the upper part of the San Andres Formation. They generally are structureless, void of fossils and organic material, and thinly bedded. Red beds are intercalated with either salt or anhydrite and may contain nodular anhydrite. In the overlying Grayburg Formation, red beds are thicker and are also associated with salt or anhydrite. Grayburg and San Andres red beds commonly are cemented with anhydrite or halite. Deposition of red beds continued, with interruption, until Late Triassic (Dockum Group).

SALT

Bedded salt is abundant in the Palo Duro Basin, but it thins and pinches out gradually to the south. Upper contacts tend to be erosional (fig. 15) and lower contacts gradational. Bedded salt may be massive and relatively dark (fig. 16), consisting of an interlocking network of subhedral to anhedral halite crystals. Vertically growing chevron crystals are also present, indicating subaqueous precipitation. Massive salt commonly is banded (fig. 16) and may contain varying amounts of siliciclastic mud, organic material, and anhydrite; potash is absent. Impurities typically compose less than 10 percent of the total rock (according to point-count analysis of nearly 400 ft of cycle 4 San Andres salt core from DOE-Gruy Federal Grabbe No. 1 and DOE-Gruy Federal White No. 1; fig. 17). Extremely coarse grained, clear halite is also present. Additionally, bedded chaotic mud salt is present, and it consists of displacive euhedral cubic crystals of halite in a matrix of mud (fig. 18). Chaotic mud salt is uncommon in lower San Andres strata, but it is the dominant salt facies in the underlying Glorieta and Clear Fork Formations and in the overlying upper San Andres and Seven Rivers Formations.

Halite also may occur as a pore-filling mineral, especially when bedded salt directly overlies porous dolomite. Ground water in the dolomite became saturated with sodium chloride and precipitated halite in the voids, rendering the dolomite nonporous.

For a more complete treatment of the various lithofacies in the study area, see Schneider (1943, 1957), Kerr and Thomson (1963), Chuber and Pusey (1967), Jacka and others (1969), Silver and Todd (1969), Barone (1976), Todd (1976), Perez de Mejia (1977), Zaaza (1978), Bein and Land (1982), and Handford and others (in press).

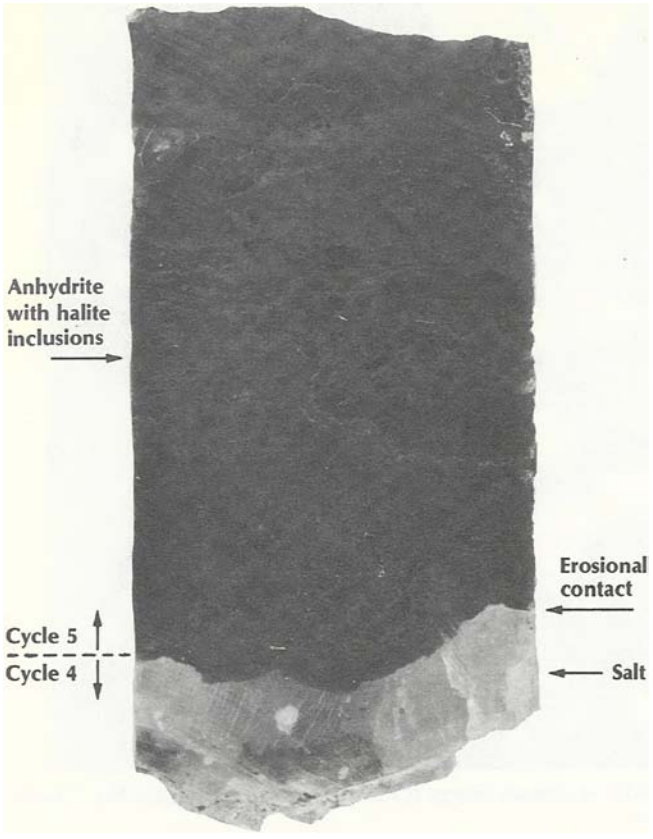

Figure 15. Erosional upper contact of San Andres cycle 4 salt, DOE-Gruy Grabbe No. 1.

Figure 16. Banded salt, DOE-Gruy Grabbe No. 1, Swisher County, Texas. Photograph by M. W. Presley.

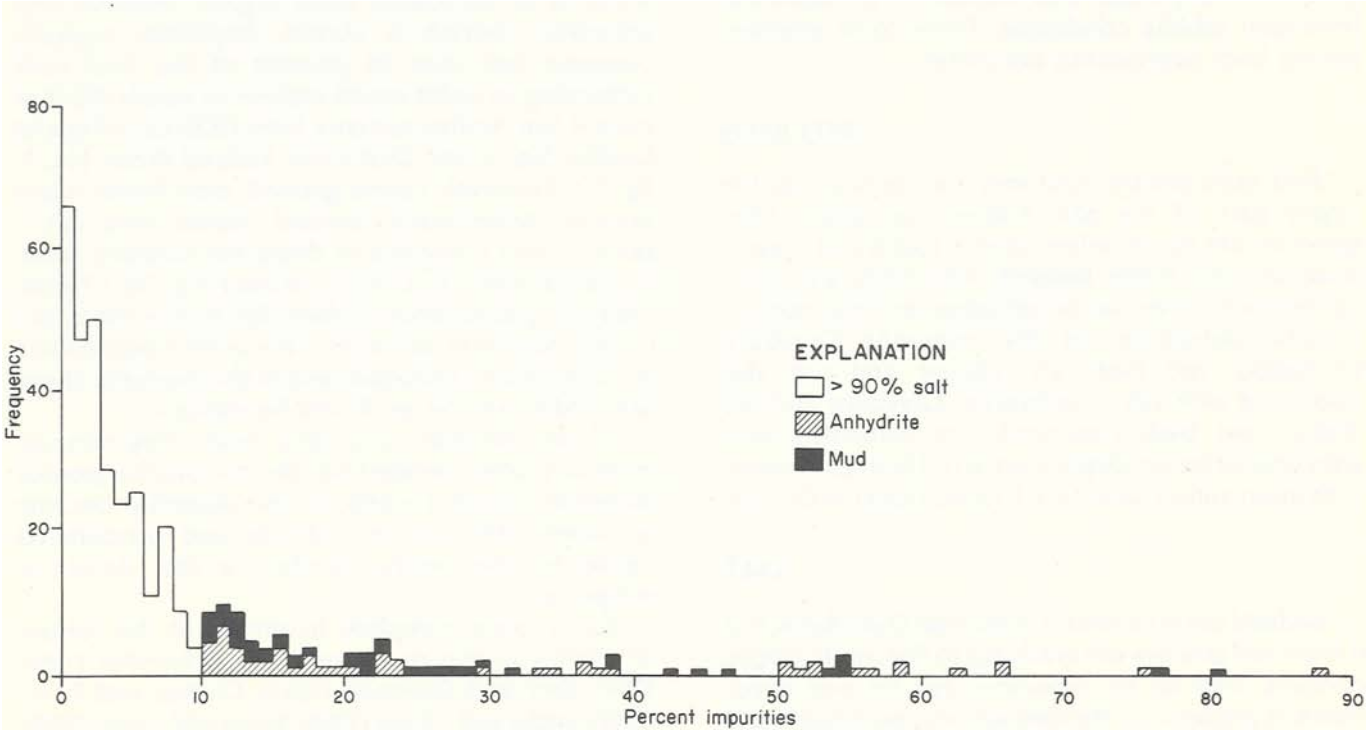

Figure 17. Histogram of impurities in San Andres cycle 4 salt, DOE-Gruy Grabbe No. 1 and DOE-Gruy White No. 1, Randall and Swisher Counties, Texas.

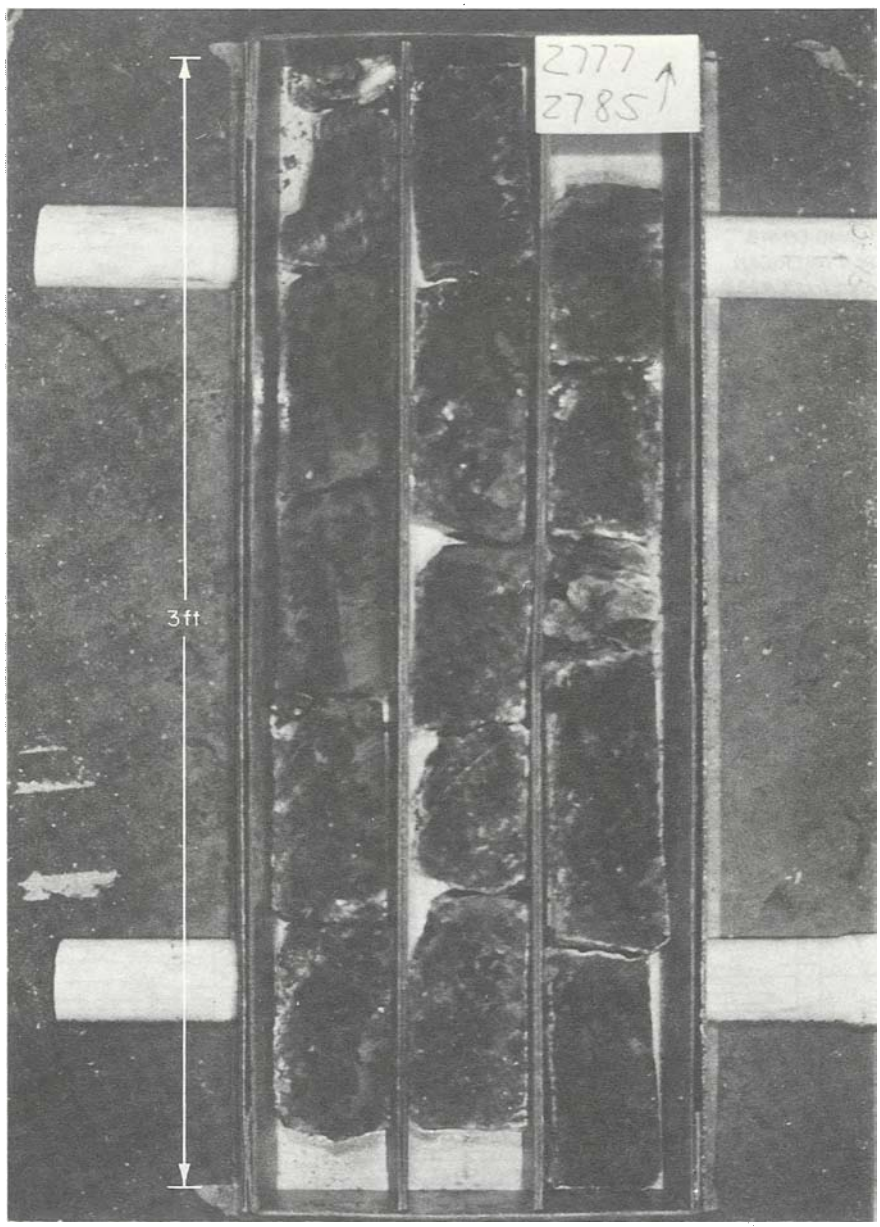

Figure 18. Chaotic mud salt, upper Clear Fork Formation, DOE-Gruy White No. 1, Randall County, Texas.

DEPOSITIONAL ENVIRONMENTS

To understand the depositional environments operative in the study area during San Andres time, it is important to understand that eustatic changes in sea level were common during the Permian. Evidence for this has been presented by Newell and others (1953, p.130), Thomas (1968), Dunham (1969a, b), Jacka and others (1969), Kendall (1969), Silver and Todd (1969), Hills (1972), Todd (1976), and Mazzullo (1982). Such features as caliche pisolites, vadose silt, and sandstone dikes were cited as evidence for periodic exposure of the shelf and shelf-margin regions; other evidence will be presented in this report. Todd (1976) further recognized that carbonate depositional facies were controlled by structure, which in turn means that structurally high areas were at least slightly positive during deposition. This is confirmed by stratigraphic thinning over structural highs (figs. 19 to 26).

Depositional environments operative during San Andres time are illustrated schematically on figure 4. During times of moderately low sea level, the Northern (inner) Shelf was separated from the deeper outer carbonate shelf to the east by a series of low-lying shoals displaying steep basinward flanks and gentle landward slopes (according to structure maps). The shoals occupied the position of the older Abo Reef shelf margin, whereas the outer shelf was simply

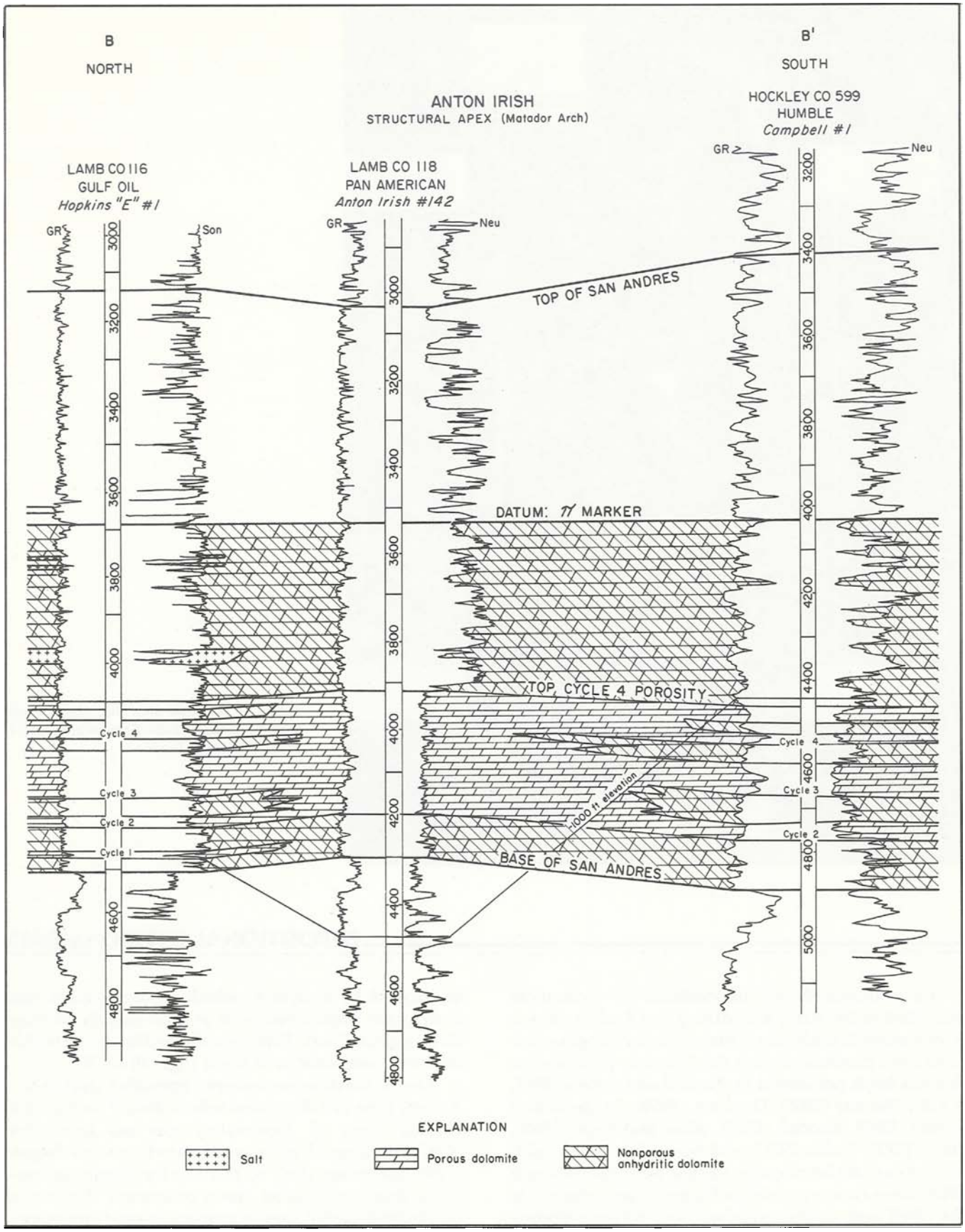

Figure 19. North-south cross section of San Andres Formation across the Anton Irish field, Texas. Line of section B-B' illustrated in figure 3.

a shallower version of the Midland Basin, where basinal shales were previously deposited in deeper water during Leonardian and Wolfcampian time. North of the shallow, sometimes saline inner shelf was an extensive sabkha and evaporite basin complex. The seaward edge of this complex was occupied by supratidal to intertidal, stromatolitic flats. When sea-level conditions were stable, these algal flats prograded seaward (southward), reducing the area of the inner shelf. An extensive brine pan or salt basin occupied the area north (landward) of the algal flats. Bein and Land (1982) concluded, on the basis of bromide geochemistry and lack of potash, that the lower San Andres salts were deposited directly by marine waters and were not leached from the surrounding terrain. Therefore, it is probable that the so-called brine pan was at times a relatively permanent body of water that was connected by tidal channels or inlets to the waters of the inner shelf during early San Andres time. Broad terrigenous mud flats, which prograded to the east, south, and west, encroached upon the salt basin. The source of these red beds probably was very distant, and transport may have been in part eolian. Occasionally, fine-grained siliciclastic sediment was transported into the sabkha and shelf environments, resulting in the deposition of the time-stratigraphic markers previously discussed.

CYCLICITY OF DEPOSITIONAL ENVIRONMENTS

Permian shelf deposits of West Texas have long been recognized as highly cyclic (Kerr and Thomson, 1963; Chuber and Pusey, 1967; Jacka and others, 1969; Silver and Todd, 1969; Perez de Mejia, 1977; Presley, 1979; Mazzullo, 1982; Handford and others, in press). These cycles tend to be upward shoaling. Large, eustatic sea-level changes of possible glacial origin are presumed to be the cause of the cyclicity. The cyclicity combined with a depositional surface of relatively low relief results in considerable vertical facies variability (through time) and great lateral facies continuity. Time-stratigraphic markers less than 10 ft thick can be traced for several hundred miles (for example, the π marker).

Slight changes in sea level obviously would have caused considerable change in the distribution of depositional environments because of the low relief of the depositional surface. Silver and Todd (1969), Hills (1972), and Todd (1976) inferred that large eustatic changes occurred. It follows, therefore, that during periods of extremely low sea level, the entire shelf would have been exposed, except possibly for the outer shelf; during periods of extremely high sea level, the entire shelf and sabkha would have been flooded by relatively normal marine water. The premise of large eustatic changes in sea level is critical to explain the depositional and diagenetic model presented for the San Andres. However, considerable disagreement exists about whether these sea-level changes actually occurred. For example, Bein and Land (1982) maintain that the facies tract can be explained by merely changing the salinity of the water body without significantly changing its size or depth. Additional evidence for sea-level changes will be presented.

Periods of high sea level are easily recognized in lower San Andres strata. Transgressive shelf dolomites (such as the cycle 4 dolomite, fig. 5) extend into the northernmost Texas Panhandle (Moore and Dallam Counties). Presley (1979) recognized five such transgressive-regressive cycles in the lower San Andres of the Palo Duro Basin (figs. 5 and 7). Barone (1976) noted four such cycles in the Northwestern Shelf. Higher order cycles were superimposed on the main depositional cycles (fig. 27). Such upward-shoaling cycles are also common in older Permian strata, as in the Wichita shelf carbonate section (Mazzullo, 1982). A cycle commonly began with deposition of a thin basal shale (fig. 7), which reflected a sudden increase in water depth, and was followed by deposition of carbonate mud containing progressively less siliciclastic sediment, as evidenced from gamma-ray logs (fig. 7). During such times, sedimentation was probably uniform throughout the entire shelf, including where surface relief existed, as reflected by the widespread distribution of carbonate facies even in the Palo Duro Basin.

As deposition progressed, water depth gradually decreased, causing a general coarsening of the sediments. Whether this was due to eustatic fall in sea level or to aggradation of the shelf by sediment is unknown; probably both were operative. At such times the surface relief strongly affected sedimentation. North of the Matador Arch, subtidal deposition gave way to intertidal and supratidal algal flats, as reflected by thinly bedded anhydrite and dolomite facies (fig. 7). This bathymetrically high belt (Handford and others, in press) separated open-marine environments of the Midland Basin to the south from the Palo Duro Basin, where a hypersaline basin or brine-pan environment developed. Tidal channels probably connected this salt basin to the shelf. Rare but heavy rainfalls may have occasionally interrupted precipitation of halite by reducing salinity and causing brief periods of dissolution and recrystallization. Increased subsidence in the central Palo Duro Basin resulted in a thickening (aggradation) of the cyclic depositional facies and permitted great thicknesses (a few hundred feet, as in cycle 4) of massive salt to accumulate. Thick interbeds of anhydrite within the cycle 4 salt exist in the southern (seaward) part of the Palo Duro Basin (Lamb, Hale, and Bailey Counties). These interbeds reflect the higher order

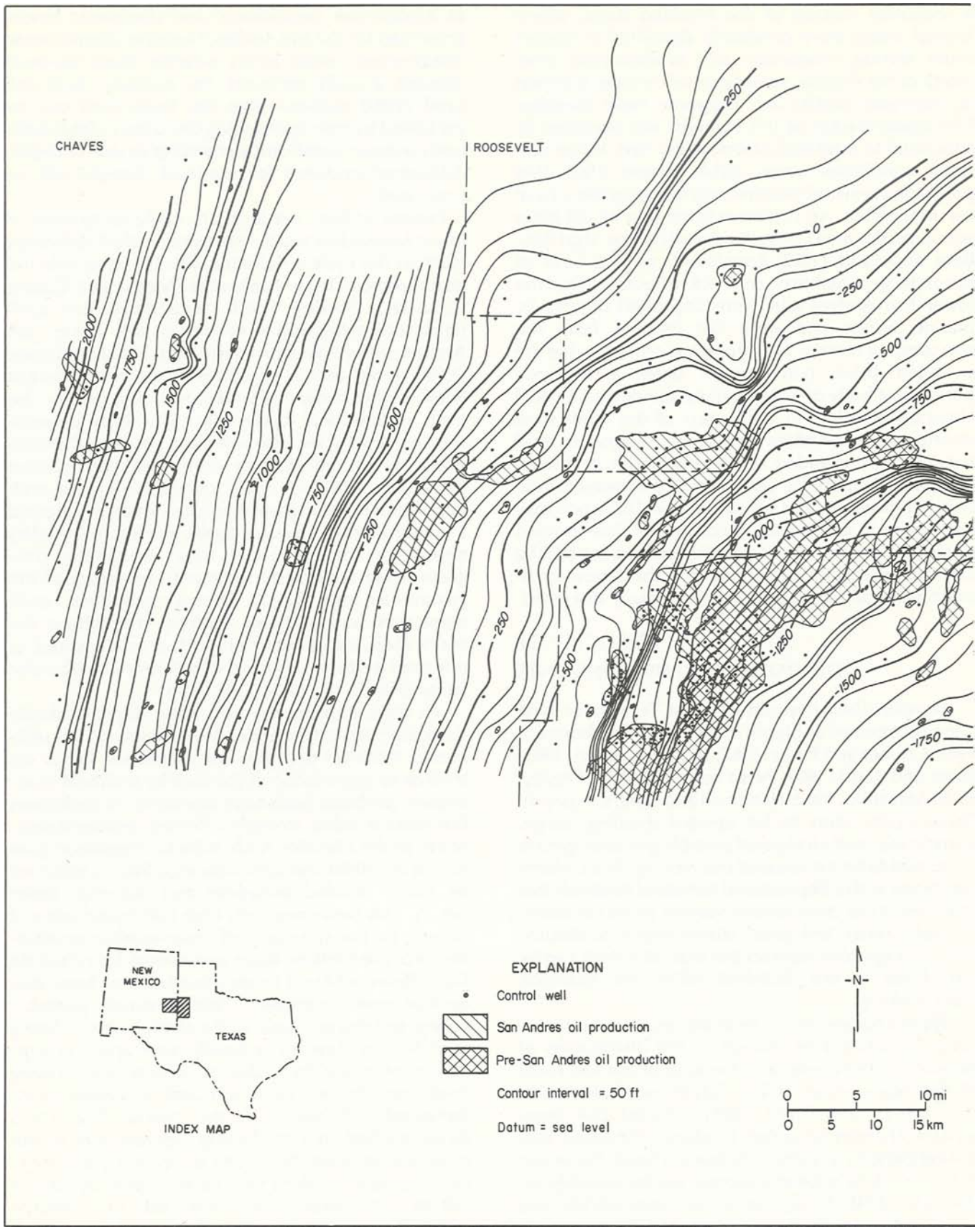

Figure 20. Structure map, base of San Andres Formation.

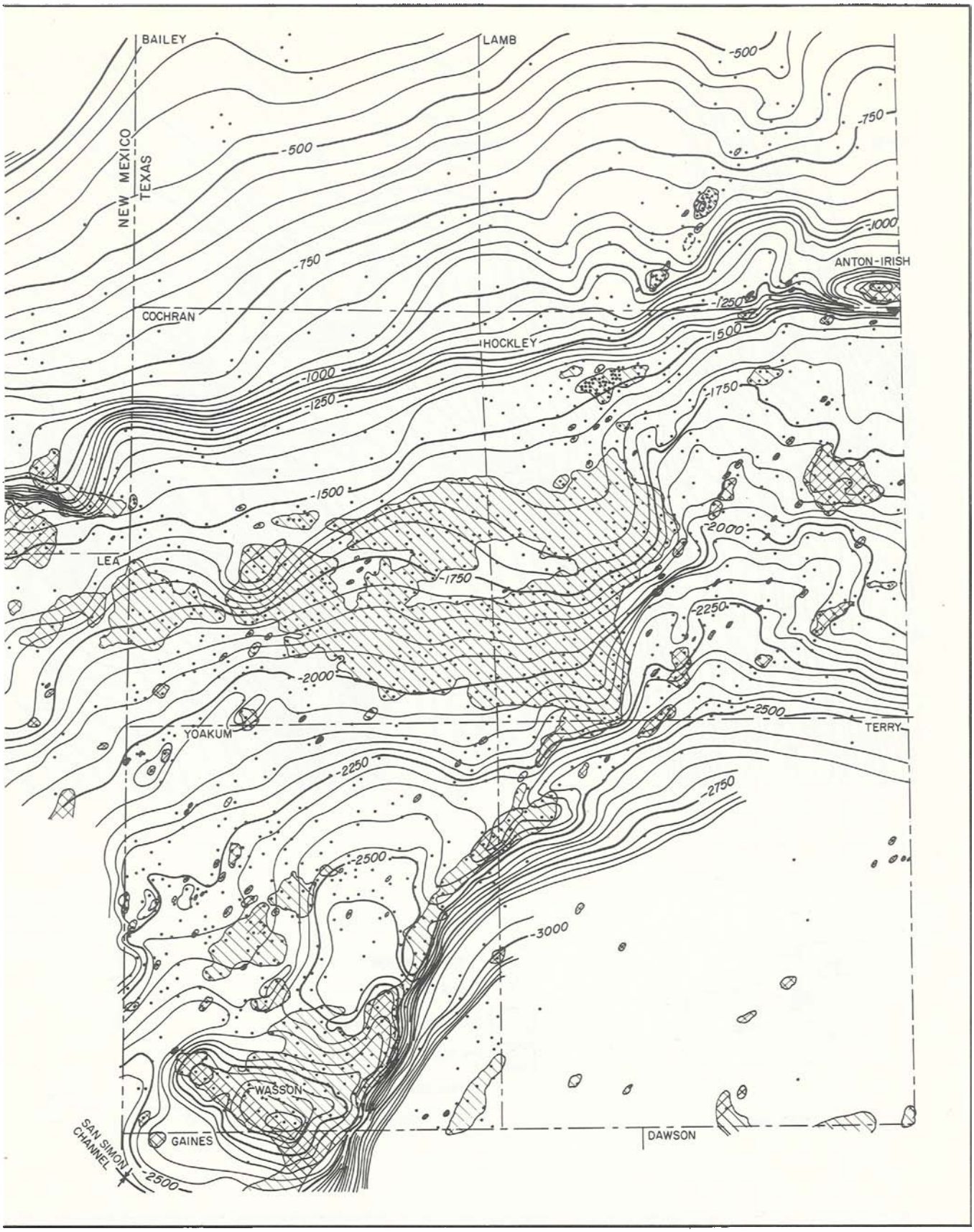

Figure 20 ***(continued)***.

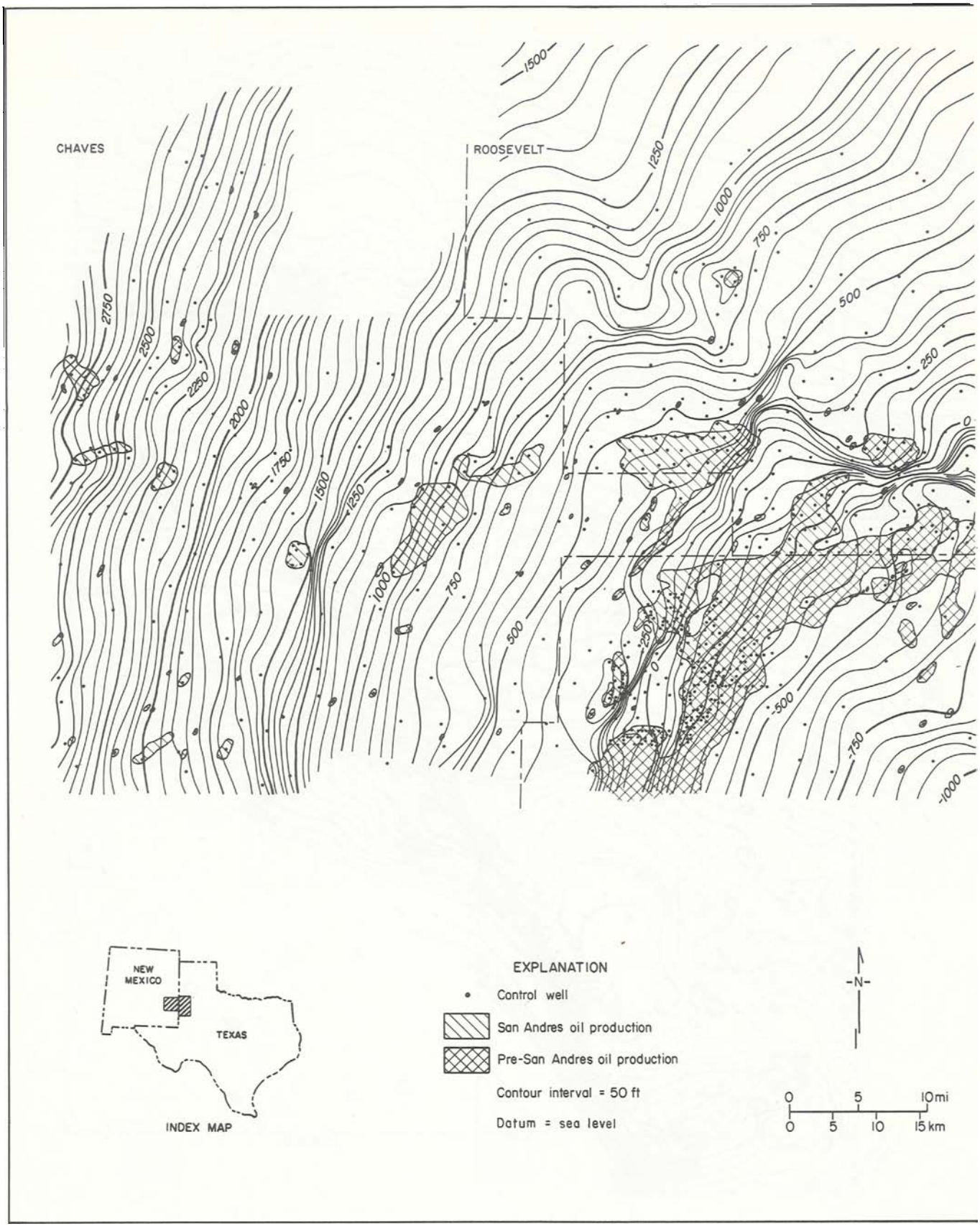

Figure 21. Structure map of π marker.

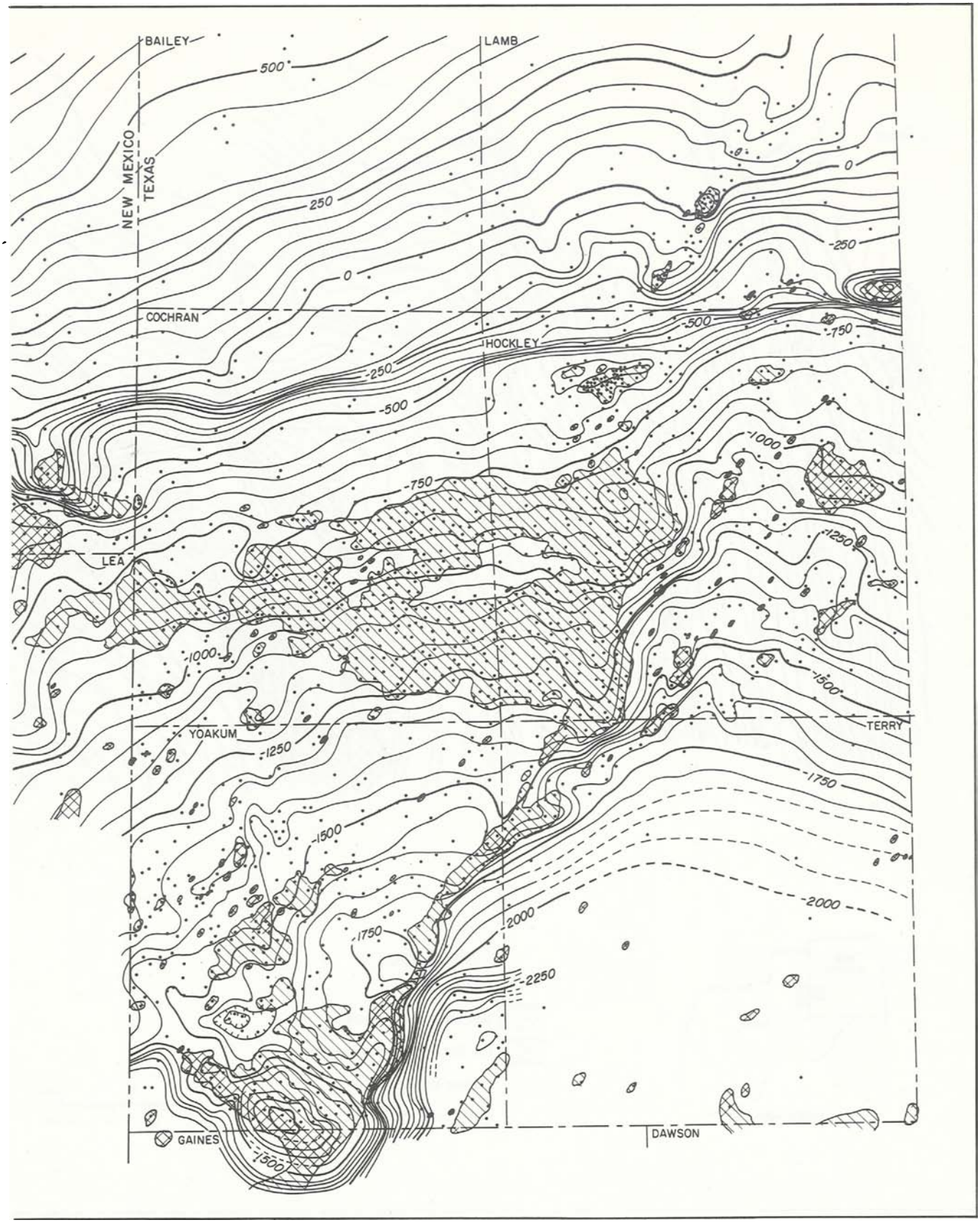

Figure 21 ***(continued)***.

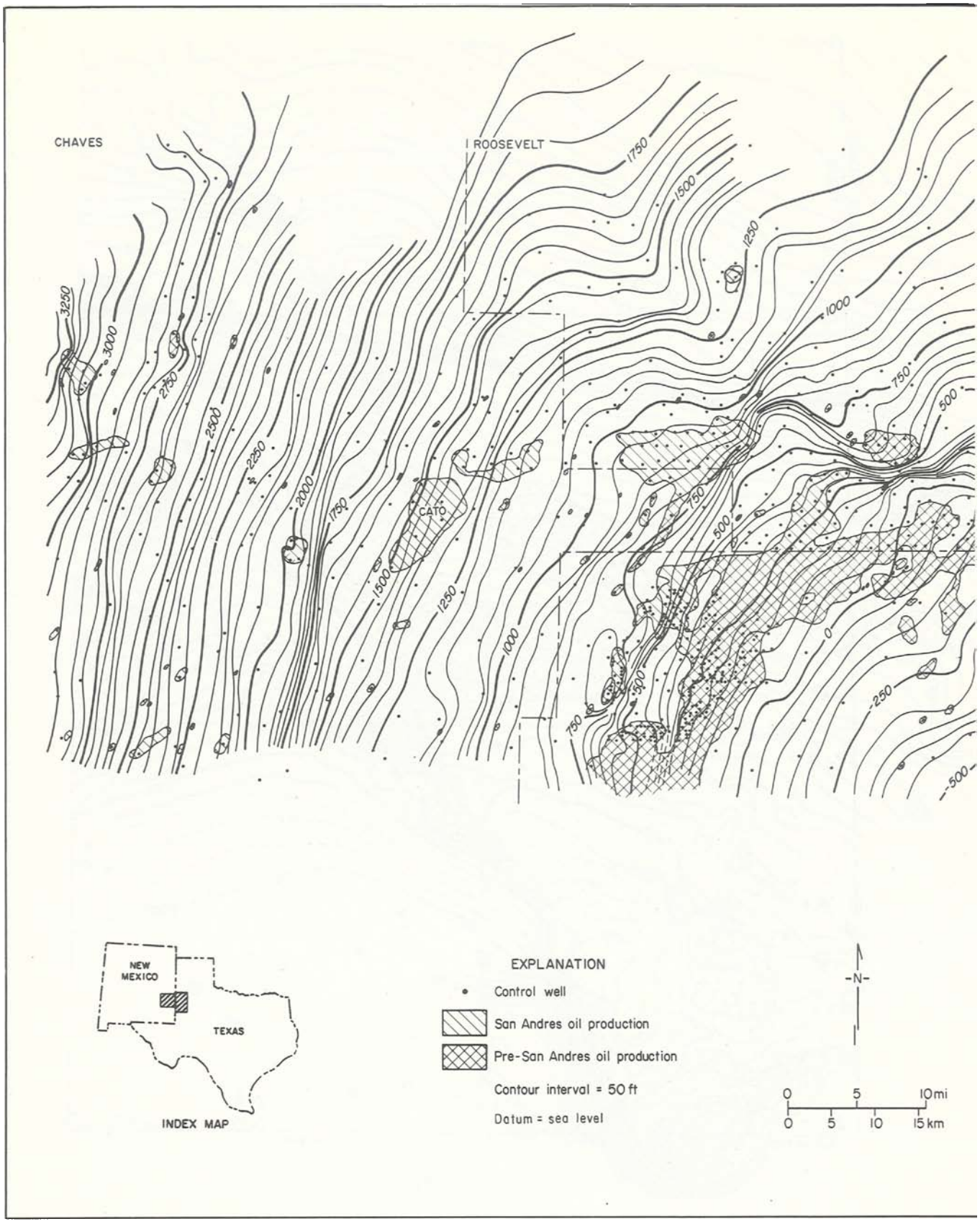

Figure 22. Structure map, top of San Andres Formation. Different marker bed is used for the top of the San Andres Formation in Yoakum and Terry Counties.

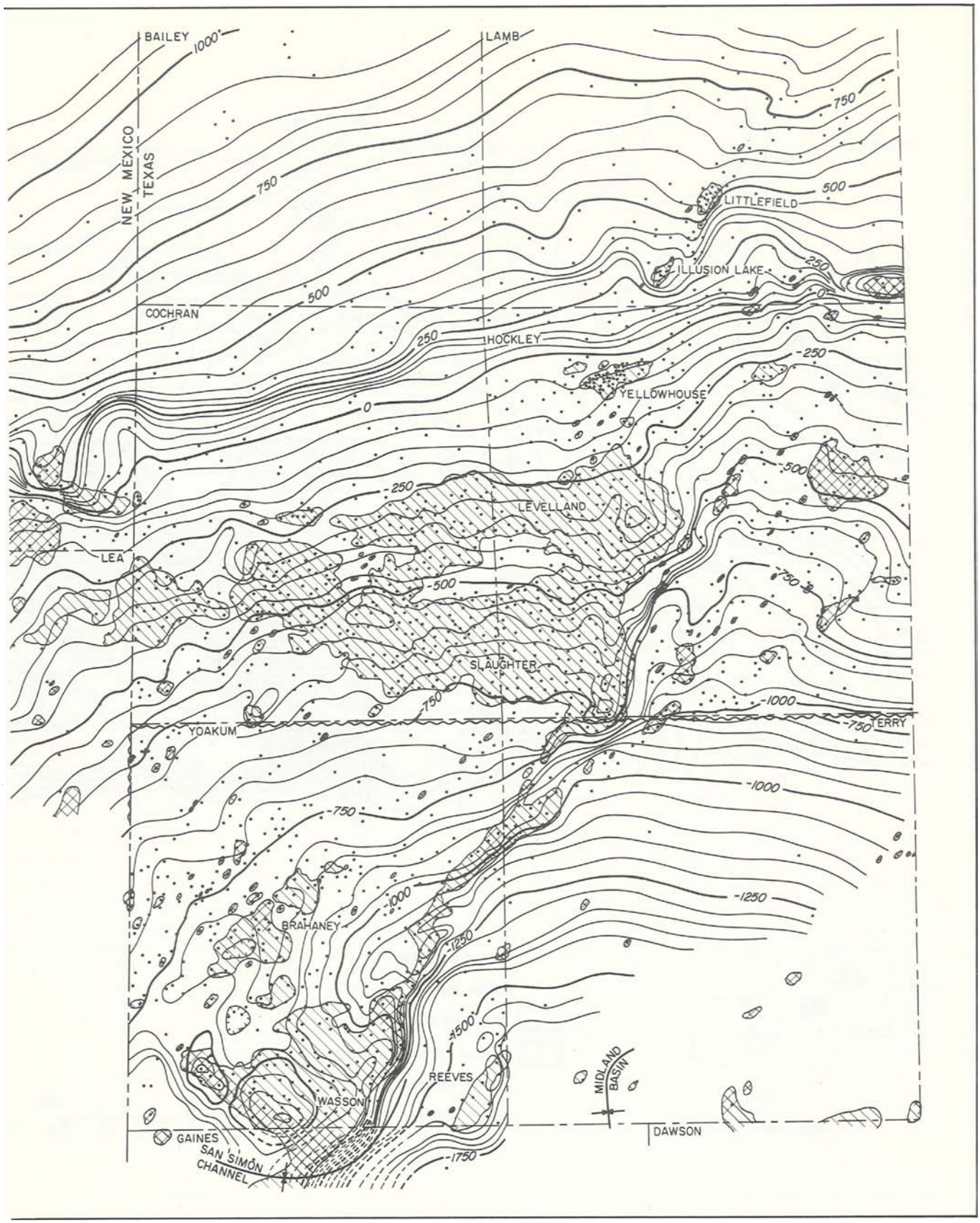

Figure 22 ***(continued)***.

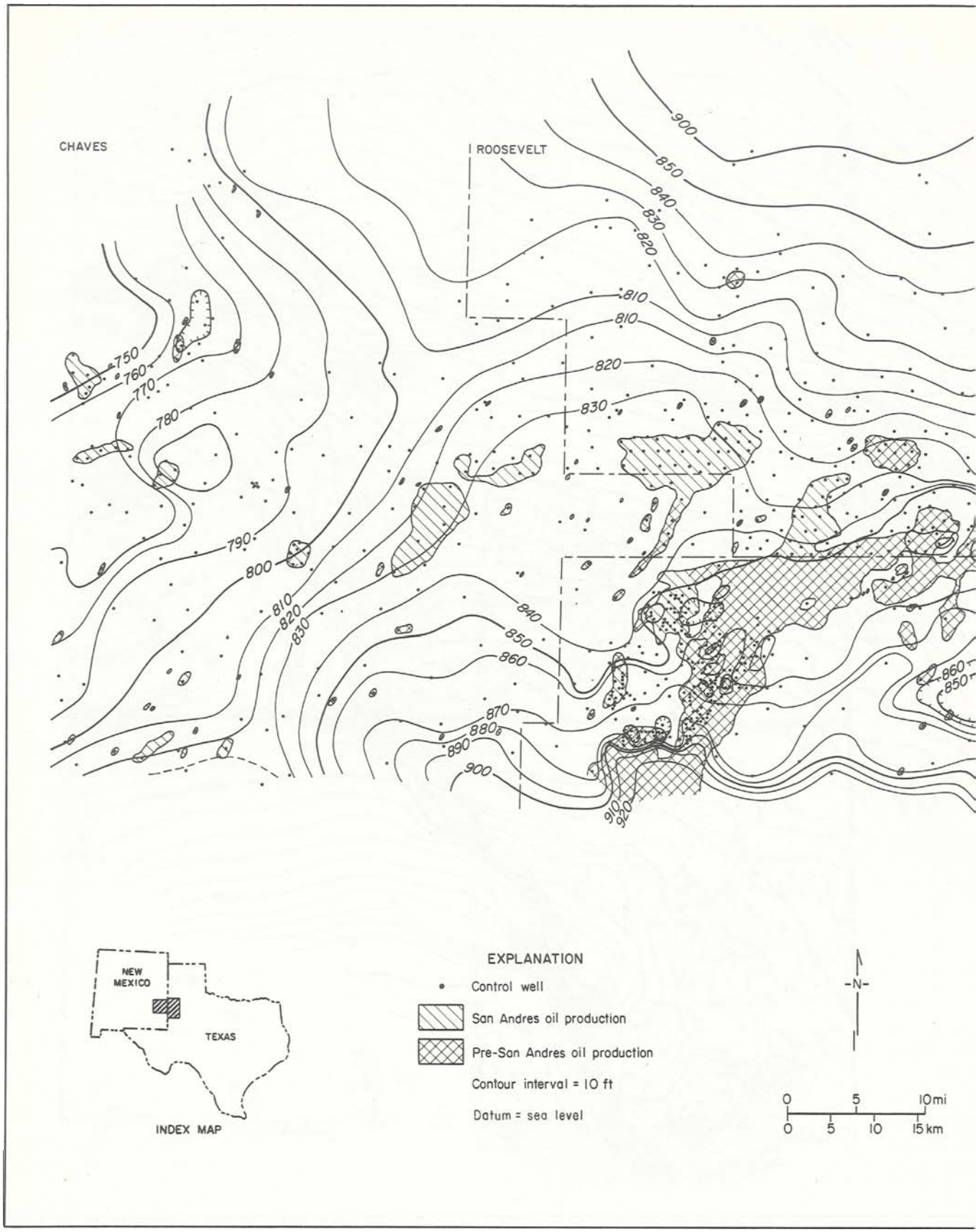

Figure 23. Isopach map, lower San Andres Formation. Hachured contours represent stratigraphic thins, not structural lows.

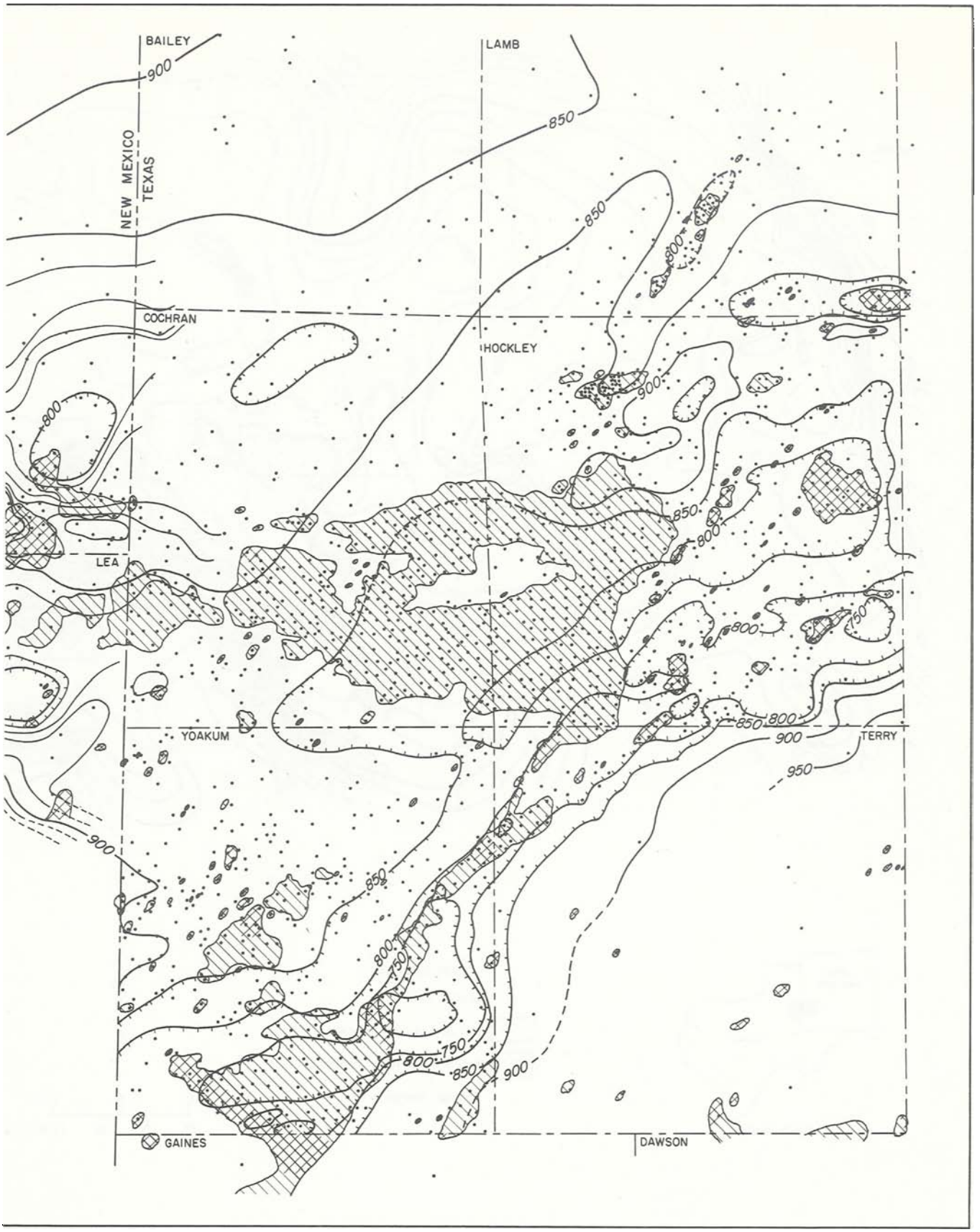

Figure 23 ***(continued)***.

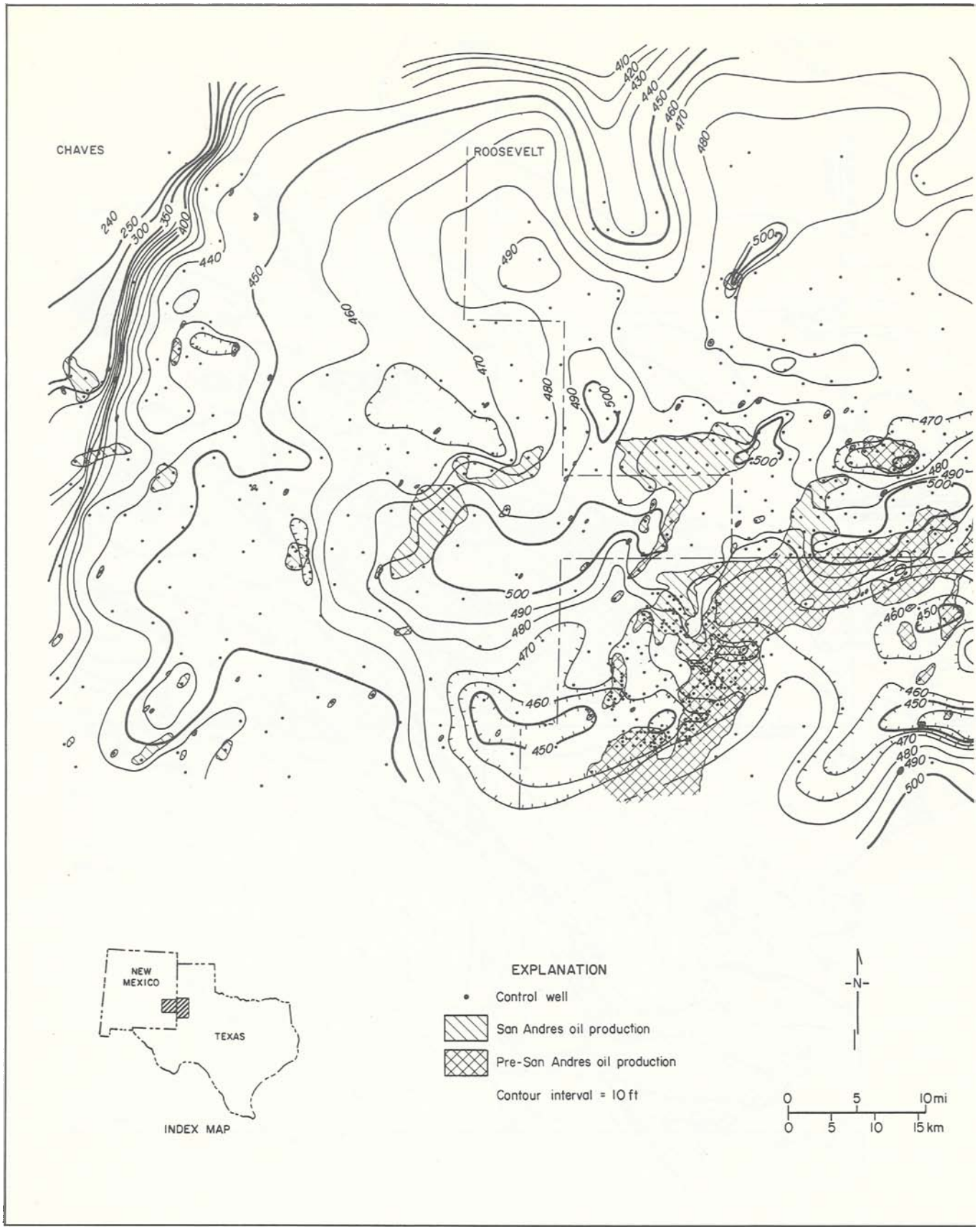

Figure 24. Isopach map, upper San Andres Formation. Hachured contours represent stratigraphic thins, not structural lows.

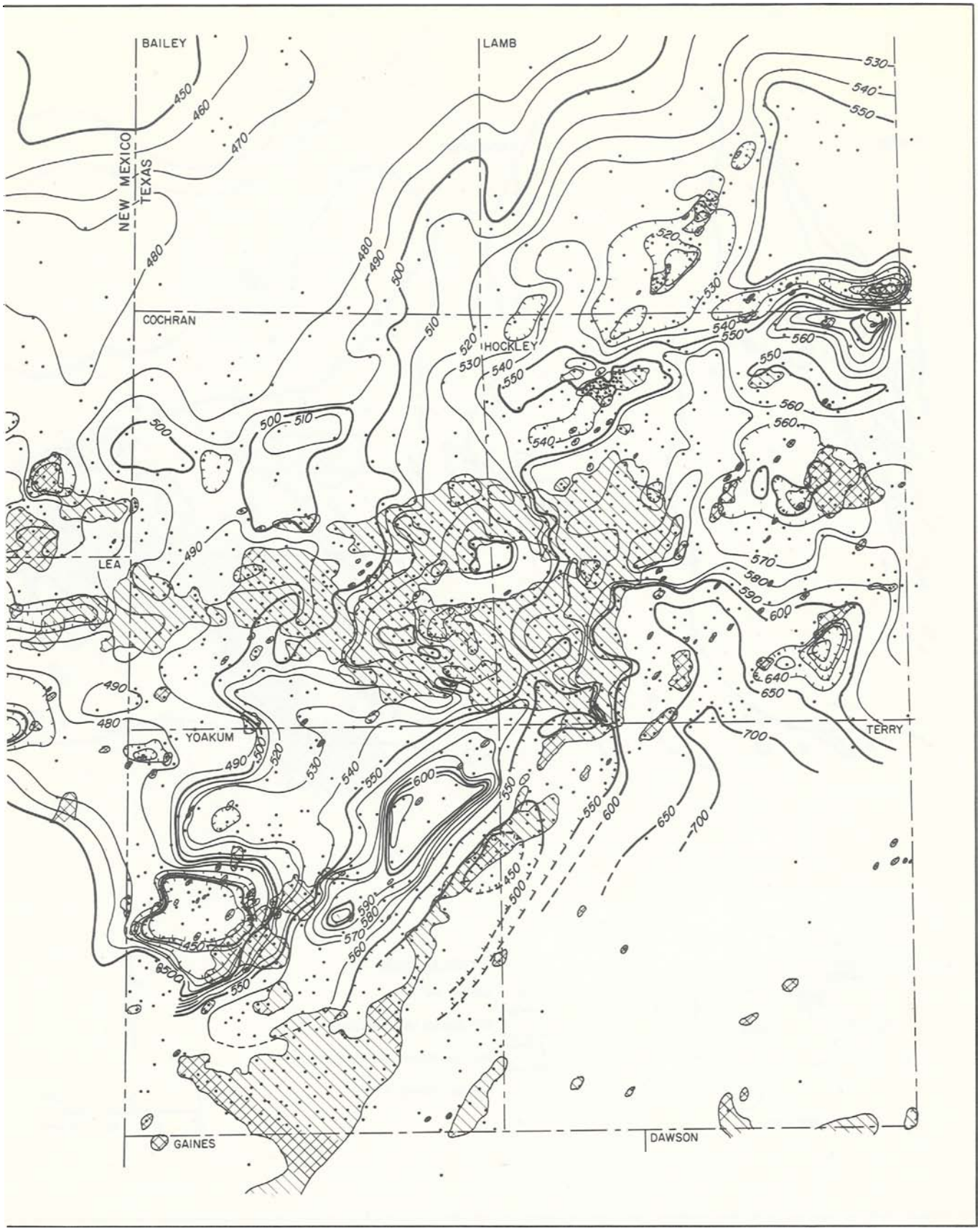

Figure 24 ***(continued)***.

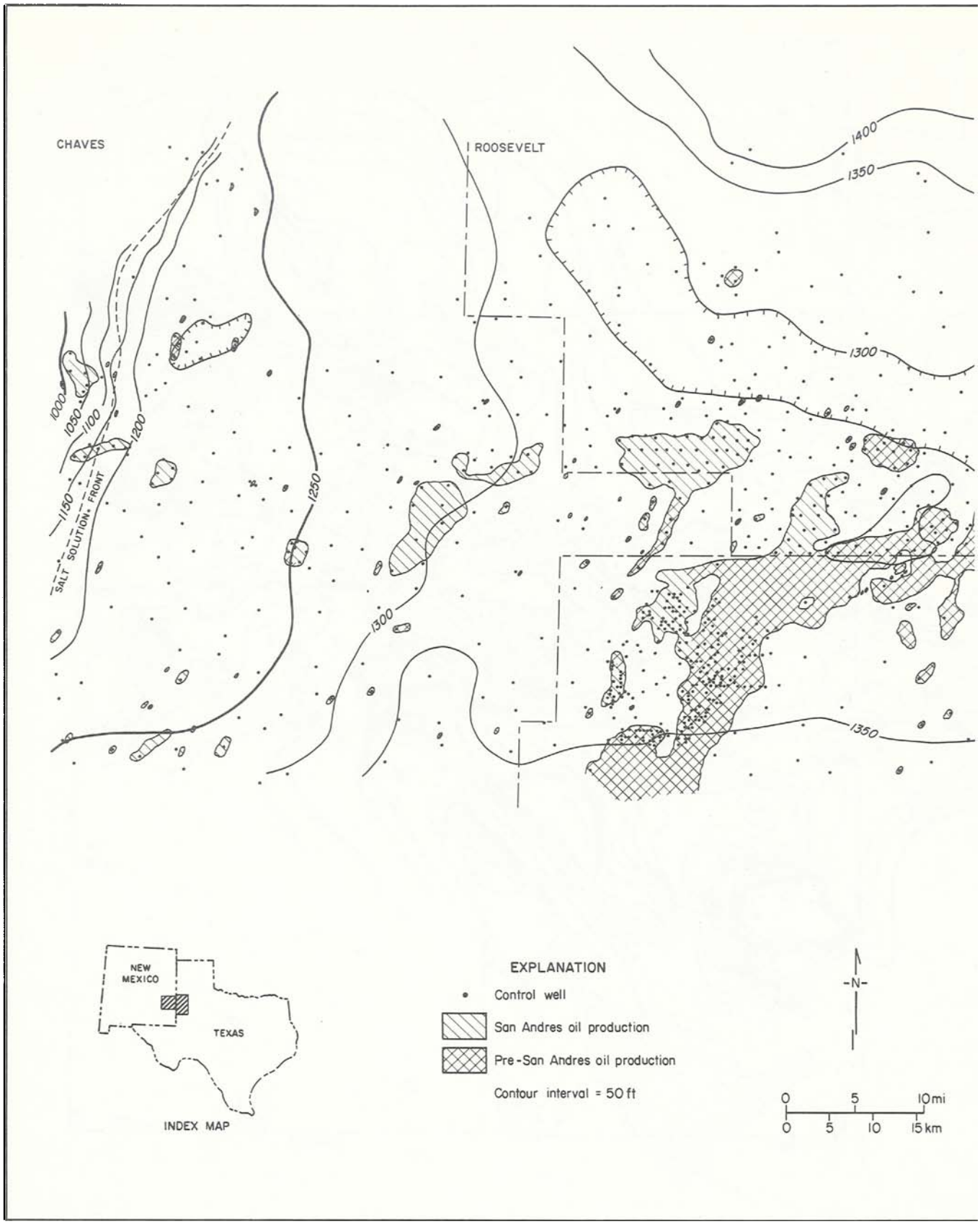

Figure 25. Isopach map, San Andres Formation. Hachured contours represent stratigraphic thins, not structural lows. Different marker bed is used for the top of the San Andres Formation in Yoakum and Terry Counties.

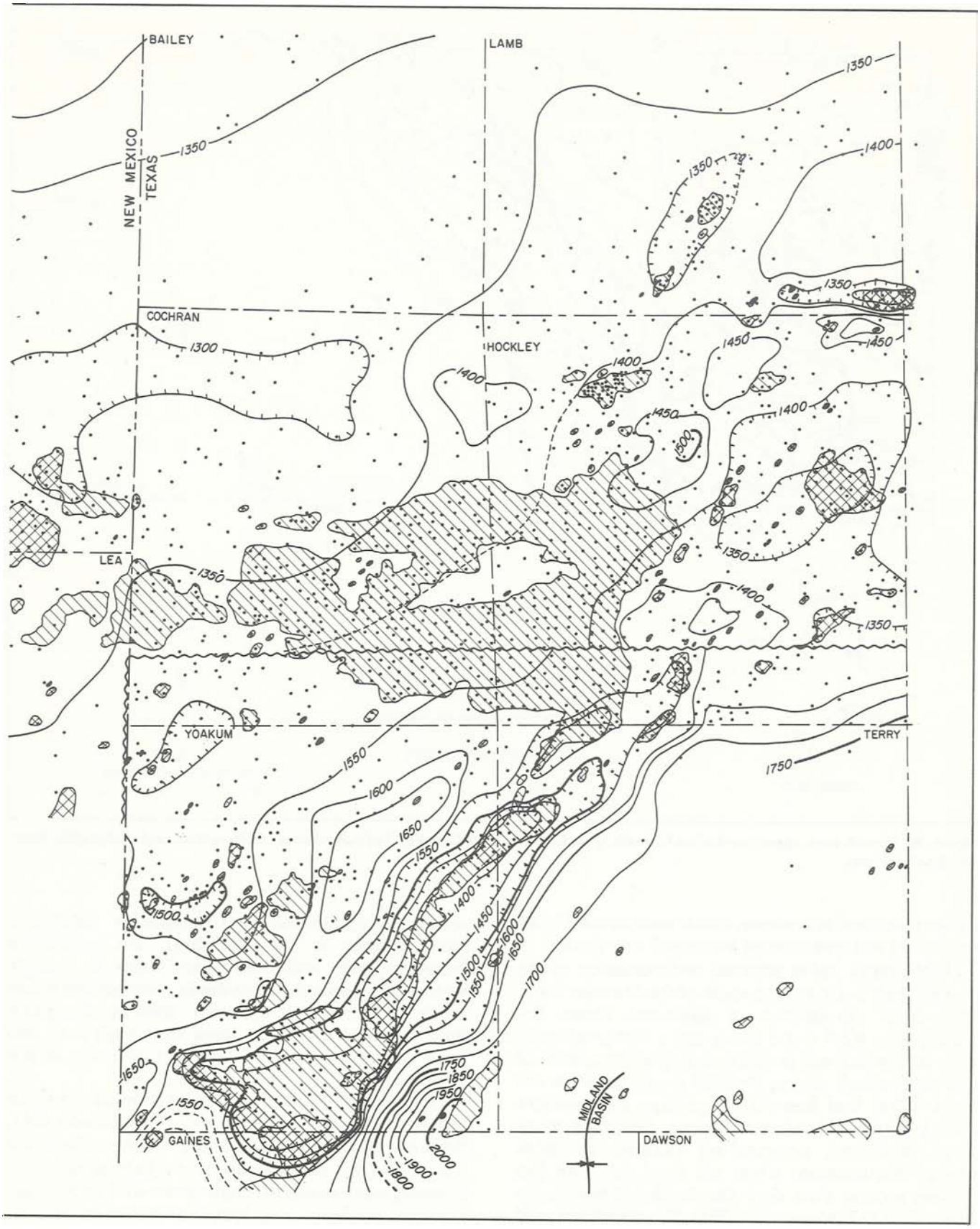

Figure 25 ***(continued).***

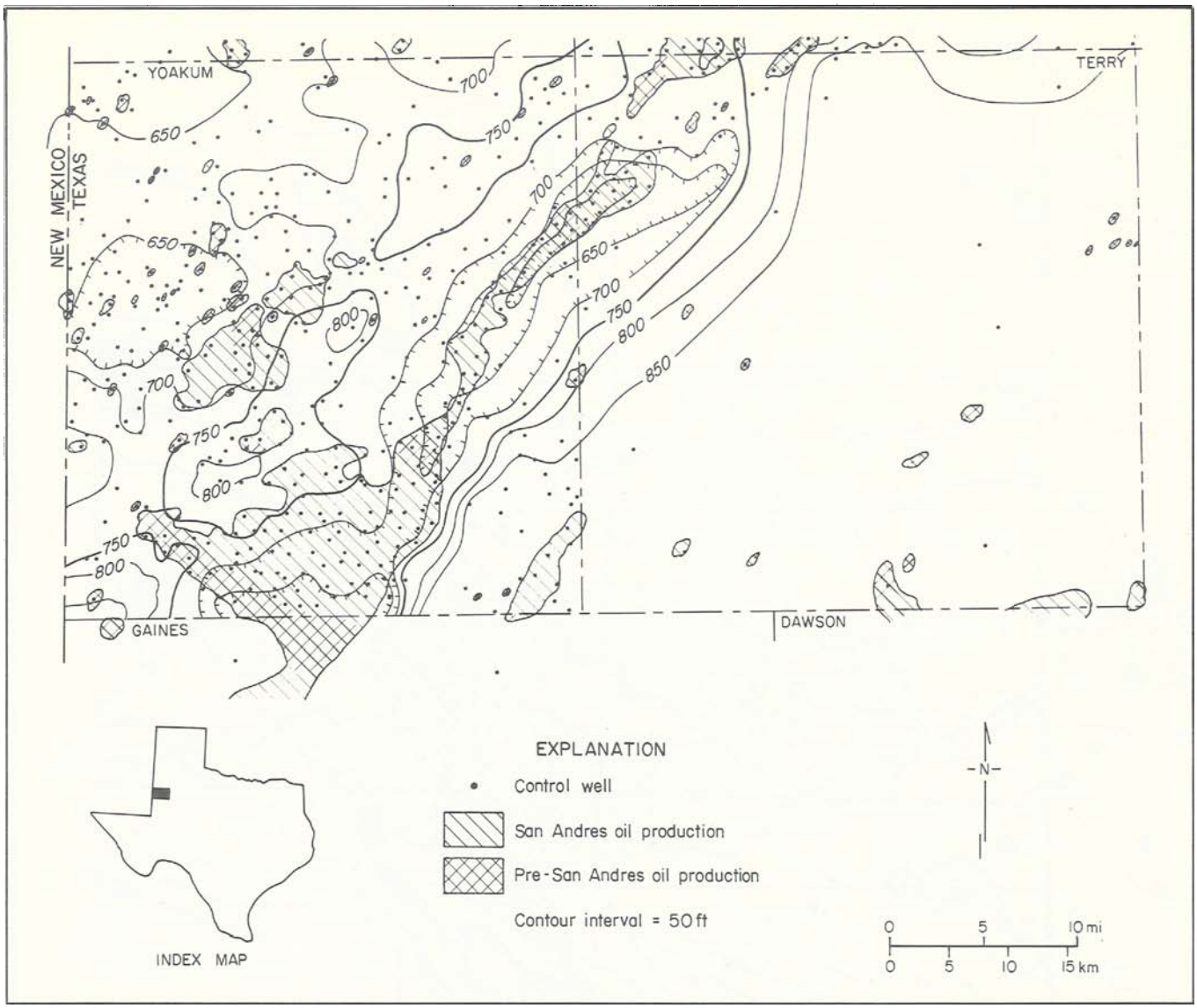

Figure 26. Isopach map, upper San Andres Formation, Yoakum and Terry Counties, Texas. Hachured contours represent stratigraphic thins, not structural lows.

cycles discussed previously, which were caused by an oscillating sea level during an overall low stand.

Bathymetric relief affected sedimentation in the marine shelf environment south of the Matador Arch. Differential compaction of sediments above the buried Abo Reef trend produced a bathymetrically high belt, which was probably occupied by a series of islands or shoals during times of moderately low sea level. What had been a low-energy environment during high sea-level stands when carbonate muds were deposited, progressively became a higher energy environment when sea level fell. The San Andres section thins over the shoals relative to the inner shelf to the west (figs. 23 to 26), an indication of longer periods of emergence along the shoals. This bathymetric relief also disrupted the deposition of siliciclastic sediments (compare figs. 28 and 29). As a result, correlation of time-stratigraphic markers is more difficult in the shoal area, and correlation between inner and outer shelf areas is virtually impossible. Apparently the shoals were barriers to the influx of siliciclastic sediment, thereby disrupting their continuity. Erosion along the shoals may also have contributed to the lack of continuity of the marker beds.

Schneider (1943, 1957) observed a similar change in sedimentation during his study of the Wasson field, the most productive field of the Northern Shelf. He found that the eastern part of the field (shoal area) contains massive reeflike carbonates with good intergranular porosity; also lentils of dolomite exist as foreset beds, reflecting the higher energy environment. In contrast, the western part of the field (inner shelf) contains finely crystalline carbonate facies

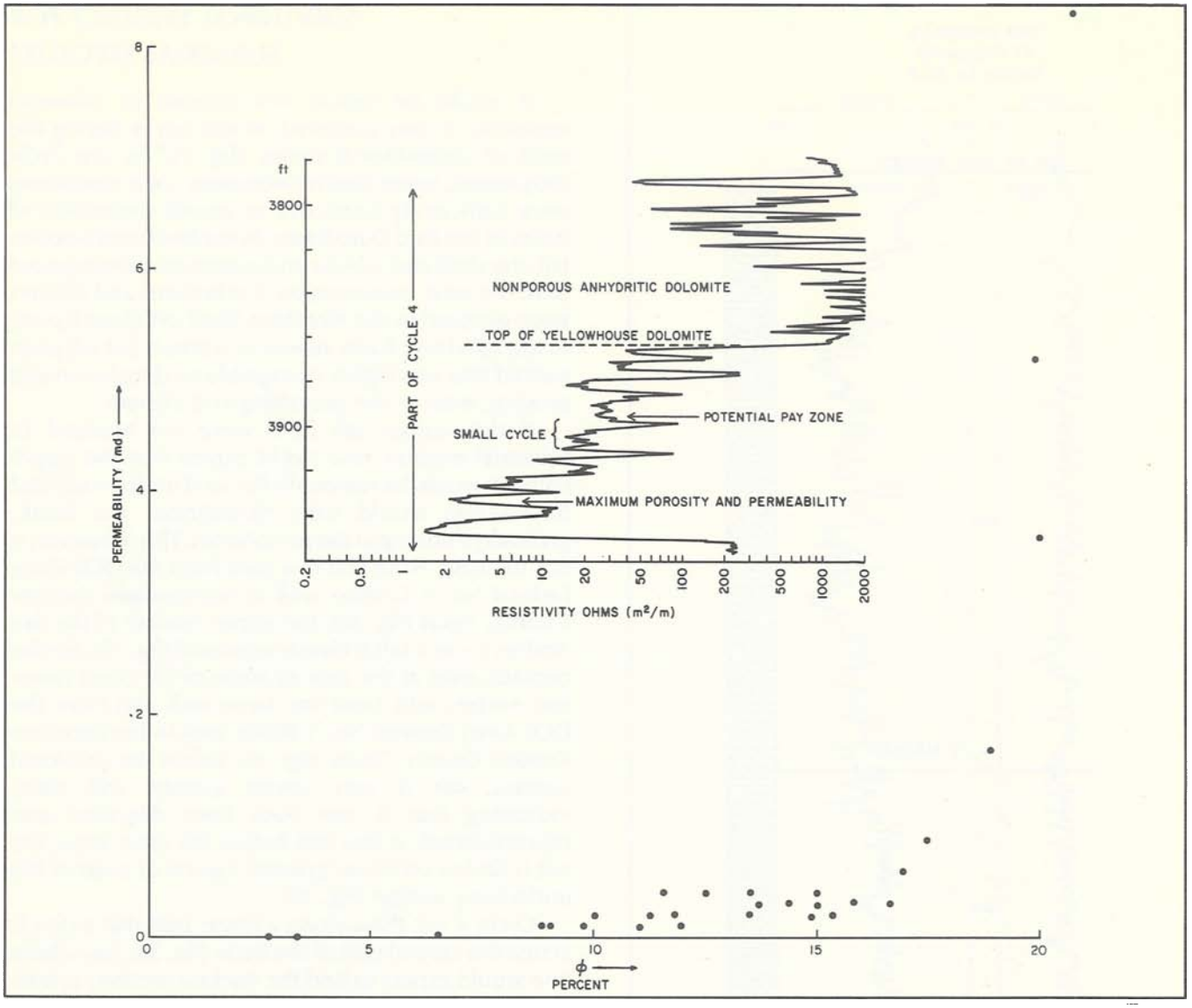

Figure 27. Plot of porosity versus permeability in the Yellowhouse dolomite; resistivity log of same interval is included, Littlefield Northeast field, Lamb County, Texas.

intercalated with more bedded siliciclastic and anhydrite strata; hence, it has lower porosity.

Chuber and Pusey (1967) defined distinctly different back-shelf and shelf-edge depositional cycles; their use of "shelf edge" is equivalent to the use of "shoals" in this report. Both cycles began with the deposition of a thin basal shale, which grades upward into dark mudstone and then into skeletal wackestones. In back-shelf areas, the wackestones grade upward into weathered stromatolites containing bird's-eye structures. Desiccation features are also present, indicating subaerial exposure near the end of a cycle. In shelf-edge areas, mud content decreases progressively upward; the cycle ended with deposition of grainstone followed by subaerial exposure. The upper and lower contacts of these depositional cycles appear to be erosional. Perez de Mejia (1977) and Amos Bein (personal communication, 1981) also have studied the inner-shelf environment west of the shoals in Yoakum County; they report the absence of packstones and grainstones, which, however, Chuber and Pusey (1967) observed along the shoal belt.

As sea level continued to fall, more inner shelf was exposed, but parts of the inner shelf may have been too deep for exposure during earliest San Andres time. Sea-level fall resulted in exposure of a broad landscape of unlithified, gypsiferous carbonate sediments south of the Matador Arch and an equally vast salt plain north of the arch. Some disagreement exists about whether this exposure occurred; therefore, additional evidence is presented in the following section.

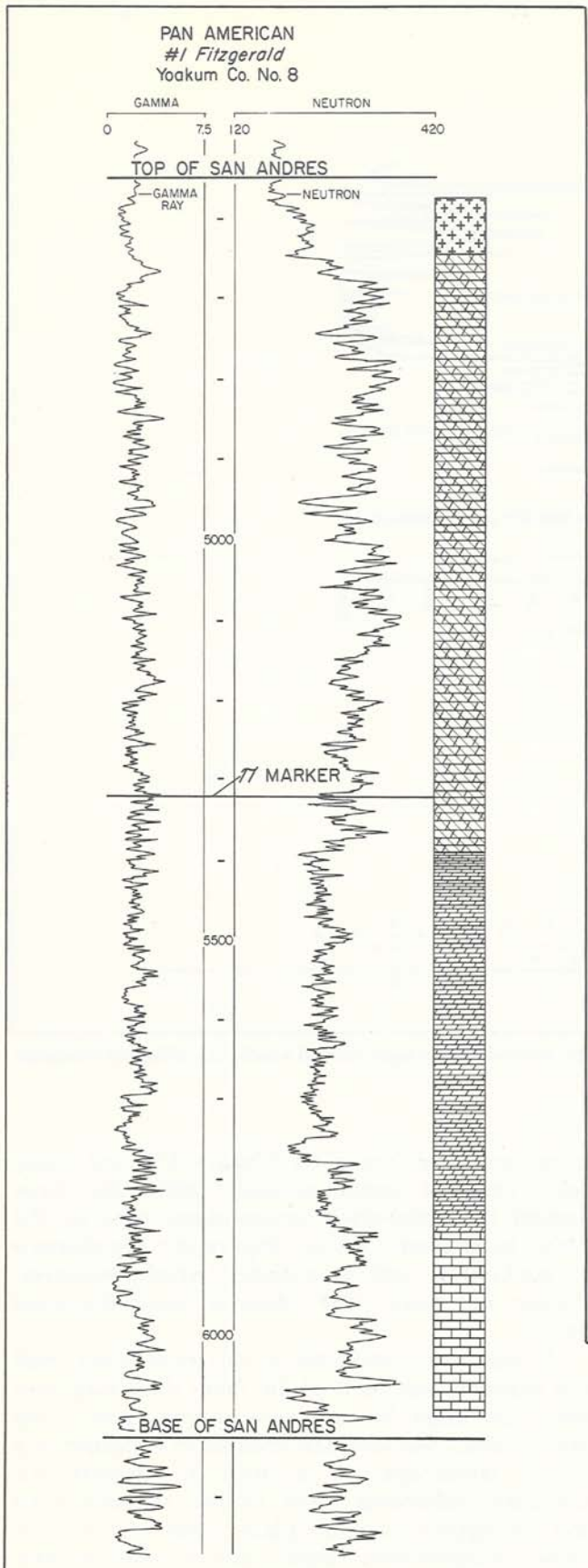

ADDITIONAL EVIDENCE FOR SUBAERIAL EXPOSURE

It would be logical that periods of subaerial exposure, if they occurred, would occur during the ends of depositional cycles (fig. 7). As the cycle progressed, water depth decreased; soon conditions were sufficiently restrictive to permit deposition of halite in the Palo Duro Basin. As sea level continued to fall, the shelf and sabkha environments were exposed until the next transgression. Carbonates and sulfates were exposed in the Northern Shelf (Midland Basin). In the Palo Duro Basin, however, a broad, flat salt plain existed that was highly susceptible to dissolution and erosion, even in the prevailing arid climate.

If the various salt beds were not exposed to subaerial erosion, one might expect that the upper contacts would be regionally flat, and uniform salt bed thicknesses would exist throughout the basin, gradually thinning at the peripheries. This, however, is not the case. Note that in a core from the DOE-Gruy Federal No. 1 Grabbe well in northeastern Swisher County, Texas (fig. 30), the upper contact of the San Andres cycle 4 salt is clearly erosional (fig. 15). Similar contacts exist at the tops of some of the other lower San Andres salts from the same well and from the DOE-Gruy Federal No. 1 White well in northeastern Randall County, Texas (fig. 30). Below the erosional contact, salt is very coarse grained and clear, indicating that it may have been dissolved and reprecipitated. A few feet below this clear zone, the salt is darker and finer grained, typical of most of the underlying section (fig. 16).

Cycle 4 salt thins along a linear belt that extends across the central part of the basin (fig. 30), just where one would expect to find the thickest section; at least 50 ft have been removed. Thin but persistent mud breaks in the upper part of the cycle 4 salt terminate along the axis of this stratigraphic thin (fig. 31), as if they were removed by a downcutting stream. No known structural anomalies exist (fig. 32) that could account for differences in thickness within the central part of the basin. Such streams would have been intermittent, flowing only during rare but heavy rainfalls typical of the climate in modern coastal

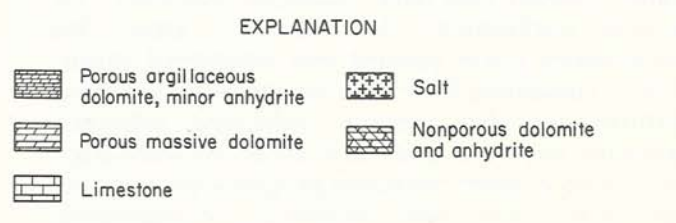

Figure 28. Gamma-ray, neutron log, and lithic interpretation, San Andres strata, Pan American Fitzgerald No. 1, Yoakum County, Texas.

sabkhas (Patterson and Kinsman, 1981). The configuration of the top of cycle 4 salt strata resembles a dissected plain (fig. 30) having runoff rills that merge to the south and empty into the deeper parts of the Midland Basin (Terry County), where permanent water probably existed at that time. Internal drainage was probably well developed within the salt basin, as suggested by local isopach thin areas (fig. 30).

On the basis of the uneven salt thicknesses of cycles 2, 3, 4, and 5 and the observed erosional upper contacts, at least two and possibly as many as four major periods of exposure can be postulated to have occurred in early San Andres time.

More evidence of subaerial exposure is present in the Tenneco No. 15 Bryson core in Yoakum County (in the shoal facies area). It contains a 19-cm-thick zone of large intraclasts in a coarsely crystalline matrix of anhydrite (fig. 8). This intraclast zone occurs near the top of the major porosity zone and is overlain and underlain by dolomitized mudstone. The overlying mudstone contains displacive nodules of anhydrite of the type described by Kerr and Thomson (1963). These nodules are absent in the intraclast zone and in the underlying mudstone. Instead anhydrite occurs as either a pore-filling cement or a replacement mineral with no displacive relationships. Minor pinpoint porosity exists in the underlying mudstone. Such sequences are not present in core taken to the west in the inner shelf.

The following interpretation of the sequence observed in the Tenneco core is offered: (1) Carbonate mud under normal (though low-energy), open-marine conditions was deposited. (2) A high-energy environment was developed owing to decreasing water depth; this caused rip-up of the surface and resulted in deposition of large intraclasts. (3) Subaerial exposure occurred, which may have caused additional cracking owing to desiccation. This period of exposure probably occurred near the end of cycle 5. (4) Influx of meteoric water followed, which then caused dolomitization of the carbonate mud (Folk and Land, 1975) and, hence, lithification. Porosity may have developed at this time through dissolution of allochems and dolomitization. (5) Deposition of

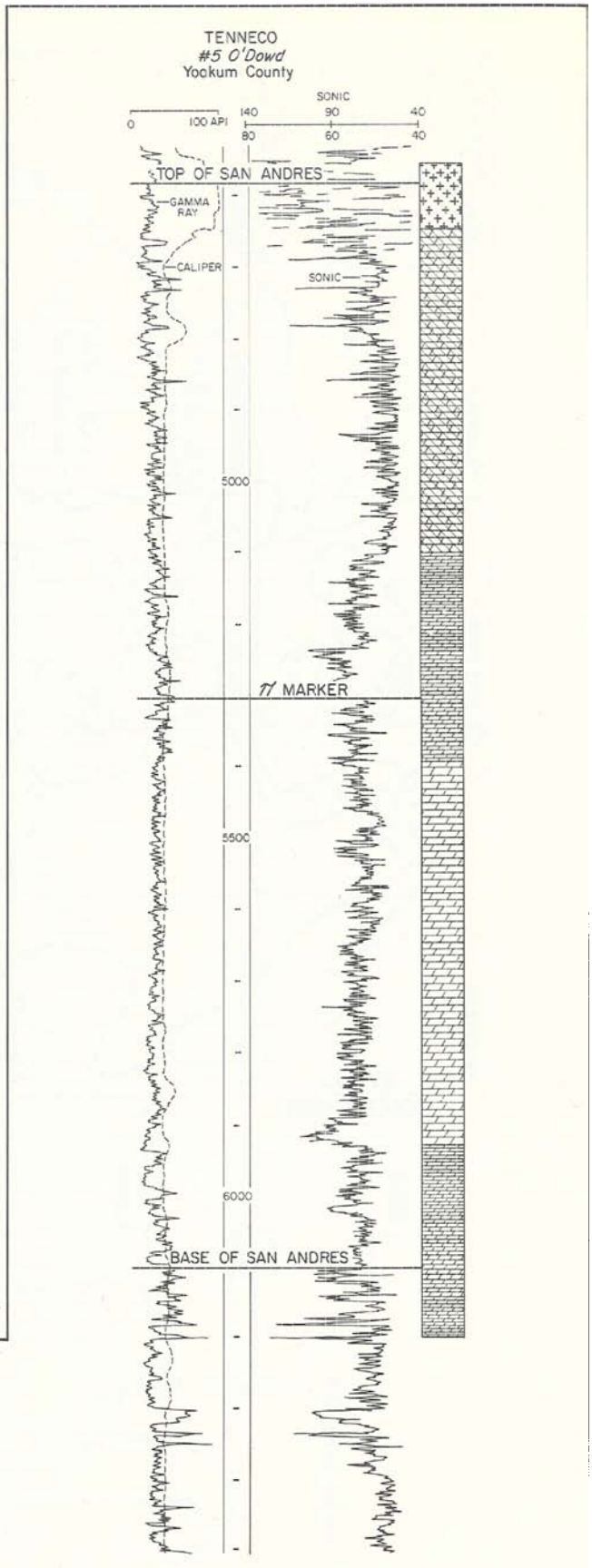

Figure 29. Gamma-ray, sonic log, and lithic interpretation, San Andres strata, Tenneco O'Dowd No. 5, Yoakum County, Texas.

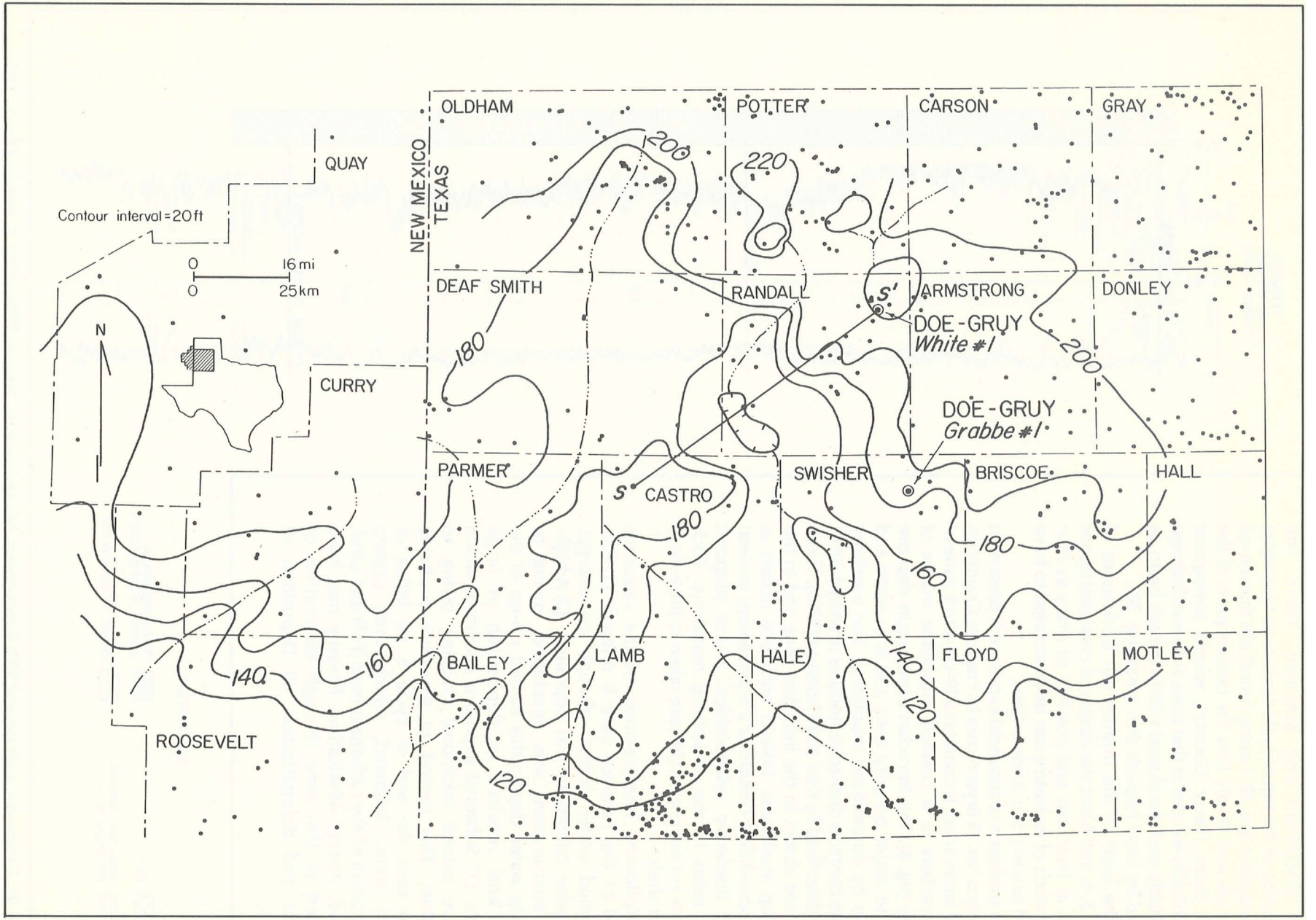

Figure 30. Isopach map of cycle 4 salt (including interbeds), San Andres Formation, Palo Duro Basin, Texas and New Mexico. Hachured contours represent stratigraphic thins, not structural lows.

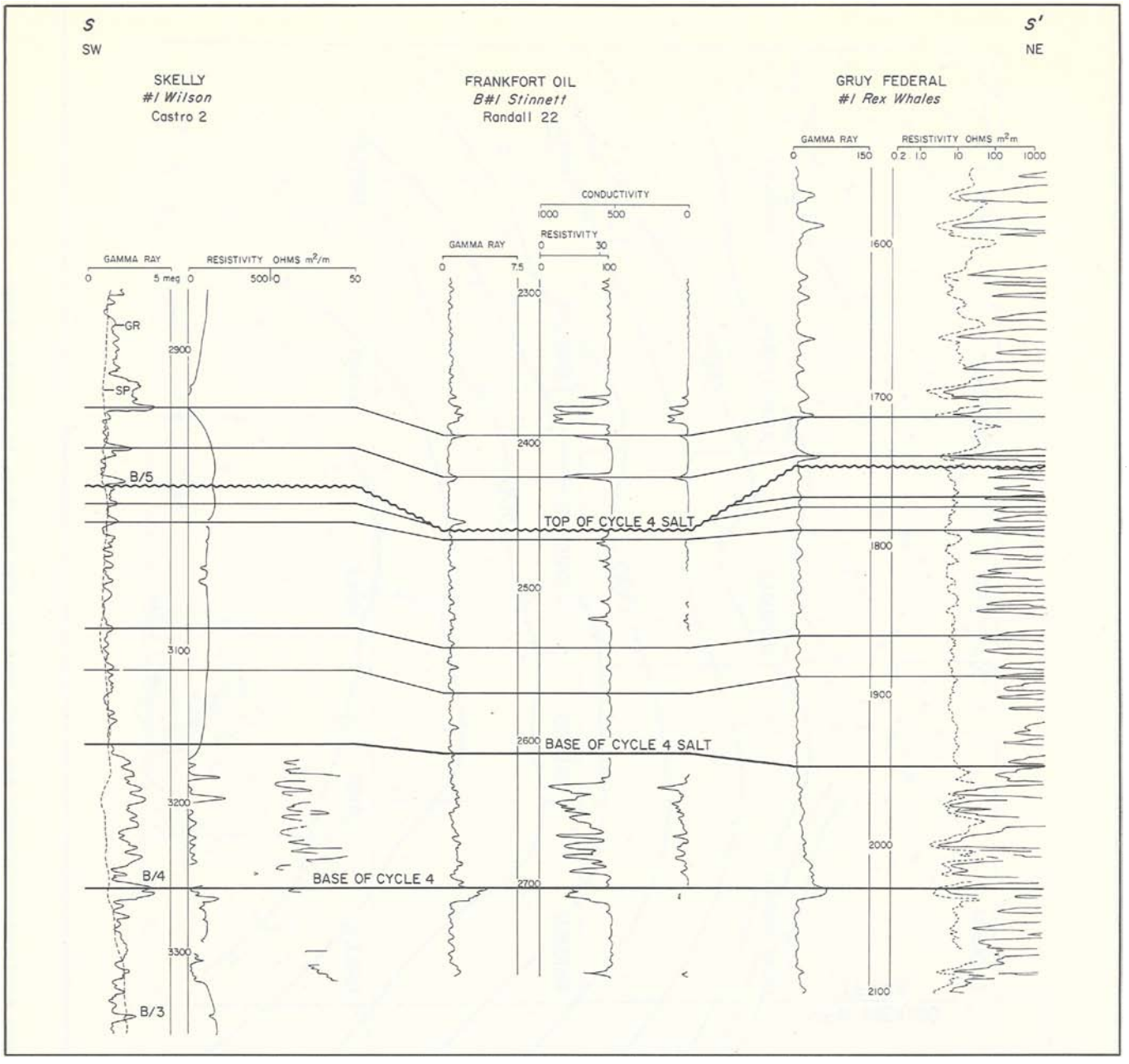

Figure 31. Cross section of cycle 4 salt, San Andres Formation, across an area of salt thinning. Line of section S-S' illustrated in figure 30.

carbonate mud resumed, caused by a rise in sea level. (6) Prograding mud-flat or sabkha environments caused a dramatic increase in salinity of surface fluids. (7) Formation of gypsum rosettes in the soft carbonate mud occurred, as it does today in Laguna Madre, Texas (Kerr and Thomson, 1963). These nodules were unable to form in the underlying intraclast and mudstone zones, which were lithified by this time. (8) Hypersaline fluids precipitated a pore-filling cement in underlying permeable units; the highly permeable intraclast zone was rapidly filled with anhydrite, rendering it impermeable. The degree to which porosity was destroyed by pore-filling anhydrite decreases with depth and is absent within the underlying major porosity zone (fig. 29).

Subaerial exposure can also be inferred from the presence of enterolithic folding in thin anhydrite beds (fig. 12c). Primary or secondary anhydrite was probably converted to gypsum, causing volume expansion and subsequent folding. Conversion from anhydrite to gypsum may have been accomplished by exposure to meteoric water. Alteration back to anhydrite occurred later either by exposure to a hypersaline brine or by burial.

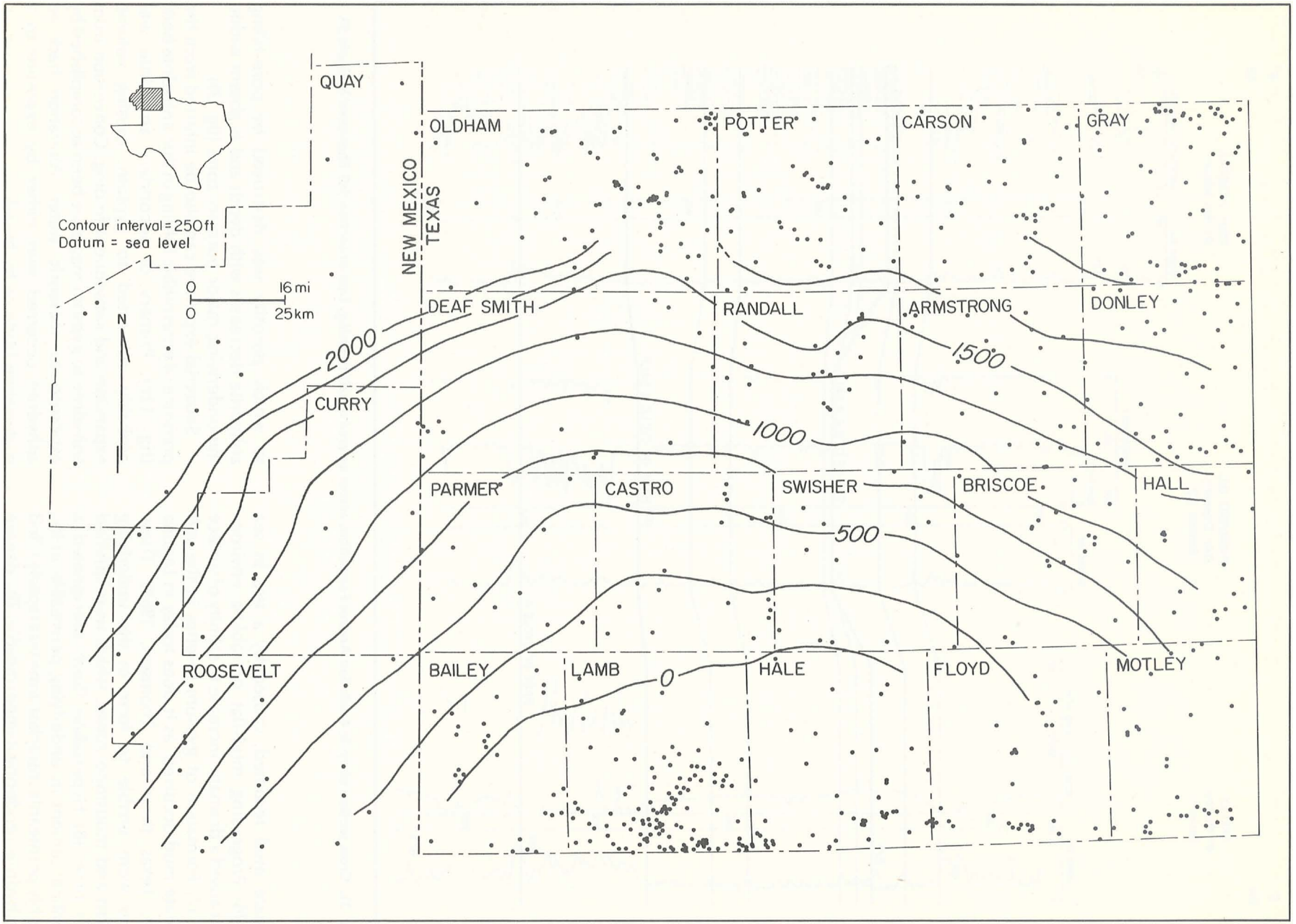

Figure 32. Structure map, basal mudstone of cycle 4, San Andres Formation, Palo Duro Basin, Texas and New Mexico.

Porosity and permeability vary considerably within oil-bearing strata of the Northern Shelf even within thin, porous intervals (Roswell Geological Society, 1956, 1960, 1967; Herald, 1957, p. 50, 144, 245, 375, 377; Chuber and Pusey, 1967; Zaaza, 1978). The results of 29 porosity and permeability measurements of the Yellowhouse dolomite (cycle 4, lower San Andres), Littlefield Northeast field, Lamb County, are shown in figure 27. The depth range of samples is small (3,880 to 3,939 ft), yet porosity varies from 2.7 to 20.7 percent and permeability from less than 0.1 to 8.3 millidarcys (md). The relation between porosity and permeability is not linear; permeability increases greatly in samples exhibiting porosity greater than 17 percent. This porosity and permeability variability in seemingly uniform lithology suggests a change in type of porosity above the 17-percent threshold.

Greater changes in permeability occur when fractures are encountered, commonly in areas where strata are draped over underlying shelf edges (fig. 33). Fractures may also allow fluid circulation, thereby enhancing dolomitization and development of secondary porosity. Such conditions were reported by Wright (1962) for carbonates in the Abo Reef trend. Dunlap (1967) reported fracture porosity in the Chaveroo field, which lies on a structural drape (figs. 1, 20 to 22). Fractures also have been responsible for the lost circulation of drilling mud in the Northwestern Shelf (Roswell Geological Society, 1956, 1960, 1967).

Coarse moldic porosity is also present in the dolomitized mudstones, but connections between such pores are poorly developed; hence, these vugs contribute little to the general permeability of the bed. Schneider (1943, p. 497) stated that coarse moldic pores "commonly fail to show saturation in an otherwise saturated sample." He considered intercrystalline and intergranular porosity to be the most effective type in the Wasson field.

Rapid changes in porosity and permeability also may be related to changes in the various carbonate facies described by Bein and Land (1982). Such subtle changes would go unnoticed in routine core and log descriptions. Large vertical variations in porosity and permeability tend to restrain oil within relatively thin reservoirs, hence preventing vertical migration and aiding in the development of updip, porosity-pinch-out traps (fig. 27).

Initial depositional porosity was destroyed early in the diagenetic process. By mid-San Andres time, the evaporitic environments that had prevailed to the north prograded over the remainder of the inner-shelf and shoal areas and caused deposition of nonporous anhydrite and dolomite strata. Hypersaline brines of a marine origin (Bein and Land, 1982) quickly seeped into underlying permeable aquifers (dolomitized packstones and grainstones), causing precipitation of coarsely crystalline anhydrite (or halite in the Palo Duro Basin) in pore spaces. Additional dolomitization may have occurred at this time (Bein and Land, 1982). Downward penetration of this hypersaline brine must have been extensive (Barone, 1976). The entire cycle 4 dolomite porosity in the Palo Duro Basin is salt filled, as evinced by two cores from the Palo Duro Basin, which indicates that brine must have penetrated at least 80 ft (the thickness of the cycle 4 dolomite). Mud-supported carbonates in the Northern Shelf resisted anhydrite precipitation, owing to the low initial permeability of the carbonate strata; it commonly maintained fine pinpoint porosity, which was produced earlier by dissolution of allochems and dolomitization of the carbonate mud.

Considering that porosity in San Andres carbonates is mostly secondary, it follows that meteoric water may have contributed greatly during times of low sea level as an agent of dissolution and dolomitization. The periodic influx of fresh water and its mixing with brine may have caused dolomitization by initiating a schizohaline environment, according to the hypothesis of Folk and Land (1975). Brines could have been supplied from the dissolution of exposed salt and the periodic wind-driven floods of marine water. It also follows that surface topography would strongly affect the path and distribution of such meteoric ground water. Thick lenses of fresh water could have developed on topographic highs (such as the shoals); dolomitization could then have proceeded along the contact of the fresh water and the underlying brine (Folk and Land, 1975). As the contact between fresh and saline water fluctuated, so should have the zone of dolomitization.

There are many ways to produce dolomite, not all of which involve mixing of fresh and saline waters. For a modern analog, the generation of protodolomite in subtidal and intertidal carbonates beneath the sabkhas of the Arabian Gulf is caused by downward-percolating brines from wind-driven floods of marine water (Patterson and Kinsman, 1982). Such brines could mix with fresher ground water as it migrates seaward; Patterson and Kinsman (1981) demonstrated that relatively fresher ground water from inland recharge areas does migrate seaward below the sabkhas of the Arabian Gulf. Alternatively, Bein and Land (1982) suggest that in the Palo Duro Basin, dense brine from the salt basin was refluxed through underlying carbonates, thereby dolomitizing the carbonate sediment. This model is especially appropriate for the Palo Duro Basin, where dolomite

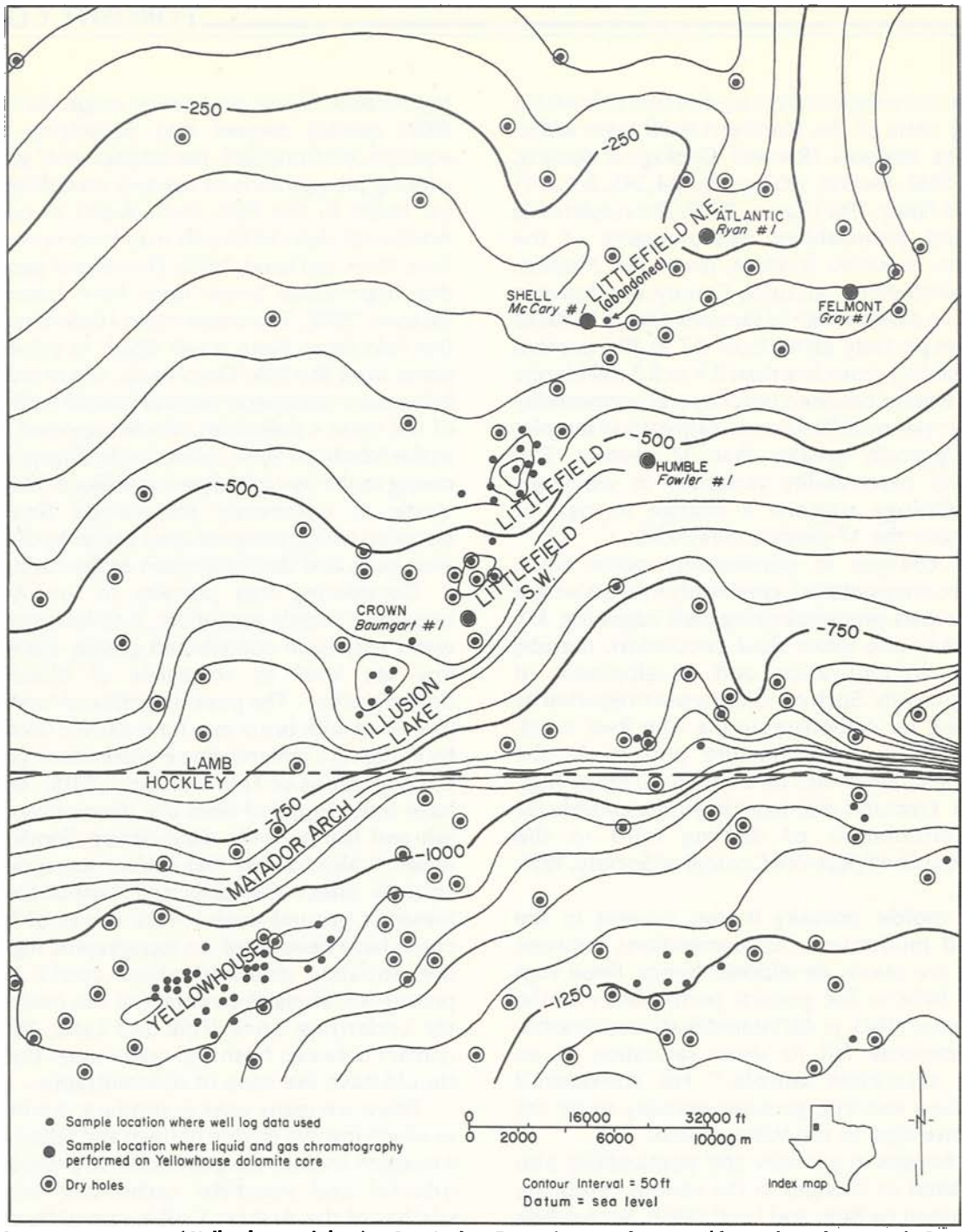

Figure 33. Structure map, top of Yellowhouse dolomite, San Andres Formation, northern Hockley and southern Lamb Counties, Texas.

(as thick as 80 ft) is intercalated within thicker beds of salt (as thick as 200 ft). Their model, however, does not explain the several hundreds of feet of massive porous dolomite occurring in the shoal area (Midland Basin); this dolomite is not in contact with salt. It is unlikely that any one model for dolomitization can be exclusively used for the entire area.

The meteoric hypothesis is supported by the fact that limestone is completely absent (fig. 29) in the shoal area, where meteoric water influx and dolomitization would have been most intense. In contrast, the lowermost San Andres carbonate muds of the inner shelf were not dolomitized (fig. 28), probably because they were submerged during the earlier periods of dolomitization and, hence, insulated from the reactive meteoric fluids. In contrast, the hingeline-associated fractures over the shoals and the greater hydraulic head (owing to

topographic relief) probably aided the downward penetration of the dolomitizing fluids along that belt (fig. 4).

The structurally low outer shelf was probably never exposed during early San Andres time. Hence, the diagenetic processes that dolomitized most of the inner-shelf and shoal areas were inoperative on the outer shelf. Consequently, lower San Andres strata consist mostly of nonporous limestone (micrite) on the outer shelf east of the shoals (fig. 5).

The presence of about 200 ft of limestone in lowermost San Andres strata on the inner shelf (fig. 28) suggests a period of prolonged submergence in some areas. Dolomitization observed in overlying strata must have occurred later during cyclic periods of exposure.

Barone (1976, p. 35) concluded that the diagenesis of the shelf carbonates was caused by the "discharge of saline meteoric ground water" from overlying sabkha deposits downward through the carbonates. Bein and Land (1982) maintained that the composition of the reactive brine was fairly uniform and of a marine origin. Bein and Land discounted the possibility of any fresh-water diagenesis. However, according to the literature previously cited concerning the periods of emergence during Permian time and the variations in stratigraphic thicknesses, one can conclude that San Andres deposits of the northern Midland Basin were exposed to meteoric fresh water. This exposure would have happened before the introduction of the hypersaline brine mentioned by Bein and Land (1982), except in the Palo Duro Basin, where halite deposition began soon after deposition of dolomite.

Bein and Land (1982) cite the absence of "blocky calcite cement" in the San Andres dolomites as strong evidence for the lack of any fresh-water diagenesis. However, the final phase of recrystallization of these carbonates could have obliterated any evidence of earlier diagenesis (R. L. Folk, personal communication, 1981). Bein and Land have studied the effects of the last reactive brine to have penetrated the carbonate strata. Their geochemical data reflect the effects of this brine and should not be used to deny earlier diagenetic changes. Furthermore, their sampling did not include dolomites from the shoal facies, where the relative effects of meteoric water would have been greater.

Although considerable evidence has been presented for periodic subaerial exposure of the Northern and Northwestern Shelves during San Andres time, this in itself is not proof that the carbonates were in fact dolomitized as a result of this exposure. Dolomitization still may have occurred during halite deposition, as described by Bein and Land (1982), or both mechanisms may have been operative. Proof may be difficult to obtain, but the distribution of massive porous dolomite on the structurally high flanks of the deep basin and the presence of nonporous limestone in structurally low areas suggest that dolomitization and porosity development, at least in the northern Midland Basin, were linked to surface topography and, hence, to meteoric processes.

OIL AND GAS PRODUCTION

PRODUCTION DATA

In 1980 San Andres reservoirs of the Northern Shelf, Texas, were responsible for 12.7 percent of total oil production for Texas; natural gas production from this area, however, was only 0.9 percent of the total for the state (Railroad Commission of Texas, 1981). Considering the relatively small area involved (roughly 3,600 mi^2), this production is impressive. These figures, however, represent a decline in production over the last several years, which, in turn, reflects the statewide trend (Railroad Commission of Texas, 1981).

The Northern and Northwestern Shelves are divided into six distinctive regions (figs. 1 and 34). These figures for total oil and gas production can be used to gauge the relative importance of each region.

Oil and gas production from San Andres reservoirs of the Northwestern Shelf, New Mexico, is dwarfed by the prolific Texas production; the Northern Shelf, Texas, has produced 36 times more oil as of January 1, 1981. Three giant oil fields (Levelland, Slaughter, and Wasson) produced 93.5 percent of all San Andres oil from both the Northern and Northwestern Shelves during 1980; these three fields, however, contain only 76.6 percent of all producing oil wells. See tables 2 and 3 for complete production data. These tables are keyed to figure 1, which shows the locations for all San Andres oil fields, including abandoned ones, in the study area. Most abandoned fields initially had marginal production (tables 2 and 3).

Gas production (mostly casing head production) from the Northern Shelf is insignificant compared with oil production. Gas-to-oil ratios are much lower (table 2) compared with the statewide average of 7.5 mcf/bbl (Railroad Commission of Texas, 1981). On a field-by-field basis, the ratios appear erratic (table 2), but if only large fields of the Northern Shelf are considered, the ratios generally fall within a narrow range (0.30 to 0.70). For both shelves, gas-to-oil ratios

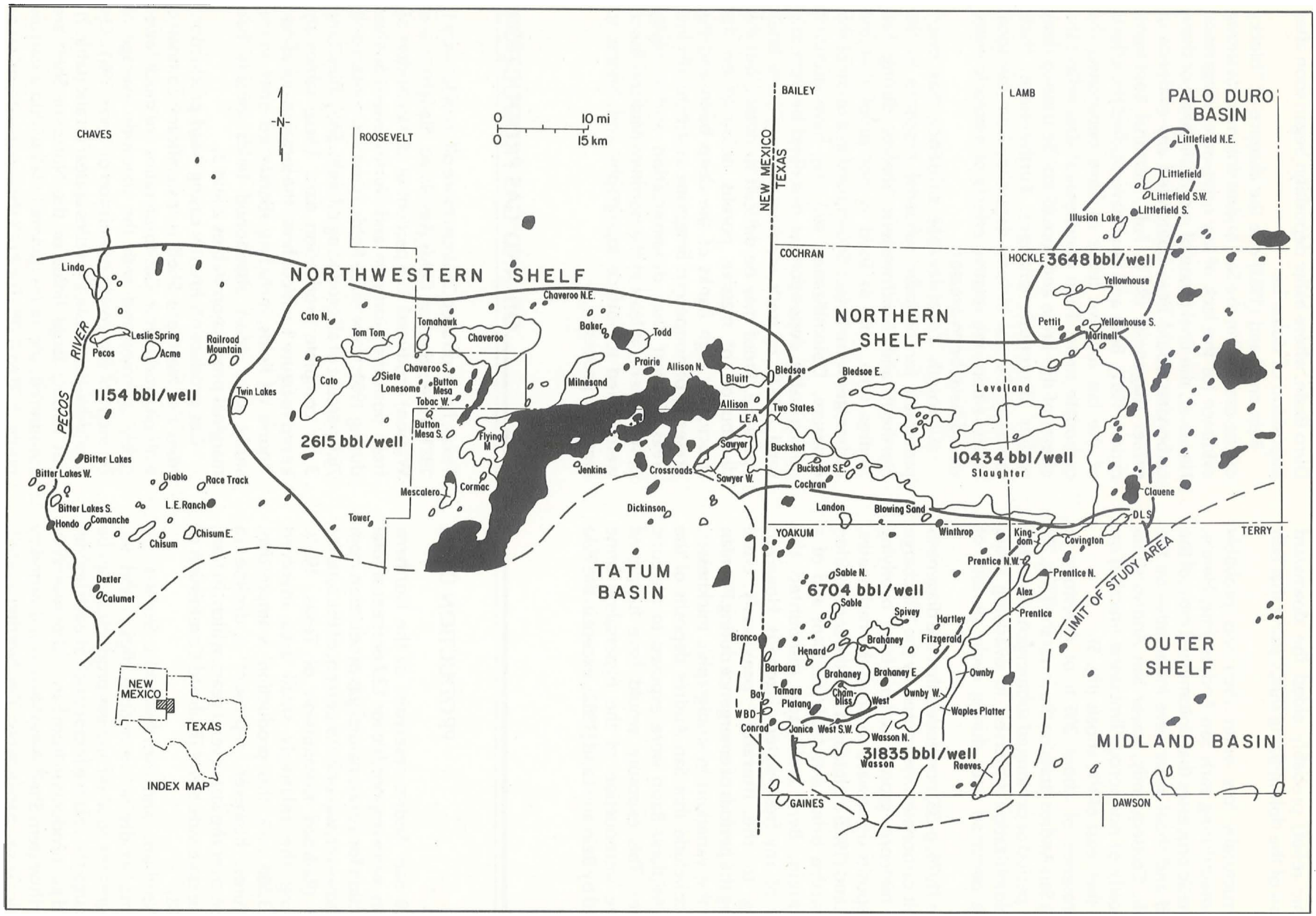

Figure 34. Map of the Northern and Northwestern Shelves showing San Andres petroleum productivity in each region. Darkened fields produce from pre-San Andres strata.

Table 2. Production data for San Andres oil fields of the Northern Shelf, Texas.

Field name	Depth to reservoir	Pay zone	1980 gas (mcf)	1980 oil (bbl)	1980 gas/oil (mcf/bbl)	Accumulative oil (bbl)	Discovery year	No. of oil wells Jan. 1,1981	1980 productivity (bbl/well)	API°
Alex	5,150		31,716	22,543	1.41	719,694	1945	8	2,818	33
Barbara	5,287		12	1,754	0.0068	8,692	1976	1	1,754	29
Bay	5,350		24	4,155	0.0058	85,377	1968	4	1,039	32
Bledsoe	4,193		94,760	12,028	7.88	174,279	1951	6	2,005	24
Bledsoe E.	4,918		0	0	-	5,330	1957	0	-	28
Blowing Sand	5,072		518	477	1.09	1,792	1974	1	477	30
Brahaney	5,301		551,634	1,481,267	0.37	32,170,903	1945	221	6,702	32
Brahaney E.	5,395		0	0	-	294	1977	0	-	29
Bronco	5,182		0	0	-	7,123	1954	0	-	31
Buckshot	5,010	S	267,778	220,644	1.21	9,641,607	1956	111	1,988	31
Buckshot SE.	5,040		4	867	0.0046	867	1980	1	867	27
Chambliss	5,248		Merged with Brahney field		-	313,275	1955	0	-	32
Clauene	5,093		0	0	-	25,219	1953	0	-	31
Coble	4,961		0	0	-	1,406	1945	0	-	30
Cochran	5,008		0	0	-	3,441	1954	0	-	31
Conrad	5,292		0	0	-	2,770	1958	0	-	33
Covington	5,020		587	8,537	0.069	317,333	1956	3	2,846	31
DLS	5,161		371,026	684,542	0.54	4,575,488	1971	59	11,602	36
Dean	5,077		0	0	-	839,724	1938	0	-	30
Duggan	5,000		0	0	-	574,172	1936	0	-	31
Fields	5,196		21	4,494	0.0047	7,267	1979	1	-	34
Fitzgerald E.	5,398		0	0	-	3,455	1960	0	-	30
Hartley	5,365		12	1,948	0.0062	53,134	1959	1	1,948	33
Henard	5,205		783	13,393	0.058	238,988	1950	7	1,913	32
Illusion Lake	4,116	Y	2,892	44,160	0.065	2,046,475	1957	16	2,760	27
Janice	5,263		5,856	3,810	1.53	202,014	1955	3	1,270	31
Kingdom	5,134		12	18,018	0.00067	31,441	1976	2	9,009	29
Kingdom USA	5,076		1	819	0.0012	819	1980	1	819	28
Landon	5,100	S	1,486	90,300	0.016	5,615,554	1945	26	3,473	32
Levelland	4,927	S,Y	10,561,840	19,031,750	0.55	331,273,210	1945	2,103	9,050	29
Littlefield	4,030	Y	997	23,295	0.043	4,666,890	1953	24	971	28
Littlefield NE.	3,871	Y	0	0	-	904	1977	0	-	30
Littlefield S.	4,082	Y	0	0	-	280	1967	0	-	32
Littlefield SW.	4,056	Y	613	5,651	0.11	32,519	1975	2	2,826	38
Marinell	4,711	Y	0	0	-	22,881	1959	0	-	32
Ownby	5,350		293,683	556,003	0.53	9,168,427	1941	45	12,356	30
Ownby W.	5,307		29,081	7,778	3.74	807,161	1953	8	972	33
Pettit	3,655		0	0	-	639	1958	0	-	31
Platang	5,137		0	0	-	12,872	1955	0	-	29
Prentice	5,294		5	115	0.043	19,426	1965	1	115	28
Prentice (5,100)	5,240		82,946	57,911	1.43	440,060	1974	12	4,826	34
Prentice N.	5,095		0	0	-	34,082	1956	0	-	33
Prentice NW.	5,164		83,323	48,278	1.72	850,782	1969	10	4,828	35
Reeves	5,544		222,662	681,268	0.33	20,907,647	1957	68	10,019	35
Rhodes	5,100		0	0	-	55,547	1940	0	-	31
Sable	5,258		125,548	426,261	0.29	6,070,844	1957	25	17,050	31
Sable N.	5,230		15	3,613	0.004	47,965	1970	3	1,204	35
Slaughter	5,000	S	12,697,665	31,245,018	0.41	828,403,420	1937	2,547	12,267	32
Spivey	5,340		1,864	21,761	0.086	221,919	1958	10	2,176	33
Tamara	5,308		0	0	-	5,399	1957	0	-	32
Two States	4,920		30,523	385	79.3	11,109	1953	1	385	30
WBD	5,288		22,303	32,235	0.69	609,143	1969	4	8,059	33
Waples Platter	5,300		Merged with Ownby field		-	1,134,419	1929	0	-	29
Wasson	4,900		38,077,218	63,356,866	0.60	1,254,293,942	1937	1,833	34,565	34
Wasson N.	5,265		3,735	10,278	0.36	77,094	1974	6	1,713	32
West	5,100		25,847	50,942	0.51	1,858,410	1938	12	4,265	32
West SW.	5,219		0	0	-	1,601	1973	0	-	36
Winthrop	5,124		0	0	-	38,185	1959	0	-	38
Yellowhouse	4,463	Y	57,895	389,124	0.15	9,404,114	1944	83	4,688	27
Yellowhouse S.	4,705	Y	1,541	8,316	0.19	486,273	1957	4	2,079	30
Totals			**63,648,426**	**118,570,000**	**0.54***	**2,528,554,800**		**7,273**	**16,303***	**31***

*Indicates an average.
SOURCE: Railroad Commission of Texas (1981) and Railroad Commission of Texas proration schedule of January 1, 1981.

Table 3. Production data for San Andres oil fields of the Northwestern Shelf, New Mexico.

Field name	Depth to reservoir	Pay zone	1980 gas (mcf)	1980 oil (bbl)	1980 gas/oil (mcf/bbl)	Accumulative oil (bbl)	Discovery year	No. of oil wells Jan. 1, 1981	1980 productivity (bbl/well)	API°
Acme	-	P_1	0	7,101	0	233,404	1950	8	888	25
Allison	4,860	-	0	0	-	118	1963	0	-	32
Allison N.	4,920	-	0	0	-	848	1964	0	-	27
Baker	-	-	-	-	-	-	-	-	-	-
Bitter Lakes	880	-	0	0	-	90	1960	0	-	26
Bitter Lakes S.	880	P_1	0	5,364	0	136,835	1960	14	383	20
Bitter Lakes W.	-	-	0	568	0	12,733	-	3	189	-
Bluitt	-	-	253,790	30,098	8.43	2,294,220	-	40	752	-
Button Mesa	4,032	-	0	0	-	860	1960	0	-	25
Button Mesa S.	-	-	0	1,578	0	108,283	-	1	1,578	-
Calumet	-	-	0	120	0	2,795	-	1	120	-
Cato	3,414	P_1, P_2	575,591	188,262	3.06	14,661,526	1966	181	1,040	26
Cato N.	-	-	0	0	-	304	-	0	-	-
Chaveroo	4,184	P_1, P_2, P_3	996,302	615,918	1.62	20,135,069	1965	355	1,735	26
Chaveroo NE.	-	-	0	0	-	10,542	-	0	-	-
Chaveroo S.	-	-	0	0	-	159	-	0	-	-
Chisum	2,023	-	0	810	0	50,082	1951	2	405	20
Chisum E.	-	-	5,520	63,969	0.086	255,672	-	23	2,781	-
Comanche	-	-	0	1,819	0	20,291	-	2	910	-
Cormac	-	-	0	539	0	6,050	-	1	539	-
Crossroads	4,837	-	0	0	-	174,919	1956	0	-	24
Crossroads E.	4,800	-	0	5,218	0	12,456	-	4	1,305	-
Dexter	-	-	0	0	-	2,318	-	0	-	-
Diablo	-	-	0	2,662	-	29,424	-	4	666	-
Dickinson	-	-	4,215	8,576	0.49	38,895	-	5	1,715	-
Flying M	4,550	P_1	180,664	381,915	0.47	6,888,305	1964	74	5,161	19
Gallina	-	-	-	-	-	-	-	-	-	-
Hondo	-	-	0	0	-	16,375	-	0	-	-
Jenkins	4,846	-	0	1,050	0	48,791	1959	3	350	17
L. E. Ranch	-	-	0	5,030	0	6,760	-	1	5,030	-
Leslie Spring	-	-	0	715	0	10,694	-	4	179	-
Linda	1,023	P_1	0	8,761	0	102,040	1963	20	438	27
Lonesome	-	-	0	0	-	2,812	-	0	-	-
Mescalero	4,063	P	222,361	132,028	1.68	5,530,555	1962	44	3,001	18
Milnesand	4,554	P_1, P_2	87,707	242,974	0.36	9,025,046	1958	91	2,670	28
Pecos	1,088	P_1	0	679	0	16,352	1961	3	226	26
Prairie	4,858	-	0	0	-	407	1959	0	-	33
Race Track	-	-	0	7,219	0	32,183	-	5	1,444	-
Railroad Mountain	-	-	638	1,347	0.47	2,607	-	2	674	-
Sawyer	5,000	-	858,586	44,978	19.1	954,641	1947	43	1,046	25
Sawyer W.	-	-	442,466	178,422	2.48	2,608,287	-	55	3,244	-
Siete	3,705	-	1,037	8,274	0.13	162,969	-	5	1,655	-
Tobac W.	4,300	-	0	0	-	355	-	0	-	-
Todd	4,440	-	148,663	39,635	3.75	2,553,639	1964	36	1,101	24
Tom Tom	-	-	182,337	335,271	0.54	1,422,800	-	71	4,722	-
Tomahawk	-	-	138,255	185,896	0.74	678,013	-	42	4,426	-
Tower	-	-	0	0	-	2,036	-	0	-	-
Twin Lakes	2,530	P_1, P_2	322,036	483,713	0.67	1,111,973	-	63	7,678	25
Totals			**4,420,168**	**2,990,509**	**1.48***	**69,365,712**		**1,198**	**2,496***	**25***

*Indicates an average.

SOURCE: Unpublished data on file at the Oil Conservation Division, New Mexico Energy and Minerals Department, and Roswell Geological Society (1956, 1960, 1967, 1977).

are much lower in small fields than in large ones. In fact, most small fields in the Northwestern Shelf report no gas production (table 3). Gas-to-oil ratios in the Northwestern Shelf are more erratic, even among large fields; in general, hydrocarbon production is more gas-rich in the Northwestern Shelf than the Northern Shelf. This difference between the two shelves, together with other compositional differences, such as the lower American Petroleum Institute(API) gravity values for Northwestern Shelf oil (tables 2 and 3), may reflect fundamental differences in source. Ramondetta (1982) suggests that the Tatum Basin is the source for Northwestern Shelf oil and the Midland Basin is the source for Northern Shelf oil, hence justifying the hydrocarbon differences exhibited by the two shelves.

STRUCTURAL CONTROL

Many researchers agree that structure was important in trapping hydrocarbons on the Northern Shelf (Schneider, 1943; Chuber and Pusey, 1967; Hills, 1972; and Otte, 1974). This is confirmed by the structure maps in this report (figs. 20 to 22, and 33).

Structural control can be subtle or obvious. Prolific San Andres and Clear Fork production exists on the large Wasson and Anton Irish structures (figs. 19 to 22); both of these well-defined domal structures display closure greater than 100 ft. In contrast, a subtle, south-plunging anticline (striking NE.-SW.) controls hydrocarbon occurrence along the eastern margin of Slaughter and Levelland fields. No San Andres production occurs east (basinward) of the anticline (figs. 20 to 22). This productive anticlinal trend, which coincides with the position of the older Wolfcampian shelf margin (fig. 2), continues to the northeast through Yellowhouse, Illusion Lake, Littlefield, and Littlefield NE. fields (figs. 20 to 22, and 33). Note the steeper basinward (southeastern) flank of this anticline and the mild structural closure along the crest where entrapment occurs (fig. 33). Similar structural drape patterns with associated fractures occur throughout the Northern and Northwestern Shelves and control some San Andres production (figs. 20 to 22). The Chaveroo field is an example of such a field on the Northwestern Shelf (figs. 20 to 22); fracture porosity has been reported in this field (Dunlap, 1967). In other fields, such as Cato or the central and western parts of Levelland and Slaughter, only a slight nosing or regional dip alone is present (figs. 20 to 22); the same is true for most of the smaller fields.

STRATIGRAPHIC CONTROL

Structural closure alone is inadequate to account for the thick oil columns observed in the Northern Shelf, such as in Wasson and Reeves fields (Chuber and Pusey, 1967). The presence of porosity pinch-outs updip from productive structures accounts for a large part of the trapped oil, especially in fields where no structures exist.

Productive areas such as the Abo Reef trend (fig. 2) rim the deeper part of the Midland Basin. This productive belt (which coincides with the shoal belt) is stratigraphically thinner, indicating that it was a depositional high (figs. 23 to 26). Schneider (1943, 1957) described the eastern (basinward) part of the Wasson field, which overlies this belt, as consisting of thick, massive reeflike dolomite with good intergranular porosity; westward this section grades into less porous, finely crystalline dolomite. The higher energy reeflike environment on the eastern shoaly part of the field is also reflected by the presence of lentils of dense dolomite occurring as foreset beds (Schneider, 1957).

In contrast, the northern and western flanks of the Wasson structure are richer in bedded siliciclastics and anhydrite, rendering the unit less porous. Much of the depositionally high area is also structurally high. Similarly, a thickened porous section occurs in the structurally high parts of Ownby field and Waples Platter field (Cooper and Ferris, 1957); these fields also occur along the shoal belt to form a northeastward extension of Wasson field (fig. 1). Wolfcampian basinal source rocks are subjacent to this belt (fig. 35). The major porosity zone in the lower San Andres Formation is thickest along this belt (despite the overall stratigraphic thinning) and thins in the updip (landward) direction in a series of steps (figs. 5 and 6). Hence, some fields, such as Wasson, Ownby, and Waples Platter, are developed on structures along the flanks of the deep basin. Carbonates along this belt have a thick porous section but are stratigraphically thin, suggesting that there was occasional emergence between periods of deposition. These types of fields are the most productive (figs. 1 and 34) because of (1) the proximity to subjacent source rocks (fig. 35 and Ramondetta, 1982); (2) the vertical fractures caused by hingeline effects allowing vertical migration of oil; (3) the considerable structural relief from the adjacent basinal area (figs. 20 to 22); (4) the sizable amount of structural closure (figs. 20 to 22); (5) the extremely thick porosity zone (figs. 5 and 6); and (6) the rapid updip pinch-out of the upper parts of the major porosity zone (figs. 5 and 6). Hence, the highly productive trend rimming the deep basin represents a series of structural traps flanked by updip porosity pinch-outs.

Another example of improved porosity over a structural high is the Anton Irish field. This high-standing structure was surrounded by prograding sabkha deposits but was not buried by the sabkhas during early San Andres time. This resulted in a relatively thick and continuous porosity zone in the

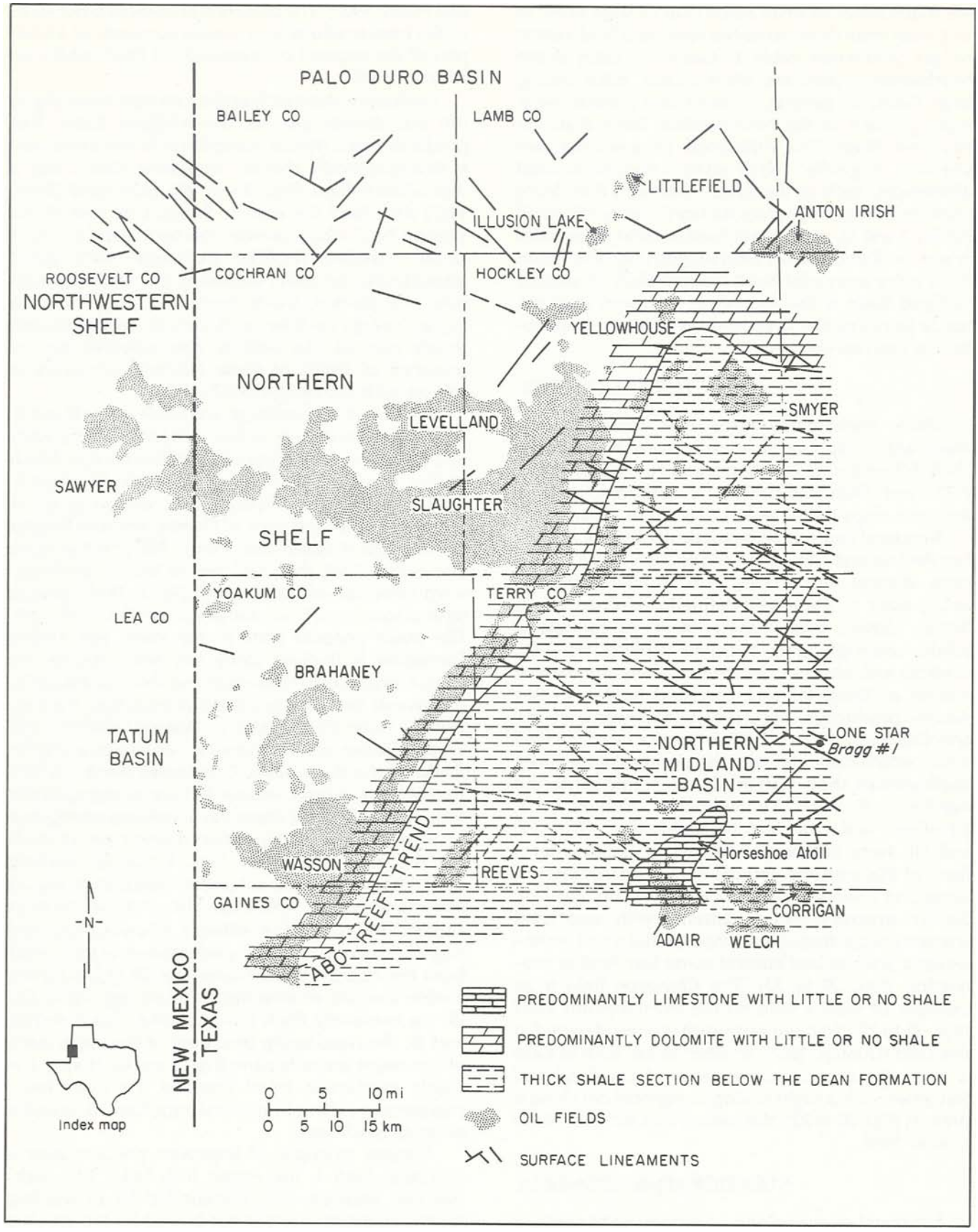

Figure 35. Distribution of source-rock facies, Yoakum, Hockley, Terry, and adjacent counties, Texas.

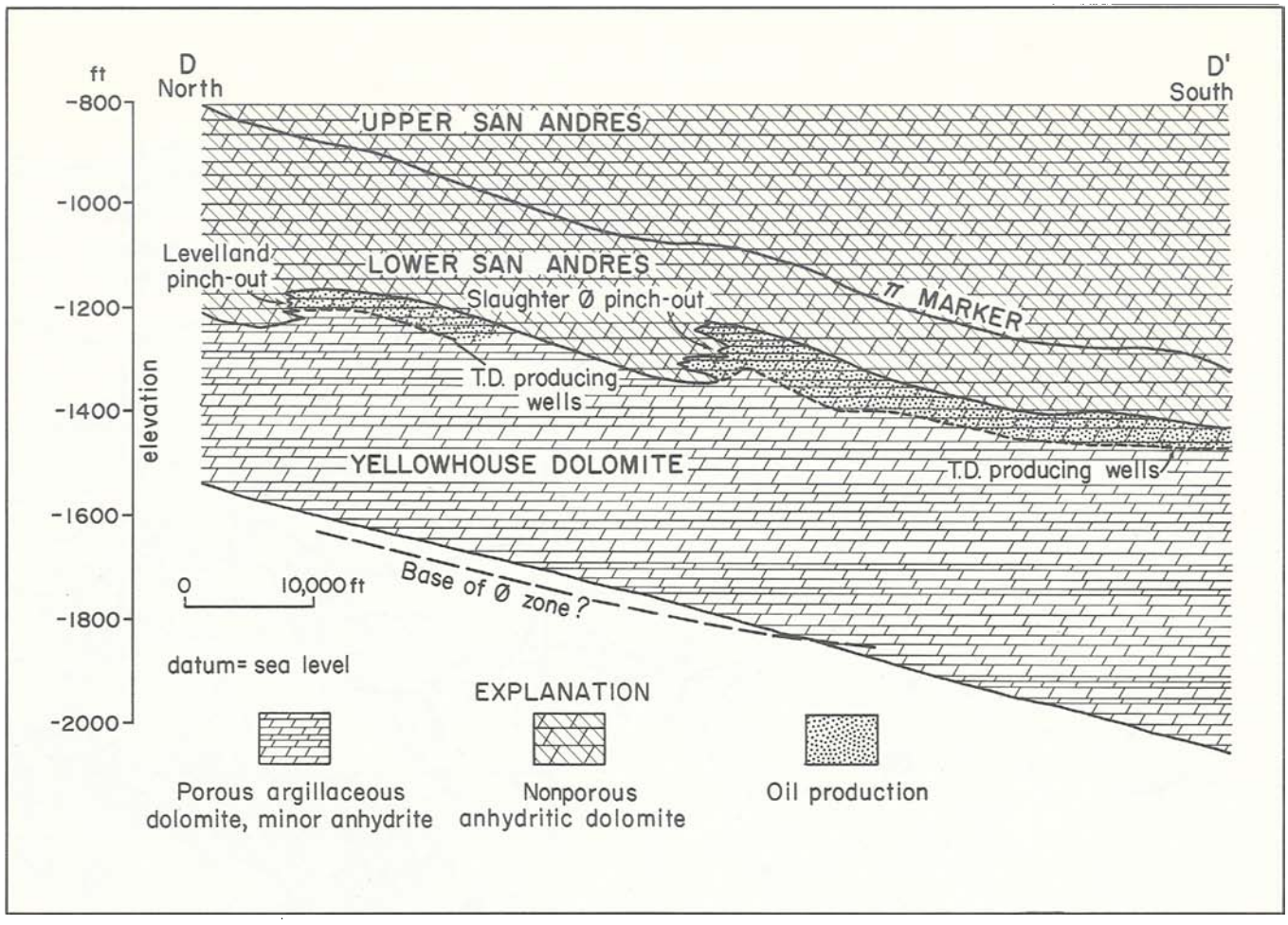

Figure 36. North-south cross section of San Andres Formation across Levelland and Slaughter fields, Texas. Line of section D-D' illustrated in figure 3.

lower San Andres (fig. 19) and Clear Fork section over the structure.

Large amounts of oil migrated updip beyond the belt that rims the deep basin. Steplike thinning of the major porous zone from the top, with little or no structural control, is largely responsible for the vast Levelland and Slaughter fields (fig. 36). Most oil production in the Slaughter field is from the stratigraphically younger Slaughter zone. This zone pinches out further updip so that in the Levelland field, the underlying Yellowhouse dolomite constitutes the top of the major porosity zone; hence, most oil production from the Levelland field is from the Yellowhouse dolomite (fig. 36). In general, the age of the pay zone increases to the north.

Isopach maps of the interval between the π marker and the Yellowhouse dolomite (cycle 4), and between π and total depth of oil wells (most of which were open-hole completions) illustrate the steplike porosity pinch-out (figs. 37 and 38). The effect is less pronounced in the Northwestern Shelf, but northern updip migration is also blocked in the north by the evaporitic barrier (Dunlap, 1967). Oil production diminishes (table 2) where the pay zone thins, as documented by a thickening of the interval between π and top of the Yellowhouse dolomite (fig. 37). Oil is not produced where this interval is greater than 420 ft (fig. 37). Because of its low density, most of the oil first entered the shallower porosity zones. Apparently oil migrated in discrete layers just below the top of the major porosity zone until the permeability of these layers diminished (fig. 36). Deeper, permeable layers extend farther north (beyond the 420-ft limit), but apparently these layers contain water only; attempts to extend the Yellowhouse - Illusion Lake - Littlefield trend farther north have been unsuccessful (fig. 33).

The San Andres pay zones of the Northwestern Shelf are stratigraphically equivalent to the Slaughter and Yellowhouse zones of the Northern Shelf. The Slaughter zone has been correlated to the Bonnie Canyon Member of the San Andres Formation in outcrop (Kelly, 1971). Dunlap (1967) divided the lower

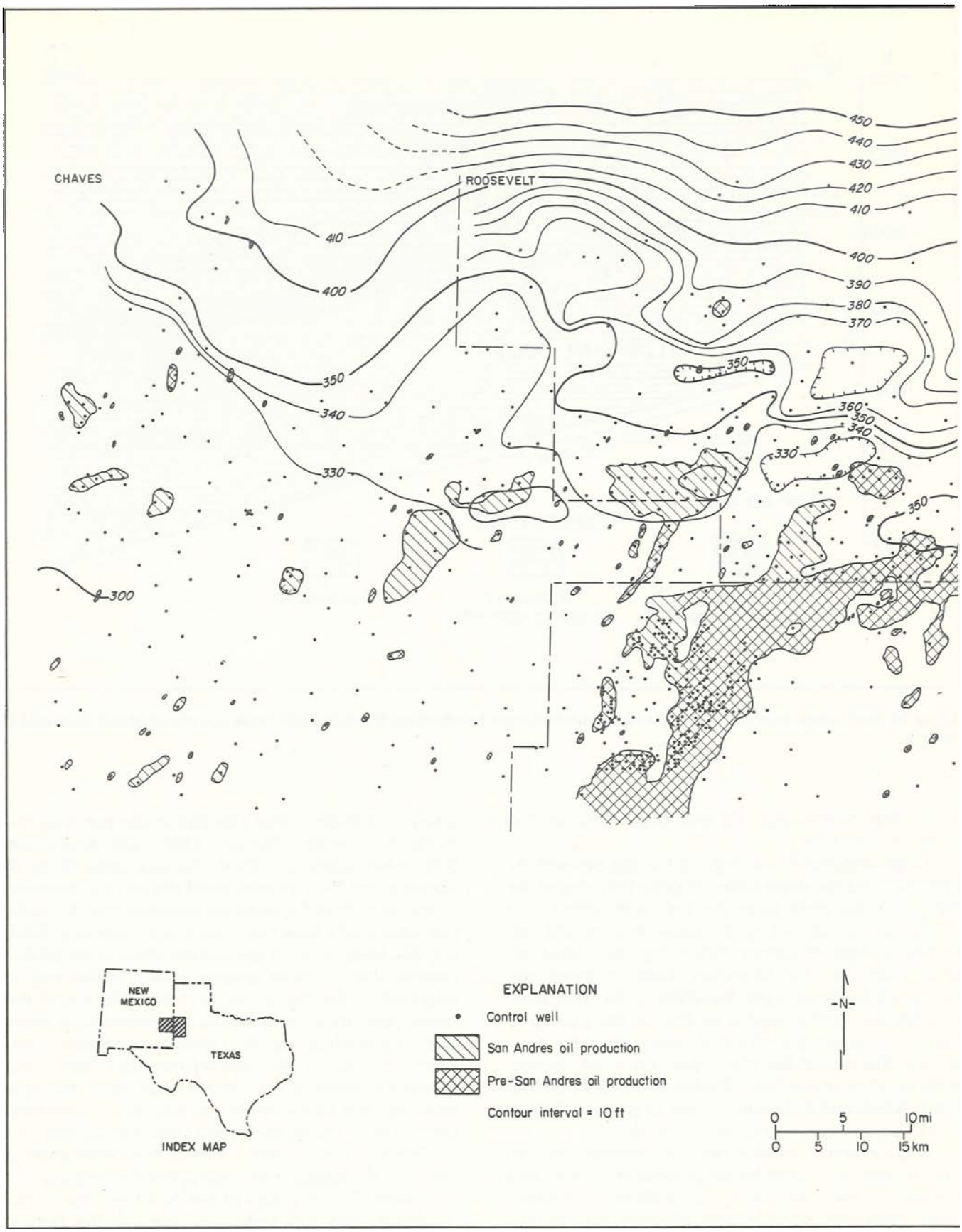

Figure 37. Isopach map of interval between the top of the Yellowhouse dolomite and the *TT* marker, San Andres Formation. Hachured contours represent stratigraphic thins, not structural lows.

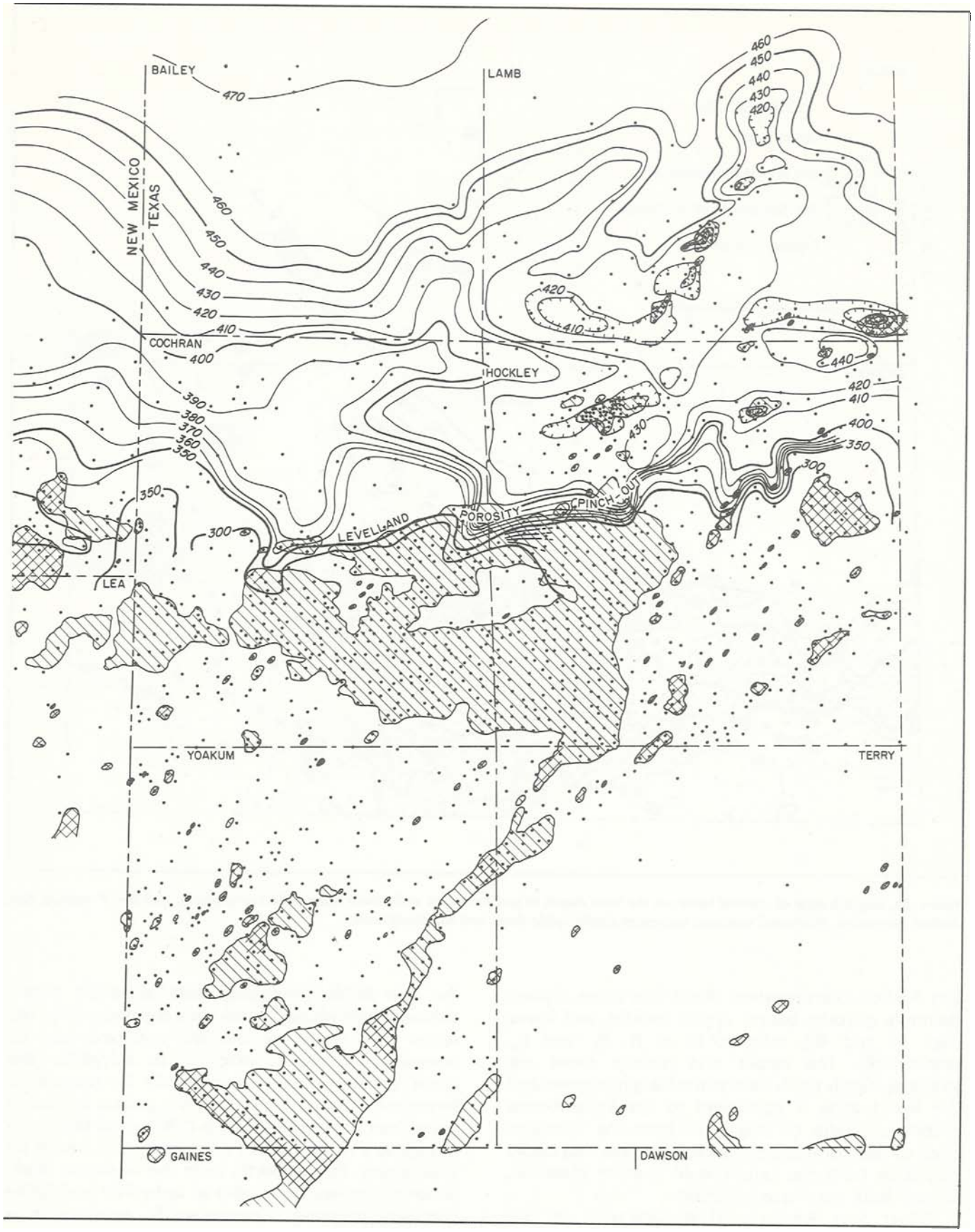

Figure 37 ***(continued)***.

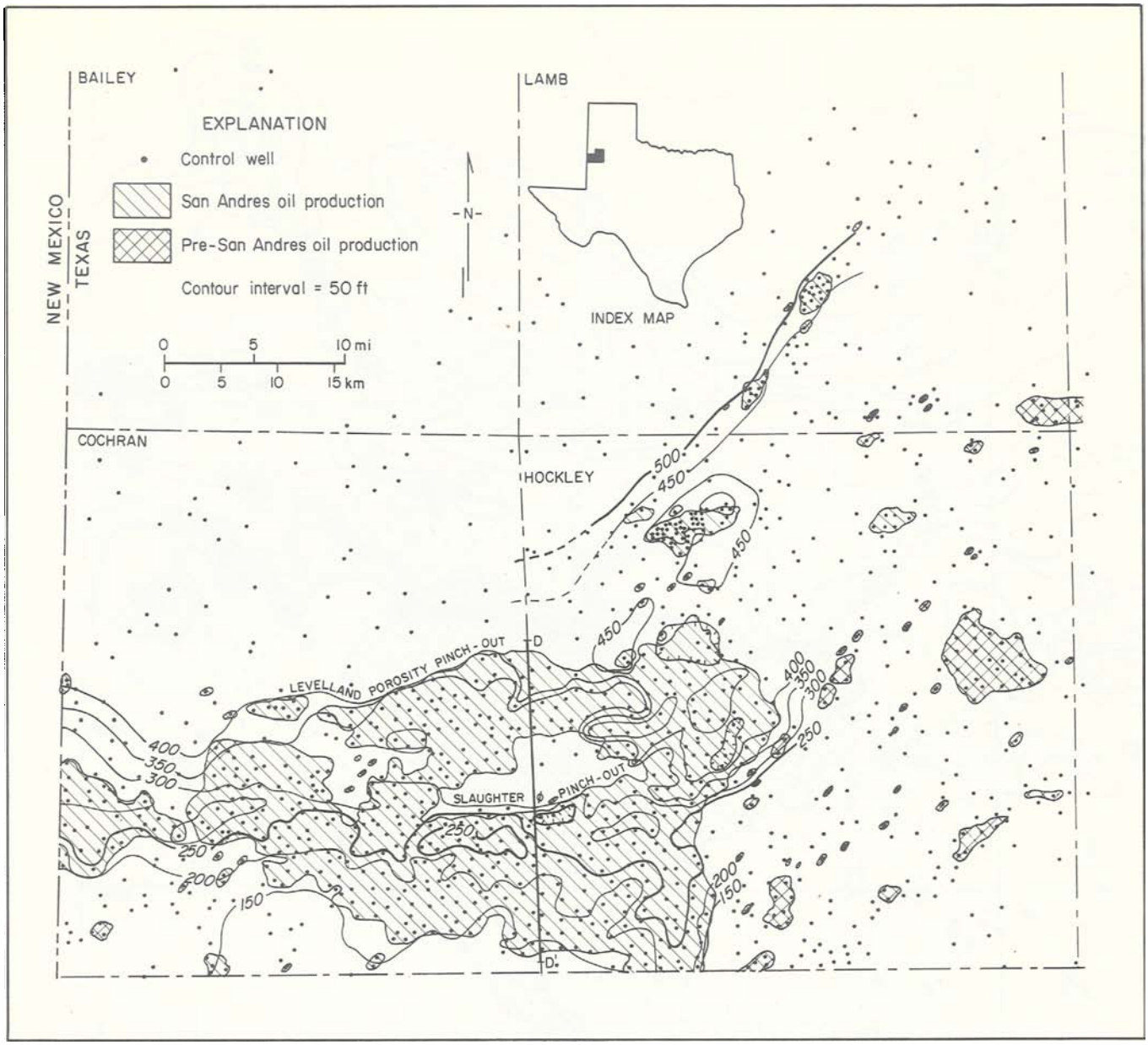

Figure 38. Isopach map of interval between the total depth of producing oil wells (with open-hole completions) and the 77 marker, San Andres Formation. Hachured contours represent stratigraphic thins, not structural lows.

San Andres (Northwestern Shelf) into three distinct dolomite porosity zones: upper, middle, and lower (figs. 39 and 40), referred to as P_1, P_2, and P_3, respectively. The upper and middle zones are stratigraphically equivalent to the Slaughter zone, and the lower zone is equivalent to the Yellowhouse dolomite. Updip oil migration from the Northern Shelf to the Northwestern Shelf is possible, but updip migration from the Tatum Basin is more plausible, though both may have occurred.

Most San Andres oil production in the Northwestern Shelf is from the upper and middle porosity zones (table 3). The Chaveroo field is one of the few fields producing from all three zones, although it produces mostly from the upper two. The upper two zones are overlain and underlain by nonporous anhydritic dolomite or anhydrite; the lower zone, however, is underlain by nonporous limestone. Toward the Tatum Basin, porous dolomites grade into limestone. Dunlap (1967) cited this facies change as a major control on porosity and, hence, oil production. To the north, as in the Northern Shelf, porosity pinches out updip as anhydrite and halite contents increase. Consequently, production is controlled by two parallel facies changes; toward the Tatum Basin, dolomite grades into limestone, and to

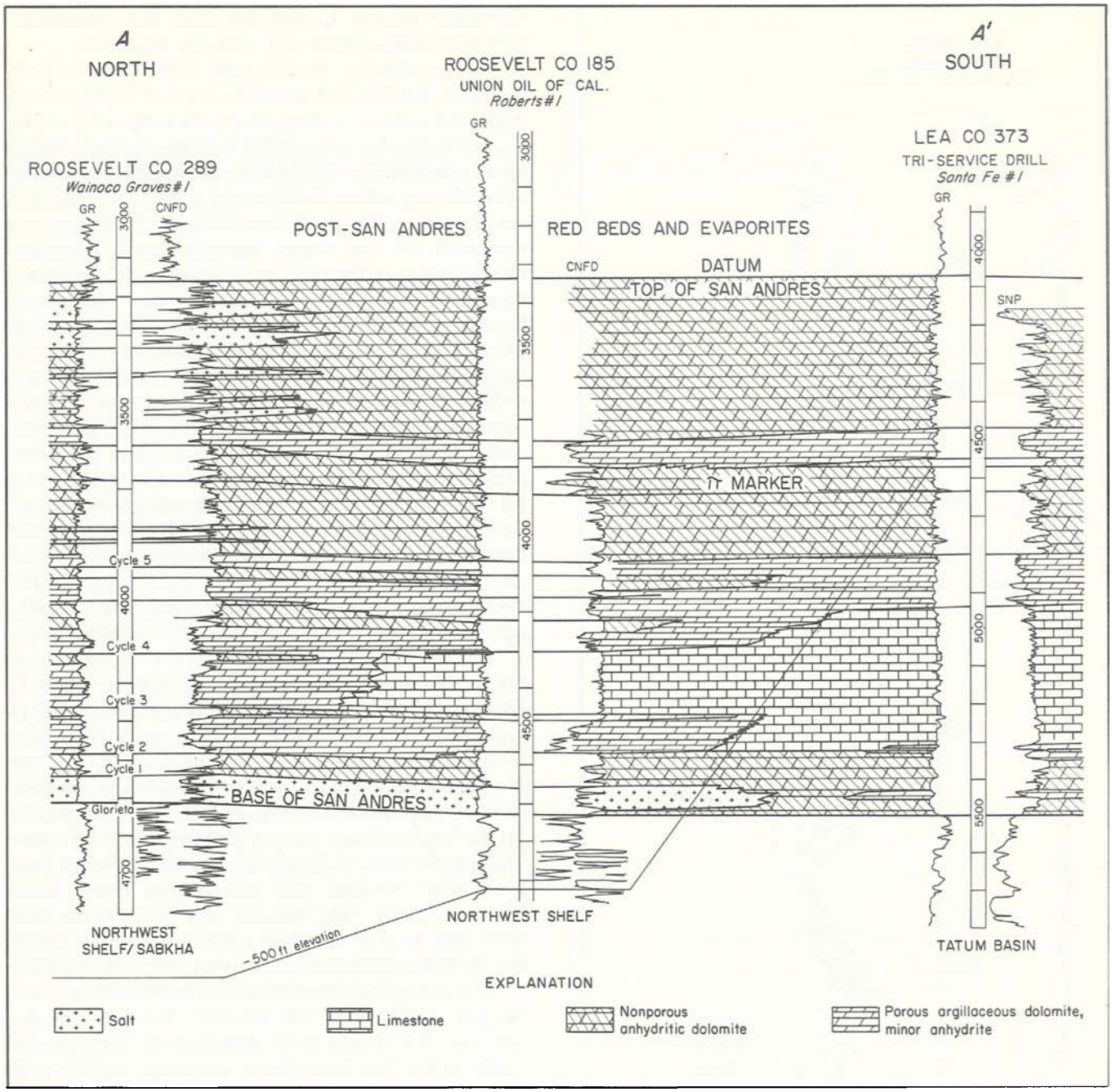

Figure 39. North-south cross section of San Andres Formation across the Northwestern Shelf, New Mexico. Line of section A-A' illustrated in figure 3.

the north, dolomite grades into anhydrite. Unlike in the Northern Shelf, there is no abrupt thickening of porosity zones around the Tatum Basin. See table 3 for the pay zones of individual fields. Figure 40 is a log illustrating the stratigraphy of the lower San Andres Formation in the Northwestern Shelf.

Total production figures do not necessarily reflect the relative productivity of various oil fields because the size of the field is not taken into account. Productivity is defined here as the amount of oil produced annually per well. The productivity of a field, therefore, depends not on its size but on such factors as porosity, permeability, thickness of the pay zone, amount of structural closure, physical qualities of the oil, and recovery techniques. Of these, the thickness of the pay zone, or oil column, is the most important. As previously mentioned, the thickness of the pay zone is related to structure. Hence, areas where the major porosity zone is thickest have the greatest potentials for having highly productive fields.

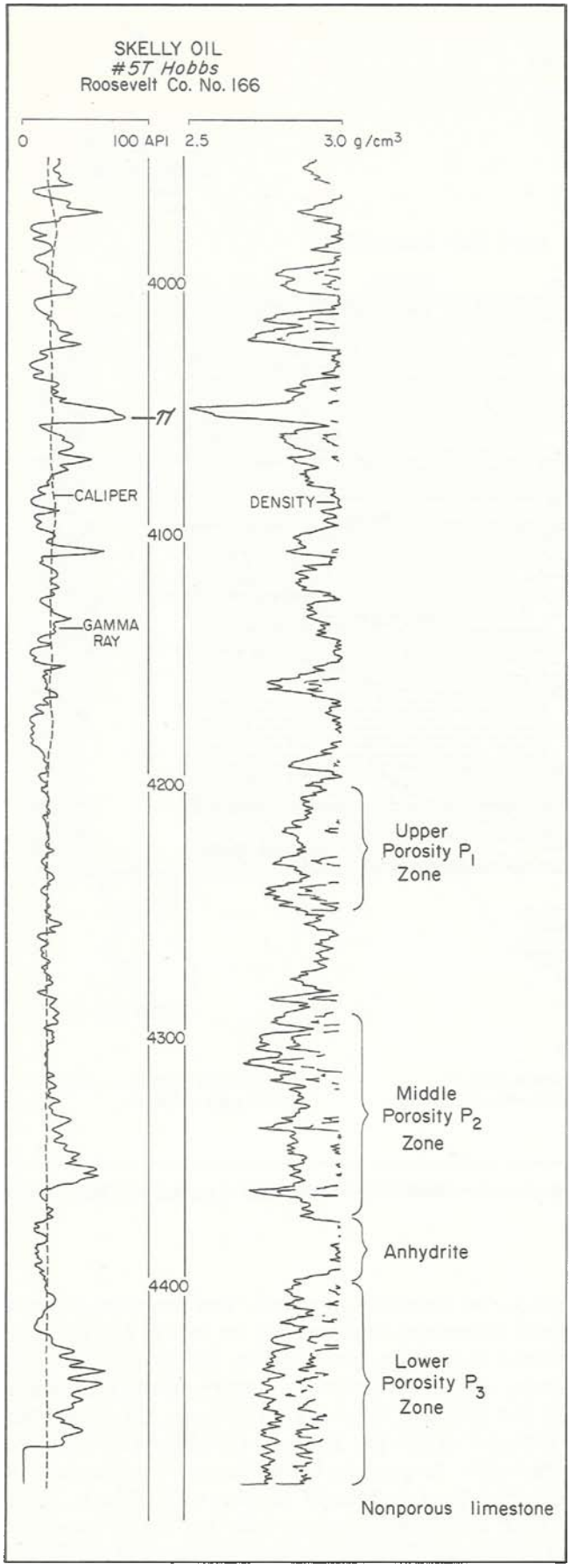

Compare figures 6 and 34; note the correlation between productivity and porosity thickness.

As previously mentioned, the Wasson field contains the thickest porosity zone. It is structurally high and overlies a hingeline with subjacent basinal source rocks. Such favorable conditions are reflected by its productivity (34,566 bbl/well for 1980), which far exceeds any other field in the study area (tables 2 and 3). As updip migration distance increases and thickness of the major porosity zone decreases northward, productivity correspondingly decreases. Compare productivities at Wasson, Slaughter, Levelland, Yellowhouse, Illusion Lake, and Littlefield fields (fig. 34; table 2). In the Littlefield field (the northernmost San Andres oil field), productivity is only 971 bbl/well (table 2). Proximity to the Midland Basin is a control on productivity; eastern Levelland and Slaughter fields in Hockley County are more productive than the western parts in Cochran County (as determined from county production figures, Railroad Commission of Texas, 1981). All production data support the model by Ramondetta (1982), which calls for vertical oil migration from deep basinal Wolfcampian shales in the Midland Basin, followed by updip migration within San Andres shelf dolomites.

Productivity is much lower in the Northwestern Shelf than in the Northern Shelf (tables 2 and 3). Likewise, productivity surrounding the Tatum Basin is higher than in fields updip from the basin. Twin Lakes field is an exception, being considerably updip from the Tatum Basin (fig. 1); this field, however, contains some structural closure (fig. 41) that may compensate for its distance from source. The field with the lowest 1980 productivity (120 bbl/well) is the Calumet field, predictably located just east of the Pecos River, Chaves County, New Mexico. The Bitter Lakes West field, just west of the Pecos River, is farthest updip, and its 1980 productivity is also very low (189 bbl/well).

The recently discovered oil in Pennsylvanian shelf-margin carbonates of western Briscoe County confirms the source-rock potential of deep basinal shales in the Palo Duro Basin. However, migration of such oil upward into younger shelf carbonates, as in the Midland Basin, is unlikely because of (1) the abundant evaporite cement in San Andres and Clear Fork carbonates of the Palo Duro Basin and (2) the lack of a sharp hingeline such as along the Abo Reef trend. Primary migration of oil from basinal shales into proximal shelf-margin deposits or fan-delta deposits, however, is entirely possible and did occur in western Briscoe County.

Figure 40. Gamma-ray, density log, and lithic interpretation of lower San Andres Formation, Skelly Oil Hobbs No. 5T, Roosevelt County, New Mexico.

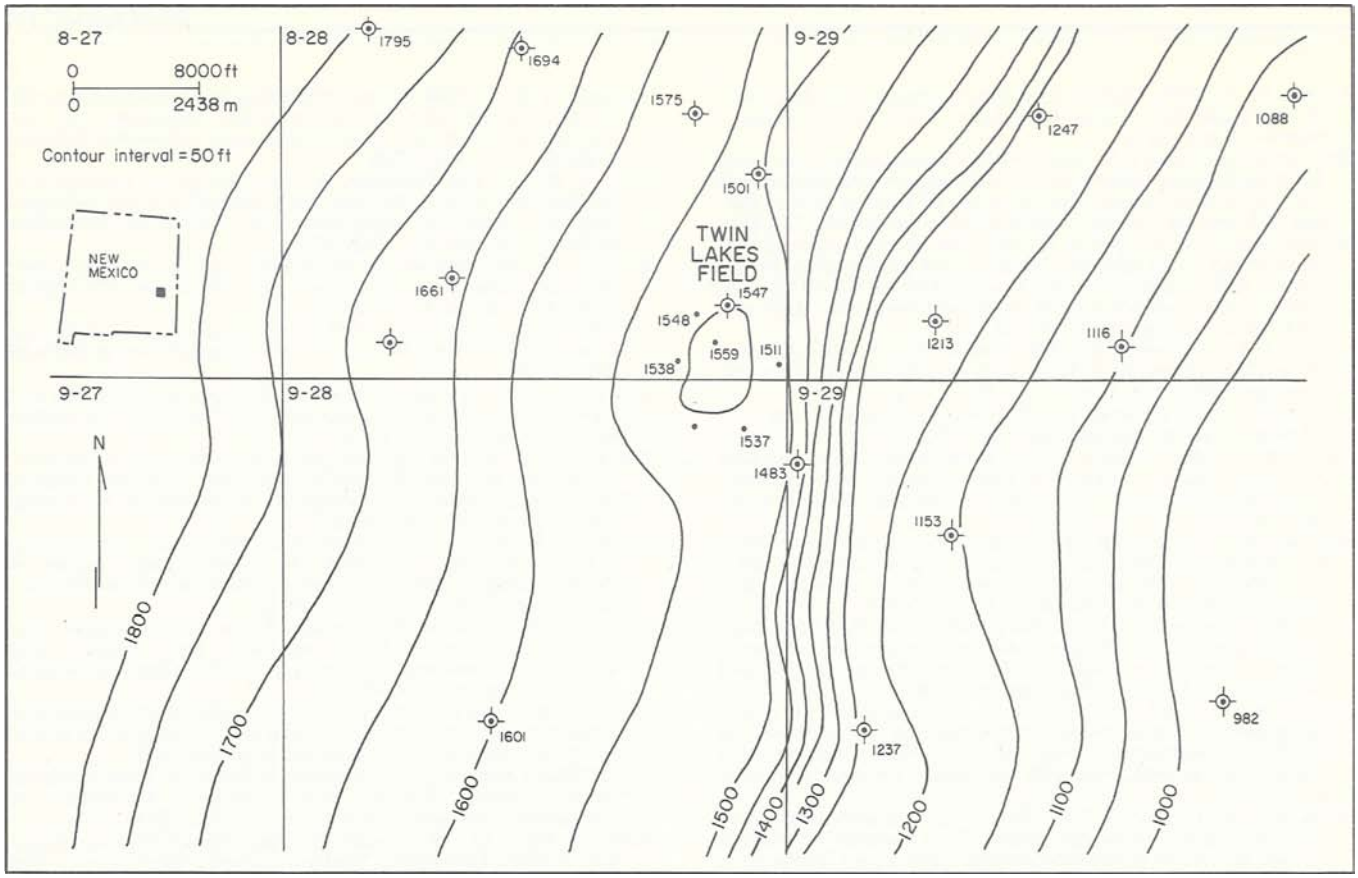

Figure 41. Structure map, π marker, Twin Lakes oil field, Chaves County, New Mexico.

CONCLUSIONS

Large, eustatic fluctuations in sea level are inferred to have enhanced secondary porosity in San Andres shelf dolomites. Dolomitization and porosity development were most intense over structurally high areas because of longer periods of subaerial exposure.

Much oil is trapped in a discontinuous, structurally high, and stratigraphically thin belt of San Andres dolomites that rims the deeper part of the Midland Basin. This belt overlies older shelf margins and is flanked on the north and west by thinning porosity zones. Lateral migration of oil updip from these traps resulted in the trapping of additional oil to the north in a series of steplike porosity pinch-outs. Many of these fields are stratigraphic traps and have only slight structural noses, if any. Salt-filled porosity in the Palo Duro Basin precludes San Andres petroleum potential north (updip) of the southernmost fringe of the Palo Duro Basin.

ACKNOWLEDGMENTS

The author gratefully acknowledges the assistance of the following persons at the Bureau of Economic Geology: Mark W. Presley, now with Delta Drilling Company, Tyler, Texas, initiated this project and provided guidance and encouragement. Michael Roberts and his staff provided the necessary computer work to compute and plot the various values on maps. Illustrations were drafted by T. M. Byrd, M. R. Davis, B. P. Holbert, J. Horowitz, and J. McClelland, under the direction of J. W. Macon and D. F. Scranton. Text photography was by James A. Morgan. Barbara Dudgeon and Ginger Zeikus typed the manuscript for this report. Typesetting was by Phyllis Hopkins, under the direction of Lucille C. Harrell. Micheline R. Davis designed and assembled this report. Editing was by R. Marie Jones-Littleton. The manuscript was critically reviewed by L. F. Brown, Jr., Amos Bein, Shirley P. Dutton, Chester M. Garrett, C. M. Jones, and Mark W. Presley.

This work was funded by the U.S. Department of Energy, under contract no. DE-AC97-80ET-46615.

REFERENCES

Barone, W. E., 1976, Depositional environments and diagenesis of the lower San Andres Formation: Texas Tech University, Master's thesis, 93 p.

Bein, Amos, and Land, L. S., 1982, The San Andres carbonates in the Texas Panhandle: sedimentation and diagenesis associated with Mg-Ca chloride brines: The University of Texas at Austin, Bureau of Economic Geology Report of Investigations No. 121, 48 p.

Chuber, Stewart, and Pusey, W. C., 1967, San Andres facies and their relationship to diagenesis, porosity and permeability in the Reeves field, Yoakum County, Texas, *in* Elam, J. B., and Chuber, Stewart, eds., Symposium on cyclic sedimentation: Midland, West Texas Geological Society, 232 p.

Cooper, C. G., and Ferris, B. J., 1957, Ownby field, Yoakum County, Texas: The University of Texas at Austin, Bureau of Economic Geology Publication 5716, p. 225-257.

Darton, N. H., 1922, Geologic structure of parts of New Mexico: U.S. Geological Survey Bulletin 726-E, p. 173-275.

Dickey, R. I., 1940, Geologic section from Fisher County through Andrews County, Texas, to Eddy County, New Mexico: American Association of Petroleum Geologists Bulletin, v. 24, no. 1, p. 37-51.

Dunham, R. J., 1969a, Early vadose silt in Townsend mount (reef), New Mexico, *in* Depositional environments in carbonate rocks, a symposium: Society of Economic Paleontologists and Mineralogists Special Publication 14, p. 139-181.

——— 1969b, Vadose pisolite in the Capitan Reef (Permian), New Mexico and Texas, *in* Depositional environments in carbonate rocks, a symposium: Society of Economic Paleontologists and Mineralogists Special Publication 14, p. 182-191.

Dunlap, W. H., 1967, San Andres oil exploration in the Cato-Slaughter trend of southeastern New Mexico, *in* The oil and gas fields of southeastern New Mexico, 1966 supplement—a symposium: Roswell, New Mexico, Roswell Geological Society, p. 21-24.

Finley, R. J., and Gustavson, T. C., 1981, Lineament analysis based on Landsat imagery, Texas Panhandle: The University of Texas at Austin, Bureau of Economic Geology Geological Circular 81-5, 37 p.

Folk, R. L., 1959, Practical petrographic classification of limestones: American Association of Petroleum Geologists Bulletin, v. 43, no. 1, p. 1-38.

Folk, R. L., and Land, L. S., 1975, Mg/Ca ratio and salinity: two controls over crystallization of dolomite: American Association of Petroleum Geologists Bulletin, v. 59, no. 1, p. 60-68.

Galley, J. E., 1958, Oil and geology in the Permian Basin of Texas and New Mexico, *in* Habitat of oil—a symposium: American Association of Petroleum Geologists, p. 395-446.

Gustavson, T. C., Presley, M. W., Handford, C. R., Finley, R. J., Dutton, S. P., Baumgardner, R. W., Jr., McGillis, K. A., and Simpkins, W. W., 1980, Geology and geohydrology of the Palo Duro Basin, Texas Panhandle—a report on the progress of nuclear waste isolation feasibility studies (1979): The University of Texas at Austin, Bureau of Economic Geology Geological Circular 80-7, 99 p.

Handford, C. R., Wiggins, W. D., Palmer, D. P., and Bassett, R. L., in press, Sedimentology, petrology, and diagenesis of Permian evaporites, Randall County, Texas: The University of Texas at Austin, Bureau of Economic Geology Report of Investigations.

Hayes, P. T., 1959, San Andres limestone and related Permian rocks in Last Chance Canyon and vicinity, southeastern New Mexico: American Association of Petroleum Geologists Bulletin, v. 43, no. 9, p. 2197-2213.

——— 1964, Geology of the Guadalupe Mountains, New Mexico: U.S. Geological Survey Professional Paper 446, p. 1-69.

Herald, F. A., ed., 1957, Occurrence of oil and gas in West Texas: The University of Texas at Austin, Bureau of Economic Geology Publication 5716, 442 p.

Hills, J. M., 1972, Late Paleozoic sedimentation in West Texas Permian Basin: American Association of Petroleum Geologists Bulletin, v. 56, no. 12, p. 2303-2322.

Jacka, A. D., Thomas, C. M., Beck, R. H., and others, 1969, Guadalupian depositional cycles of the Delaware Basin and Northwest Shelf, *in* Cyclic sedimentation in the Permian Basin—a symposium: West Texas Geological Society Publication No. 69-56, p. 152-196.

Kelly, V. C., 1971, Geology of the Pecos country, southeastern New Mexico: New Mexico State Bureau of Mines, Memoir 24, 75 p.

Kendall, G. St. C., 1969, An environmental reinterpretation of the Permian evaporite/carbonate shelf sediments of the Guadalupe Mountains: Geological Society of America Bulletin, v. 80, no. 12, p. 2503-2526.

Kerr, S. D., Jr., and Thomson, A., 1963, Origin of nodular and bedded anhydrite in Permian shelf sediments, Texas and New Mexico: American Association of Petroleum Geologists Bulletin, v. 47, no. 9, p. 1726-1732.

King, P. B., 1942, Permian of West Texas and southeastern New Mexico: American Association of Petroleum Geologists Bulletin, v. 26, no. 3, p. 535-763.

Lee, W. T., and Girty, G. H., 1909, The Manzano Group of the Rio Grande Valley, New Mexico: U. S. Geological Survey Bulletin 389, p. 1-141.

Lewis, F. E., 1941, Position of the San Andres Group, West Texas and New Mexico: American Association of Petroleum Geologists Bulletin, v. 25, no. 1, p. 73-103.

Mazzullo, S. J., 1982, Stratigraphy and depositional mosaics of lower Clear Fork and Wichita Groups (Permian), northern Midland Basin, Texas: American Association of Petroleum Geologists Bulletin, v. 66, no. 2, p. 210-227.

Newell, N. D., Rigby, J. K., Fischer, A. G., Whiteman, A. J., Hickox, J. E., and Bradley, J. S., 1953, The Permian reef complex of the Guadalupe Mountains region, Texas and New Mexico: San Francisco, W. H. Freeman, 236 p.

Otte, C., 1974, Hydrocarbon accumulation in San Andres Formation of Permian Basin, southeast New Mexico and West Texas: American Association of Petroleum Geologists Bulletin, v. 58, no. 5, p. 909-910.

Patterson, R. J., and Kinsman, D. J. J., 1981, Hydrologic framework of a sabkha along Arabian Gulf: American Association of Petroleum Geologists Bulletin, v. 65, no. 8, p. 1457-1475.

——— 1982, Formation of diagenetic dolomite in coastal sabkha along Arabian (Persian) Gulf: American Association of Petroleum Geologists Bulletin, v. 66, no. 1, p. 28-43.

Perez de Mejia, D., 1977, Facies and diagenesis of Permian, lower San Andres Formation, Yoakum County, West Texas: The University of Texas at Austin, Master's thesis, 137 p.

Presley, M. W., 1979, San Andres facies patterns, Palo Duro and Dalhart Basins, Texas: American Association of Petroleum Geologists Bulletin, v. 63, no. 8, p. 1427-1428.

Railroad Commission of Texas, 1981, 1980 annual report of the Oil and Gas Division, 666 p.

Ramondetta, P. J., 1982, Genesis and emplacement of oil in the San Andres Formation, Northern Shelf of the Midland Basin, Texas: The University of Texas at Austin, Bureau of Economic Geology Report of Investigations No. 116, 39 p.

Roswell Geological Society, 1956, 1960, 1967, 1977, Oil and gas fields of southeastern New Mexico, a symposium: Roswell, New Mexico, 4 volumes.

Sax, N. A., and Stenzel, W. K., 1968, Oils from Abo reservoirs of the Northwest Shelf, *in* Basins of the southwest, v. 2: Midland, West Texas Geological Society, p. 42-52.

Schneider, W. T., 1943, Geology of Wasson field, Yoakum and Gaines Counties, Texas: American Association of Petroleum Geologists Bulletin, v. 27, no. 4, p. 479-523.

——— 1957, Wasson field, Yoakum and Gaines Counties, Texas: The University of Texas at Austin, Bureau of Economic Geology Publication 5716, p. 377-384.

Silver, B. A., and Todd, R. G., 1969, Permian cyclic strata, northern Midland and Delaware Basins, West Texas and southeastern New Mexico: American Association of Petroleum Geologists Bulletin, v. 53, no. 11, p. 2223-2251.

Thomas, C. M., 1968, Vadose pisolites in the Guadalupe and Apache Mountains, West Texas, *in* Guadalupian facies, Apache Mountain area, West Texas: Society of Economic Paleontologists and Mineralogists, Permian Basin Section Guidebook Publication 68-11, p. 10-31.

Todd, R. G., 1976, Oolite bar progradation, San Andres Formation, Midland Basin: American Association of Petroleum Geologists Bulletin, v. 60, no. 6, p. 907-925.

Wright, F. W., 1962, Abo Reef: prime West Texas target: Oil and Gas Journal, v. 60, no. 32, p. 188-194.

Zaaza, M. W., 1978, The depositional facies, diagenesis, and reservoir heterogeneity of the upper San Andres Formation in West Seminole field, Gaines County, Texas: University of Tulsa, Ph.D. dissertation, 210 p.